Auditory and Tactile Detection by the West Indian Manatee

David Mann, University of South Florida
Gordon Bauer, New College of Florida
Roger Reep, University of Florida
Joseph Gaspard, Trainer – Mote Marine Laboratory & Aquarium, UF Ph.D. Student
Kim Dziuk, Trainer – Mote Marine Laboratory & Aquarium
LaToshia Read, Trainer – Mote Marine Laboratory & Aquarium

Introduction

Endangered Florida manatees (*Trichechus manatus latirostris*) inhabit shallow waters of rivers, bays, estuaries, and coastal areas, where their primary food source, light-dependent vegetation, concentrates them in shallow water areas. Much of their environment overlaps with humans, and as a result they suffer mortality and injury from boats, water control structures, and fisheries gear (U.S. Fish and Wildlife Service, 2001), in addition to a variety of natural causes. Thirty-one percent of all manatee deaths in the period from 1976-2000 were attributable to human-related causes. This is undoubtedly an underestimate of human impact since the cause of 30% of deaths during this period could not be determined, some due to the degree of carcass decomposition. The Florida Manatee Recovery Plan (U.S. Fish and Wildlife Service, 2001) explicitly identified the need to reduce mortality and/or injury caused by vessels (Goal 1.3, p. 56, 60), water control structures (Objective 1.6, p. 60), and fisheries and entanglement (Objective 1.7, p. 63). Manatee casualties caused by human activities can be minimized through an understanding of how manatees sense their environment and in some critical instances fail to sense it. The Recovery Plan (2001, p. 79) explicitly recognized this need in calling for study of sensory processes. In the long-term, understanding of the auditory/tactile habitat of the manatee will be critical to protecting them. To address the Recovery Plan sensory objectives, we investigated the abilities of manatees to hear and feel different types of auditory/tactile stimuli in a controlled environment in order to understand how well they can detect boats and other sound sources (such as depth finders), as well as static objects (such as water control structures, crab pots and traps) through the changes made in water flow patterns.

Reduction in watercraft related manatee deaths and injuries appear to be critically related to audition. Whether manatees can detect and localize boat engine noise and the frequencies that are best detected is currently a topic of debate. Many aspects of detection remain to be explored. Recently we assessed the ability of manatees to localize sounds in a four-speaker, 180° array (Colbert et al., in press) and in an eight-speaker array that encircled the manatee (Colbert et al., 2008). In general, we found that manatees were quite good at localizing broadband stimuli, but quite poor at determining the direction of unmodulated tonal sounds. Their ability to localize underwater sounds over 360° is quite impressive given that sound travels approximately five times faster underwater than in air, thus potentially reducing the usefulness of time of arrival cues in sound localization. One possible explanation is that the manatee body provides

substantial sound shadowing over a broad frequency range, which could provide sound localization cues.

Early reports of manatee hearing using auditory evoked potential (AEP) techniques suggested that manatees had greatest hearing sensitivity at lower frequencies (Bullock et al., 1980; Bullock et al., 1982). Anatomical analysis (Ketten et al., 1992) also indicated adaptations for low frequency hearing. More recent reports of AEP studies of both West Indian and Amazon manatees (*Trichechus inunguis*) indicate higher frequency hearing, with greatest sensitivity in the 10 – 25 kHz range and upper limits as high as 60 kHz (Klishin et al., 1990; Mann et al., 2005; Popov & Supin, 1990). A behavioral audiogram for West Indian manatees reported by Gerstein et al. (1999) was consistent with the high frequency ranges found in the later AEP studies. Although some of the discrepancy between the early and later studies might be accounted for by differences between in-air measures, such as used by Bullock, which appear to yield lower frequency detection estimates, and in-water measures, the question of frequency sensitivity remains open because of the small sample sizes (usually 1 – 2 animals) and potential variability among techniques.

Furthermore, manatee responses to vibrational stimuli may be mediated by more than one sensory mechanism. Gerstein et al. (1999) reported the interesting observation that one of his subjects, Stormy, detected low frequency sounds, under 400 kHz, but with a different behavioral topography. Stormy rotated his body and ducked his head before responding. Gerstein suggested that the low frequency response could be mediated by a vibrotactile sense, rather than audition. At this point, however, we do not really know if the low frequency responses were mediated by audition or a vibrotactile sense.

To address manatee hearing and vibrotactile capabilities within the context of understanding their responses to anthropogenic disturbance we investigated the sensory performance of manatees in three areas, and placed manatee hearing within the context of boat noise.

1) Behavioral audiograms. We assessed the ability of manatees to detect sounds at different frequencies in quiet conditions.
2) Masked audiograms. We assessed the ability of manatees to hear in noise.
3) Tactile assessment. We initiated assessments of the ability of manatees to detect low frequency, putatively vibrotactile stimuli.
4) Boat noise assessment. We recorded boat noise in Sarasota Bay next to a manatee idle speed zone.

These four lines of investigation served several important purposes. The auditory research extended the work of Gerstein (1999) by testing a range of acoustic signals in noise as well as in quiet conditions. The audiograms double the sample size of subjects tested for frequency sensitivity using behavioral measures, validate the partial auditory evoked potential audiogram done with the same animals (Mann et al., 2005), and validate our directional hearing studies (Colbert et al., in press; Colbert et al., 2008) by identifying the sensitivity of the subjects to the frequencies tested. The tactile studies provide the first glimpse of the mechanisms manatees use to detect low frequency signals. The noise assessments place our laboratory findings of manatee senses within the natural context of

field conditions where manatees are vulnerable to harm from vessel strikes. These experiments, as a group, provide information important for understanding the sensory abilities of manatees to detect boat noise.

Experiment I. Auditory Frequency Sensitivity (Behavioral Audiogram)

We previously conducted studies on the hearing sensitivities of Hugh and Buffett using auditory evoked potential techniques (Mann et al., 2005). Results of these tests indicated that the frequency range of their frequency detection extended from 4 kHz (lowest frequency tested) to 40 kHz. We also indirectly measured the temporal resolution of the manatee auditory system using the Envelope Following Response (EFR) technique. Animals with higher temporal resolution abilities show responses to signals with higher rates of amplitude modulation (AM). Both Hugh and Buffet could follow AM rates up to 600 Hz. To put this in perspective, dolphins, which have extremely high levels of temporal resolution, can detect changes in AM rates up to about 1100 Hz, while humans are sensitive only to about 200 Hz. Thus, manatees have an intermediate temporal resolution. These results suggest relatively high frequency sensitivity of manatees, which is often related to temporal resolution.

In this study we determined the audiogram under quiet background conditions resembling rivers (about 50 dB re 1 $uPa^2/(Hz)$). We presented low tones corresponding to the range of boat noises, mid-range tones corresponding to natural vocalizations, and high tones assessing the upper limits of hearing.

Methods

Subjects
Subjects were two male, Florida manatees (*Trichechus manatus latirostris*), Hugh and Buffett, ages 22 and 19 respectively at the start of testing.

Training
Both Hugh and Buffett were highly trained manatees (Colbert & Bauer, 1999; Colbert, Fellner, Bauer, Manire, and Rhinehart, 2001; Bauer, Colbert, Gaspard, Littlefield, and Fellner, 2003; Mann et al., 2005). They have been trained to approach visual targets, depress tactile targets while blindfolded, breathe into a mask for respiration and hormonal analysis, accept insertion of needle electrodes for brain evoked potential studies of hearing, and press targets in response to high and low frequency sounds.

Procedure
Training was done with standard conditioning techniques. Subjects were reinforced with favored food items, such as beets, apples, and carrots for desired responses. Undesirable responses were ignored. The sounds were delivered through a speaker based on quasi-random schedules in which half the trials were sound present and half were "catch" (sound absent) trials. The 50/50 split prevented a response bias based on probability of sound presentation. The subjects were tested using a go/no-go format and were

reinforced for touching the response paddle, a speaker blank, when a sound was emitted or remaining at station for 10 secs if no sound was generated. Subjects were called back to the center station between trials. The minimum inter-trial-interval (ITI) was 30 secs.

Each subject was trained to station for each trial 1 m below the water surface by pressing the post-nasal crease underneath a PVC horizontal bar in response to a specific pulsed tone. This apparatus was positioned approximately 3 m in front of a transducer which was mounted independently. The sound stimuli used overlapped those used in our underwater evoked potential audiogram study (Mann et al., 2005). A light signaled the subject that a stimulus window, sound present or sound absent, would begin 2 secs from onset. Sound stimuli were 2 secs in duration, which video analysis indicated did not allow subjects to move from the stationing bar before the signal termination. A modified staircase method was used (Cornsweet, 1962). For each tone frequency, testing started at a sound intensity level that was easily detectable (e.g., 15 dB above estimated threshold) based on previous published reports and AEP studies with Hugh and Buffett. After a correct response, the sound intensity was dropped 6 dB. After an error sound intensity was raised 3 dB, followed by 3 dB drops for all correct responses thereafter. A session consisted of eight to ten sound intensity reversals. A threshold was defined as two consecutive sessions with mean amplitude levels of reversals differing by no more than 6 dB.

The location of the subject at the central station was monitored by overhead video in order to assess exact head position. Only trials where head position was appropriate (i.e., 3 meters from the speaker) at the initiation of a test sound were kept for analysis. All responses were automatically recorded and stored, so that an ongoing record of correct trials and latency (time from test signal to speaker touch) could be maintained. To control for motivational artifacts blocks of trials were started with 4 “warm-up” trials. The sound stimuli for these trials were easily detected training stimuli (e.g., 15 dB above estimated threshold). Performance accuracy of 75% on these motivation assessments were required to keep session trials for analysis. Otherwise, a session was abandoned or data were not used for detection analysis.

To review the full sequence for a trial:
1) Subject was called to station by a pulsed tone from a central speaker;
2) Subject aligned itself facing an underwater speaker;
3) Trial initiation was signaled with a light 2 secs prior to the stimulus window;
4) Subject approached and touched a response manipulandum to its left if the sound was played, or remained at station for 10 sec if no sound was played;
5) The correct response was followed immediately by an acoustic secondary reinforcer;
6) The subject returned to the central station to be fed by a trainer “blind” to the test condition. The “blind” status of the trainer was maintained by wearing headphones playing masking noise. If the subject made an incorrect response he was called back to the center station for the next trial, to be initiated no sooner than 30 secs (the minimum inter-trial interval) after the last sound. The sequence of trials was determined quasi-randomly by the computer.

Experimental Layout
The sound speaker was located 1 meter from the water surface and 3 m from the subject (Figure 1). The response paddle was located at the same depth but 1 meter to the subject's left.

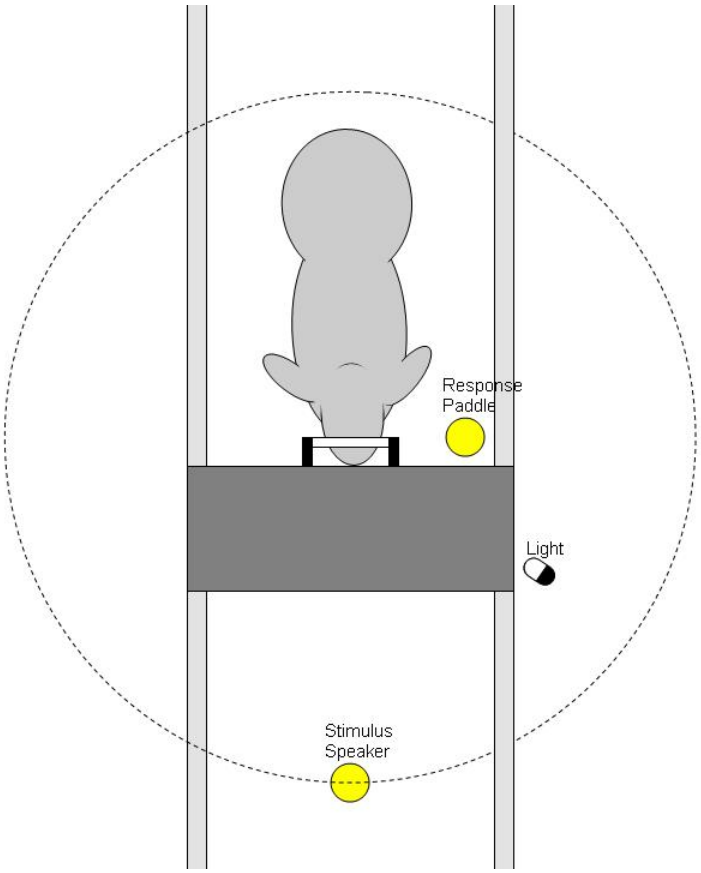

Figure 1. Audiogram layout. The manatee stationed with its head facing the transducer 3 meters away.

Signal Generation
Signals were generated digitally by a Tucker-Davis Technologies Real-Time Processor (RP2.1), attenuated with a programmable attenuator (PA5) to control level, and amplified with a Hafler Power Amplifier. The status of a switch at a speaker was monitored by the digital inputs on two RP2's. A digital output on an RP2 was used to control the light indicating the start of a trial. A separate D/A channel was used to generate the signal to the stationing speaker at the manatee start station.

All experiments were programmed in MATLAB with a graphical user interface. All signals had a 10 ms rise-fall time to eliminate transients. The signals received by the manatees were monitored for all experiments with a Reson calibrated hydrophone. The computer randomized the timing of sound presentation and recorded the latency to respond.

Results and Discussion

The behavioral audiogram for Hugh and Buffett is presented in Table 1 and Figure 2. Figure 2 also displays their AEP audiogram, and the behavioral audiogram for two previously tested manatees, Stormy and Dundee, reported by Gerstein and colleagues (1999). The results of the audiogram with Hugh and Buffett represent the means of at least two staircase runs. The one exception is at 90.5 kHz, where the result from Buffett is from one staircase. Blocks were dropped if the manatee did not achieve better than 75% correct on catch trials. Hugh and Buffett had similar sensitivity, with best sensitivity for Buffett between 16-32 kHz and Hugh between 8-22.627 kHz. The audiograms also show sensitivity down to 250 Hz, the lowest frequency tested.

The form of the audiogram is similar to that reported by Gerstein et al. (1999), with the exception of considerably higher frequency detection by one of our subjects. In general, we found higher threshold levels, some of which might be attributable to masking (see critical ratios in next section).

Table 1. Behavioral audiogram measurements for Hugh and Buffett. The frequency is the test frequency. The threshold dB Level is the average across multiple sessions of interpolated hearing threshold at the specific frequency. The false alarm rate is the proportion of sound absent trials that the manatee incorrectly responded to as if sound were present.

Buffett

Frequency (kHz)	Threshold dB Level (dB re 1 µPa)	False Alarm Rate
0.25	116.1	0.09
0.5	103.4	0.12
1	99.7	0.20
2	96.4	0.12
4	86.7	0.10
8	70.3	0.11
16	60.7	0.18
22.627	64.3	0.15
32	63.7	0.16
64	105.1	0.15
76.1093	128.4	0.17
90.5	141.1	0.11

Hugh

Frequency (kHz)	Threshold dB Level (dB re 1 µPa)	False Alarm Rate
0.25	125.6	0.15
0.5	112.9	0.16
1	104.9	0.12
2	97.0	0.17
4	78.6	0.13
8	71.7	0.19
16	70.7	0.18
22.627	71.0	0.19
32	97.6	0.13

38.0546	121.3	0.10

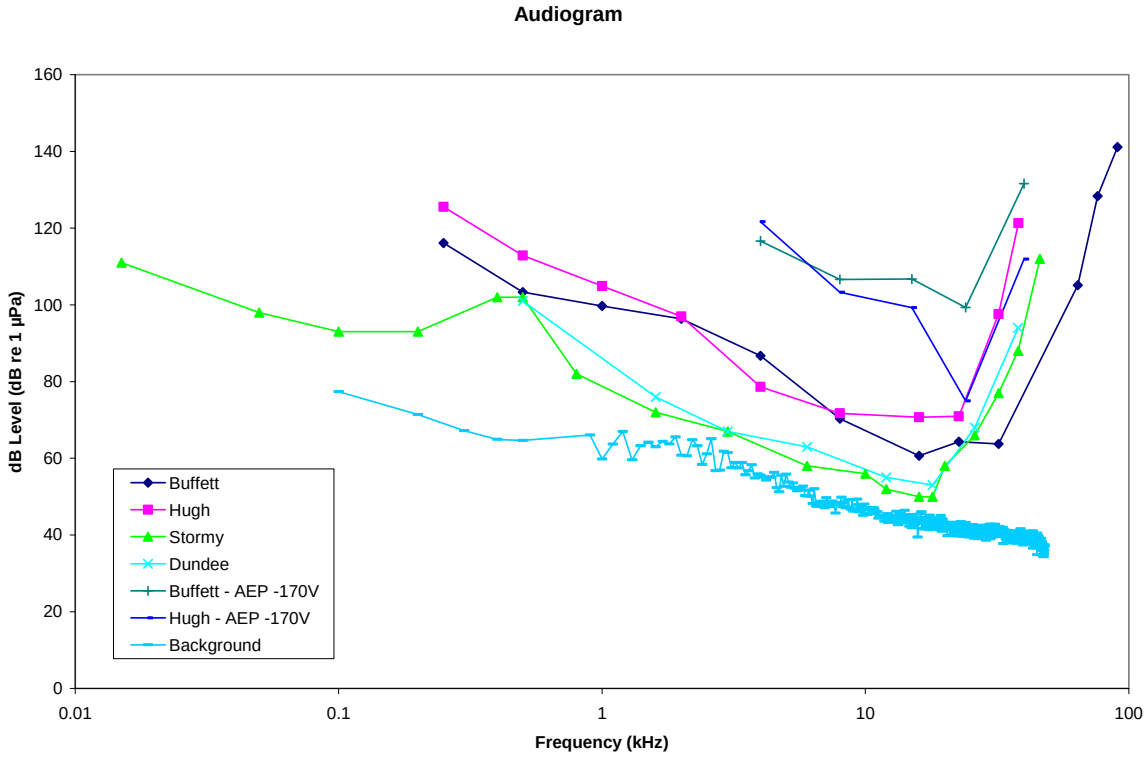

Figure 2. Behavioral audiogram of Buffet (blue diamonds) and Hugh (pink squares). Behavioral audiograms of Stormy and Dundee (Gerstein et al., 1999) and evoked potential audiograms of Buffett and Hugh (Mann et al., 2005) are plotted for comparison. The light blue line (rectangles) represents typical background noise in the test tank during the Hugh-Buffett audiograms.

Experiment II. Masked Hearing Thresholds and Critical Ratios

Background noise can often mask the ability to detect a sound (consider how difficult it is to hear someone talking when at a party). Critical ratios provide estimates of that ability to hear sound in the presence of background masking noise. In this experiment we measured hearing sensitivity under noisy conditions (about 90 dB re 1 uPa/sqrt(Hz)) resembling a coastal environment..

Methods

Subjects
The same subjects were used as for Experiment I.

Procedures
The same testing procedures were used as in Experiment I. The test stimuli were a subset of the frequencies used for the audiogram measured in low-background noise conditions.

One-octave wide noise bands centered on the test tone frequency were used as maskers, with the spectrum level sound level 7-12 dB above the thresholds in quiet from the audiogram. The same speakers were used to play the noise and the test tone signals (these signals were mixed by a summer before playing). Sound levels were calibrated at the position of the head of the manatee when the manatee was not present using a calibrated pressure hydrophone with a flat frequency response from 0 – 170 kHz. The noise used in masking experiments was normalized by the computer system so that it was flat across the frequency spectrum (most speakers do not have a flat response across the frequency spectrum).

Results and Discussion
The results of the critical ratio measurements are listed in Table 2 and shown in Figure 3. The 10% energy curve that is plotted on the graph is approximately followed by most mammals for which there are critical ratio measurements. The critical ratios for the ringed seal and bottlenose dolphin are shown for comparison. What seems unique about manatees is that their critical ratios are quite low, especially at 8 kHz compared to the ringed seal. This would mean that their hearing thresholds would not be elevated as much by the presence of background noise, and which also suggests that their auditory system has relatively narrow filters in this frequency range. Since the same speaker is used to present the masking noise and the test tone, it is not possible that they are obtaining spatial masking release. It is also interesting to note that many manatee vocalizations are tonal harmonic complexes that often include a tonal component in the 4-8 kHz range.

Table 2. Critical ratio measurements for Hugh and Buffett. The frequency is the test frequency. The masked threshold is the threshold measured in presence of the background noise. The background noise level is the spectrum level background noise centered at the test frequency. Only data with a false alarm rate <25% are included in this table.

Buffett

Frequency (kHz)	Masked Threshold Level (dB re 1uPa)	Background Noise Level (dB re 1uPa^2/Hz)	Critical Ratio
4	123.8	93	30.8
8	103.8	82	21.9
16	99.6	73	27.0
22.627	107.0	76	31.0
32	98.2	70	28.2

Hugh

Frequency (kHz)	Masked Threshold Level (dB re 1uPa)	Background Noise Level (dB re 1uPa^2/Hz)	Critical Ratio
4	114.9	85	29.9
8	102.3	84	18.3
16	105.1	77	28.1
22.627	110.1	76	34.1

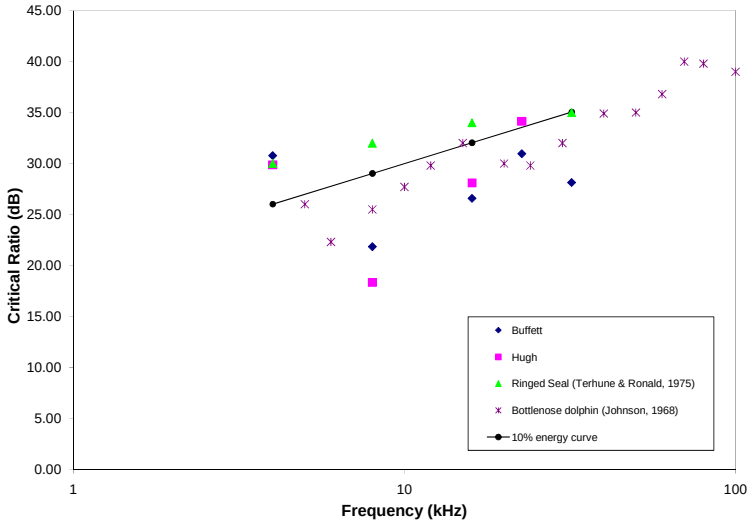

Figure 3. Critical ratios for Hugh and Buffett. Also shown for comparison are the critical ratios for the ringed seal (Terhune and Ronald, 1975), the bottlenose dolphin (Johnson, 1968) and the 10% energy-level calculated as 10*log(frequency (Hz) * 0.1).

Experiment III. Vibrotactile Frequency Sensitivity (Behavioral Tactogram)

Evidence for a vibrotactile sense derives from two lines of evidence, one behavioral and the other anatomical. The behavioral evidence was provided by Gerstein et al. (1999) in reporting the manatee audiogram. He described a variety of different response characteristics to sounds under 400 Hz that differed from responses to higher frequencies. These included; 1) a long training time, despite the fact that the subject, Stormy, had already learned the required response (a paddle press) to sounds above 400 Hz, 2) different response topography (rotating the body and ducking the head), and 3) a response curve with a disjunction (a change in sensitivity pattern) at 400 Hz.

The anatomical evidence comes from an intriguing discovery and hypothesis by Reep, Marshall, and Stoll (2002). Reep's careful analysis of the body hairs of the manatee indicated that they are all sensory hairs (i.e., vibrissae). Manatees are the only animal so far reported to have vibrissae exclusively covering the entire body. From this finding, they surmised that these sensory hairs might serve as a three dimensional array for monitoring water flow, a mammalian analog to the fish lateral line system.

Methods

Subjects
Subjects were the same as for the audiograms.

Procedures
The procedures were similar to those used for the audiogram. We tested the sensitivity of the rostral vibrissae, primarily those of the oral disk. Although we hypothesized that the postcranial vibrissae would be more sensitive to hydrodynamic stimuli, we began training with the facial region due to the similarity of this protocol with previously trained behaviors. The subject was trained to position itself facing a sinusoidally oscillating sphere 10 cm away on the midline at a depth of 0.75 m, and driven by a computer-controlled calibrated vibration shaker (Data Physics – Signal Force, Model V4). The subject placed the postnasal crease (located caudal to the oral disk; Reep et al., 1998) under a horizontal bar, which allowed exact measurement from a fixed benchmark of the distance between the oral disk and the oscillating sphere (Figure 4). Pink noise (151 db re 1 μPa) was played to the manatees throughout the sessions to control for auditory cues that might be detected by the cochlea. Stimuli were 3 sec duration with $\cos^2$ rise-fall times of 300 ms (cf. Dehnhardt et al., 1998).

Each subject was trained using standard conditioning techniques (Colbert et al., 2001) in a go/no-go response paradigm. Presentation of signal-present vs. signal-absent trials were counterbalanced and controlled for standard animal biases (e.g., perseveration, alternation, and double alternation) using quasi-random schedules. The subject indicated detection of vibrations by withdrawing from the horizontal stationing bar and pressing a target lateral to the head. A no-go response was defined operationally as ten seconds

without pressing the target. Correct responses were followed by a secondary, whistle reinforcer followed by a food reward.

A staircase method was used. Each frequency was started at ~24 dB above threshold based on preliminary testing and dropped in 3 dB increments if the subject responded correctly. Thresholds were determined as the average of the amplitudes for 8 reversals (i.e., 8 transitions in which the amplitude increased or decreased). We ran a second day to confirm the threshold. We tested the following frequencies: 5, 10, 15, 20, 25, 50, 75, 100, 125, and 150 Hz. 150 Hz is below the apparent functional hearing limit of 250 Hz (see above) or 400 Hz (Gerstein et al., 1999). If we did not get agreement between days within 6 dB, we ran sessions until we achieved two consecutive stable sessions of 8 reversals.

Equipment

A dipole shaker (Data Physics – Signal Force, Model V4) with a 5.08 cm diameter plastic sphere on a stainless steel extension (Coombs, 1994)) was used to generate the stimuli (Figure 5). The dipole shaker generates a localized flow that decreases in amplitude as $1/\text{distance}^3$, as opposed to a monopole source that decreases in amplitude as $1/\text{distance}^2$ (Kalmijn, 1988). The dipole source is easily characterized and is useful for determining thresholds for detection of near-field signals. The vibrissae are likely important in detecting other types of water flow, such as river currents and vortices shed by other swimming manatees. However, it is extremely difficult to generate and characterize these types of stimuli in the tanks typically used to house manatees. Use of a dipole shaker generated localized, controlled, and calibrated stimuli that allowed us to determine sensitivity over specific parts of the body (e.g., the oral disk on the face).

For calibration we embedded a 3-dimensional accelerometer (Dimension Engineering) into the sphere to measure its movement. We have also potted a 3-dimensional accelerometer and mounted it to a neutrally buoyant frame to measure the motion received at the location of the manatee. The thresholds presented here are based on the measurements from the accelerometer located at the position of the manatee.

Results and Discussion

A summary of the training trials is presented in Table 3 and a summary of the testing trials is presented in Table 4. False alarm rates by test data are shown in Table 5. False alarms are errors of commission; the manatee reports a signal present when in fact the signal is absent. The results of the tactogram measurements are shown in Figure 6 as a function of displacement, velocity, and acceleration (because the signals are sinusoidal, velocity can be calculated from the acceleration by dividing by 2*PI*F; displacement can be calculated from the velocity by dividing by 2*PI*F)

For the majority of frequencies tested, the tactogram shows remarkable sensitivity. In terms of displacement, the manatees could sense displacements of less than 1 micron at most test frequencies. As startling as this level of sensitivity appears, the relatively low false alarm rates at some frequencies suggest that the thresholds listed are probably conservative. Manatees are likely to be more sensitive than we report. Hugh in particular

seemed to employ a very conservative response strategy. Sensitivity diminished at the lowest frequencies tested (5 - 15 Hz).

Any vibrating source (whether monopole or dipole) generates acoustic pressure (that we detect with our ears) and acoustic particle motion. Vibrissae are not the only sensory system capable of potentially detecting stimuli from the dipole shaker. We are currently conducting vibrissae blocking experiments that will confirm whether the responses we have measured are the result of detection by vibrissae.

Table 3. Number of training trials for tactogram measurements. These trials were conducted after initial training to familiarize the animals with each test stimulus frequency.

	Hugh	Buffett
Frequency	# of Trials	# of Trials
50	82	61
25	12	8
20	4	0
15	12	0
10	43	17
5	28	12
Total	181	98

Table 4. Number of testing trials for tactogram measurements

	Hugh	Buffett
Frequency	# of Trials	# of Trials
150	72	104
125	82	78
100	108	112
75	70	54
50	118	109
25	58	62
20	55	45
15	59	47
10	73	127
5	0	33
Total	695	771

Table 5. False alarm rates for testing trials for Buffett and Hugh.

Buffett

Date	Frequency	FA
1/16/2009	150	0.00%
1/15/2009	150	0.00%
1/14/2009	150	0.00%
1/13/2009	125	0.00%
1/9/2009	125	7.00%
1/8/2009	125	0.00%
11/21/2008	100	5.56%
11/20/2008	100	23.80%
11/25/2008	75	0.00%
11/24/2008	75	0.00%
12/2/2008	50	0.00%
12/1/2008	50	8.33%
11/28/2008	50	7.69%
11/26/2008	50	0.00%
11/19/2008	50	6.67%
12/4/2008	25	5.88%
12/3/2008	25	15.38%
12/12/2008	20	0.00%
12/9/2008	20	10.00%
12/17/2008	15	9.00%
12/16/2008	15	16.67%
12/31/2008	10	7.69%
12/30/2008	10	15.38%
12/18/2008	10	16.67%
12/5/2008	10	7.14%
1/7/2009	5	12.50%
1/2/2009	5	13%

Hugh

Date	Frequency	FA
1/15/2009	150	17.00%
1/14/2009	150	0.00%
1/13/2009	125	0.00%
1/9/2009	125	7.00%
1/8/2009	125	0.00%
11/21/2008	100	11%
11/20/2008	100	0.00%
11/25/2008	75	0.00%
11/24/2008	75	5.88%
1/16/2009	50	0.00%
12/2/2008	50	0.00%
12/1/2008	50	0.00%
11/28/2008	50	7.69%
11/26/2008	50	6.67%
11/19/2008	50	0.00%
12/4/2008	25	0.00%
12/3/2008	25	0.00%
12/12/2008	20	7.14%
12/9/2008	20	0.00%
12/17/2008	15	0%
12/16/2008	15	0.00%
12/31/2008	10	0.00%
12/30/2008	10	0.00%
12/18/2008	10	0.00%

Figure 4 – Experimental setup showing the shaker with a black PVC stationing apparatus. The task of the manatee is to station on the black PVC (see photo on right) and then upon detecting the movement of the dipole to touch the yellow response paddle shown on the left.

Figure 5. Dipole shaker with sphere mounted in the end. The ball contains a three-dimensional accelerometer that is used to measure the acceleration of the ball for each test frequency. The cage is used for mounting the shaker to the side of the tank and also protecting the shaker from the manatee.

Table 6. Thresholds for the facial tactogram. Values were calculated for the location of the manatee when at station.

Buffett

Frequency (Hz)	Displacement (um)	Velocity (mm/s)	Acceleration (mm/s^2)
5	4.21623713	0.132456996	4.161259253
10	1.078611477	0.067771158	4.258187433
15	0.309515583	0.029171156	2.749316724
20	0.174102515	0.021878367	2.749316724
25	0.150309012	0.023610484	3.708726213
50	0.03845254	0.012080222	3.795113544
75	0.0079021	0.003723777	1.754788477
100	0.001874412	0.001177728	0.739988165
125	0.003083508	0.002421781	1.902062459
150	0.00132033	0.001244382	1.172802205

Hugh

Frequency (Hz)	Displacement (um)	Velocity (mm/s)	Acceleration (mm/s^2)
10	1.523579208	0.095729305	6.014849621
15	0.309515583	0.029171156	2.749316724
20	0.146489011	0.018408352	2.313261734
25	0.150309012	0.023610484	3.708726213
50	0.034270862	0.010766509	3.382398507
75	0.003960432	0.001866309	0.879477582
100	0.00314677	0.001977174	1.242295105
125	0.002594448	0.002037675	1.600386112
150	0.000934722	0.000880955	0.830280377

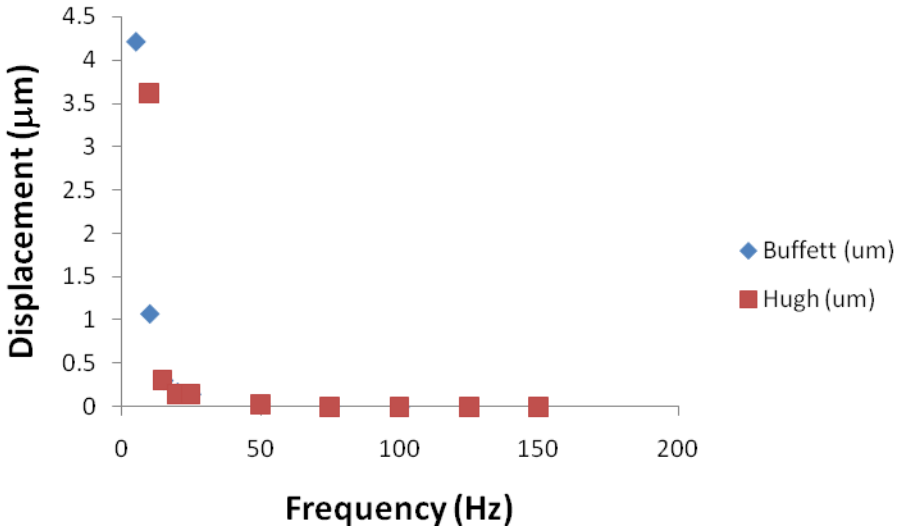

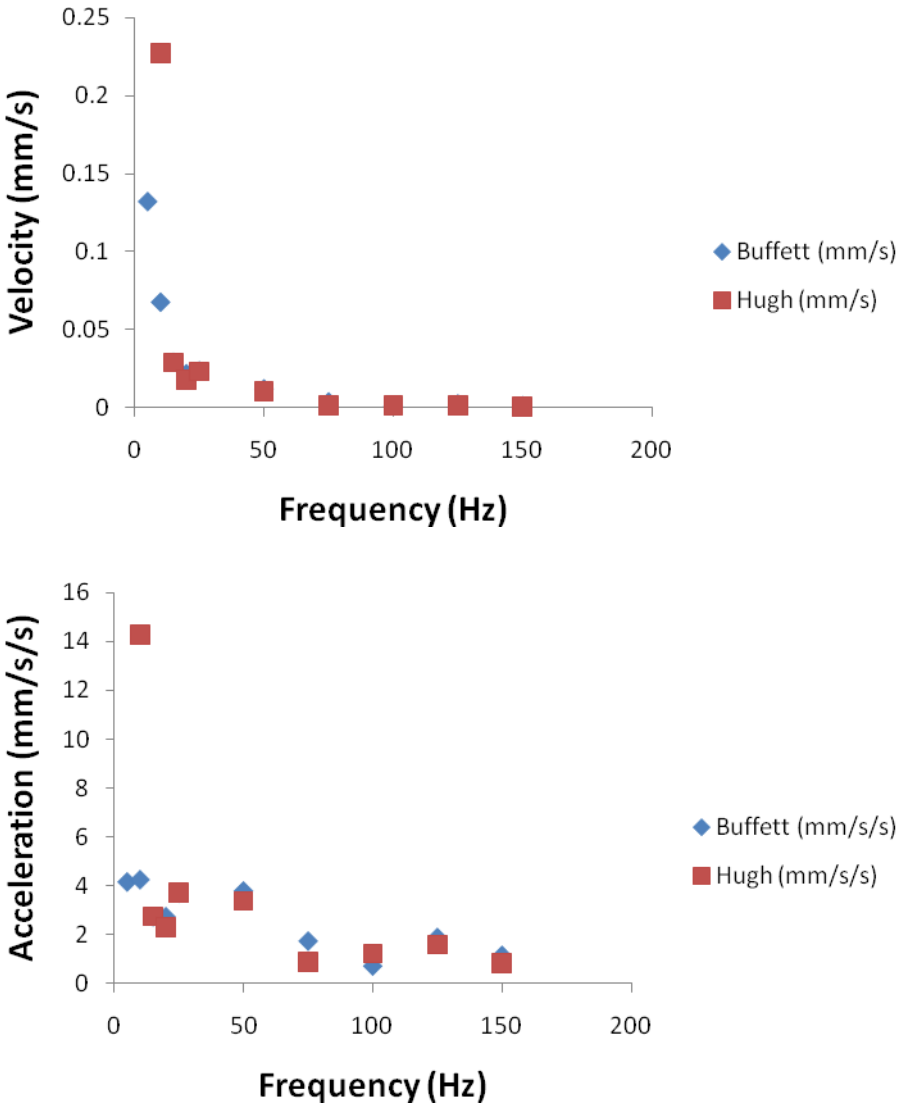

Figure 6. Manatee tactograms showing sensitivity in terms of threshold displacement, velocity, and acceleration. Calibrations were performed with an accelerometer. The velocity was calculated by dividing the acceleration by 2*PI*frequency, and the displacement was calculated by dividing the velocity by 2*PI*frequency.

Experiment IV: Boat Noise Recordings

Methods

Boat noise recordings were made with boat approaches at four different speeds using three different boats (the boat names and their engine sizes are: Nai'a - 225 HP Yamaha 4-stroke, Fregatta - 150 HP Yamaha 4-stroke, Mini Mako - 115 HP Yamaha 4-stroke). The two lowest speeds correspond to Idle speed and Slow speed as dictated by boating regulations. Recordings were made in Sarasota Bay just outside a manatee idle speed zone where the water depth was 4 m. Two Reson TC4013 hydrophones (sensitivity -212 dBV/uPa, 2 Hz-180 kHz) were used with VP1000 amplifiers (32 dB gain, 100 Hz high pass filter) to record boat approaches at 15 cm depth and 1 m depth. The signals from each hydrophone were recorded on a calibrated m-audio recorder sampling at 24-bit resolution and 96 kHz. Two vessels were used to make the recordings. The recording vessel was anchored with all systems off. The approach vessel used a GPS system to measure boat speed. The approach vessel passed approximately 1-2 m from the recording vessel. If other vessels were in the area, their distance from the recording boat was determined with laser range finders.

Recordings were cropped so that the end of the recording corresponded to 5 seconds after the boat pass. Acoustic analyses were done by analyzing 1 second segments of each recording with MATLAB (Mathworks, Inc.) and are presented as times relative to the boat passing. Frequency spectra were calculated with a 96,000 point FFT.

Background noise was taken from a 13 second recording made at the same time and location as the boat noise recordings. This recording was analyzed by frequency averaging 1s segments.

Results

Spectrograms of the approach and passing sequences are shown in Figures 7-57. The fastest approach was loudest at the time of passing. The recordings at 15 cm depth were lower in amplitude than those recorded at 1 m depth.

The audiograms and audiograms adjusted for critical ratios were overlaid on the power spectra and showed that all of the boat approaches would be easily detectable by manatees (e.g. Figs. 8-10, 12-14, 16-19, and 22-24). It appears that the approaches of the Idle and Slow speed boats would be detectable before those from fast moving boats, but because the starting distance was kept constant, the recording times for the fast moving boats were shorter.

Faster boats produced louder sounds than slower boats (Figures 7-57). In one case, the sound from an idle speed boat was masked by another boat passing at a distance of 225 m (Figure 53). The background noise levels were relatively low at the recording site in Sarasota Bay, especially in comparison to the sound levels from boats (Figure 58). Sound measurements at the time of closest approach showed that the peak sound levels increased with increasing speed (Figure 59). The rms sound levels were approximately similar for boats traveling at speeds higher than 20 mph. Note that the rms measurement

is essentially a time-averaged measurement, thus the similarity in levels is due to the faster moving boats not spending as much time near the measurement hydrophone.

The depth sounder on the moving boat was on for these recordings. The pings from the depth sounder were readily apparent for the slower moving boats prior to passing, and are apparent in the power spectra as increased energy between 30-48 kHz (Fig. 23 and 24). For the fastest moving vessels, these signals were not as easily detectable on the spectrograms.

Conclusions

Manatee tonal hearing thresholds are typically near or below natural ambient background noise spectrum level (i.e. in 1 Hz wide frequency bins) over a large frequency range (8-40 kHz) (Figure 58). Using the critical ratio as an estimate of the auditory bandwidth of the manatee assuming an equal-energy conversion, allows the audiogram thresholds to be adjusted down to estimate broad-band detection thresholds. These adjusted broad-band thresholds suggest that manatee hearing is well below natural background levels between 2-40 kHz. Since boat noise spectra are similar to ambient noise spectra, detecting the presence of a boat noise is essentially equivalent to detecting an increase in the background noise levels. The just detectable increment in sound level for a broad-band noise in humans is <2 dB for sensation levels 10 dB and higher (Miller, 1947). To put this into perspective, *assuming* that manatees have similar just detectable increments in noise levels, one can judge from a spectrogram whether manatees can detect a boat. For frequencies above 2 kHz, if a boat signal can be seen on a spectrogram, it is likely that a manatee can hear it.

Recordings were made at two depths, 15 cm and 1 m, to measure how the received sound field may vary as a function of the depth of the head. The 15 cm depth is the approximate position of the ears as the manatee takes a breath. All of the recordings show that the sound level is lower for the 15 cm position compared to the 1 m position. Even with this decreased sound levels, the recordings show that manatees should be able to detect slow and idle speed boat at least 40 sec prior to the boat passing even if it is near the surface.

The boat noise measurements show that even though slower moving boats produce less noise than fast moving boats, they are all detectable minimally 15 seconds prior to the boat passing if no other boats are present. The signals from the slow and idle speed boats are detectable over a longer period in our tests (at least 40 s prior to passing). Since our measurements were made starting approximately 100 m from the recording vessel, we did not measure the high speed boats at distances that would take 40 sec to approach the recording vessel. For the 35.2 mph vessel, 40 sec would correspond to a distance of 629 m. However, it is possible that faster moving boats could mask boats that were closer, but moving at a slower speed (Figure 53 and Figure 59.

The spectrograms also show that there are two additional cues that manatees could potentially utilize to detect the presence of an approaching boat. The first is obvious, as a boat approaches it gets louder. The second cue is more subtle, and that is in shallow water there are frequency patterns of constructive and destructive interference that change as a function of boat distance. This is most apparent in Figure 7, which shows that as the boat approaches bands of higher intensity decrease in frequency. After the boat passes, these frequencies increase in pitch. The rate of pitch change is a function of boat speed. The pitch changes faster the faster the boat is traveling.

All of these data taken together suggest that manatees should be able to hear single boats moving at all speeds. Previous research in our laboratory (Colbert et al., in press; Colbert et al., 2005) indicates that manatees are also good at localizing broadband sounds, such as those produced by boat engines. Studies of the behavioral responses of manatees show that they do respond to boat approaches, where they often head for deep water, sometimes crossing the path of the oncoming boat to reach deep water (e.g. Miksis-Olds et al., 2007). It is important to note that the recordings of boat noise were made in one location at one time. It is likely that the situation could be different in other circumstances, such as boats traveling in channels with measurements made in adjacent shallow water areas. Furthermore, in more complex situations with multiple boats, it is possible that high speed boats at a distance could mask the approach of slower speed vessels. Still, the confirmed reports of manatee collisions with small boats that resulted in death suggest that manatees that are killed by boat strike are hit by faster moving vessels (Calleson and Frolich, 2007). The area over which masking by faster moving boats is an issue could be reduced by decreasing the maximum boat speed. For example, assuming a conservative spherical spreading loss sound propagation model, a 6 dB decrease in sound level would lead to a 4 times smaller area of equivalent masking (with a cylindrical spreading model the area of potential masking would be 16 times smaller). Based on peak sound levels at passing this reduction could be achieved by changing maximum speed from 35 mph to 20 mph (Figure 60).

Nai'a - 225 HP Yamaha 4-stroke
35.2 mph

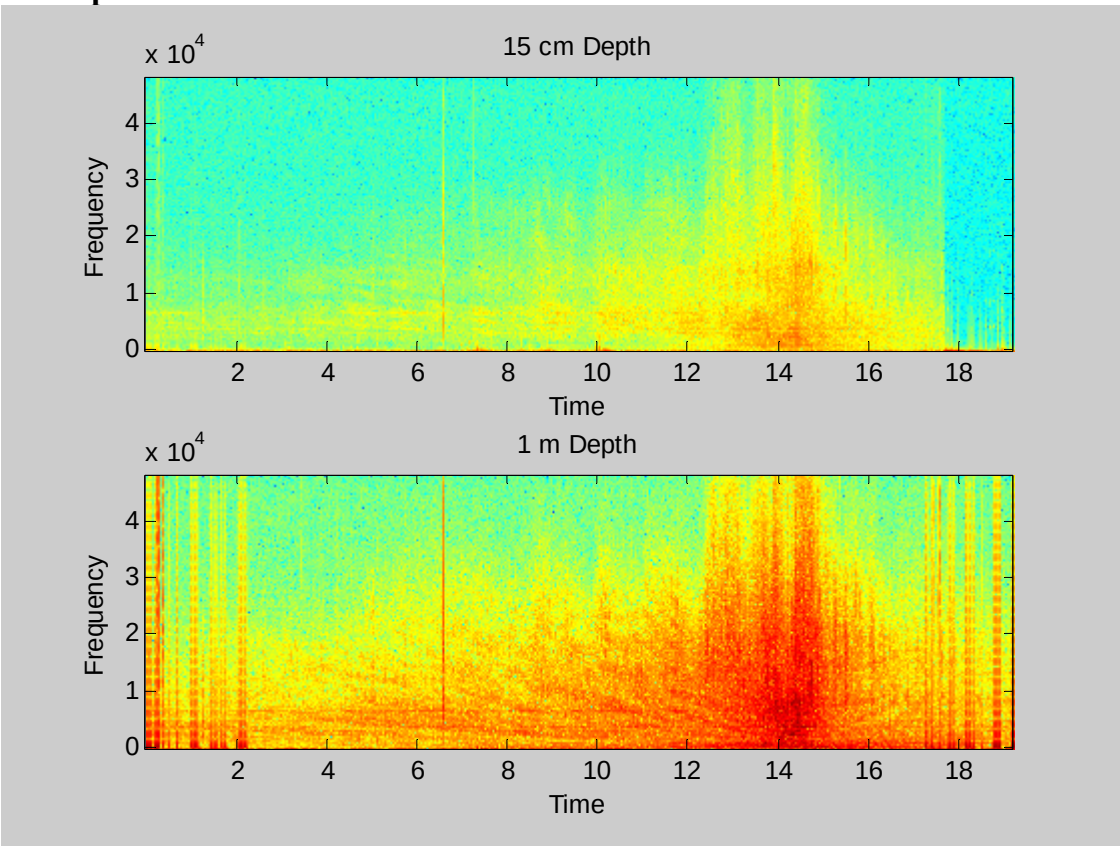

Figure 7. Spectrogram of approach sequence with vessel traveling 35.2 mph. Top plot is with hydrophone at 15 cm depth. Bottom plot is from a hydrophone at 1 m depth.

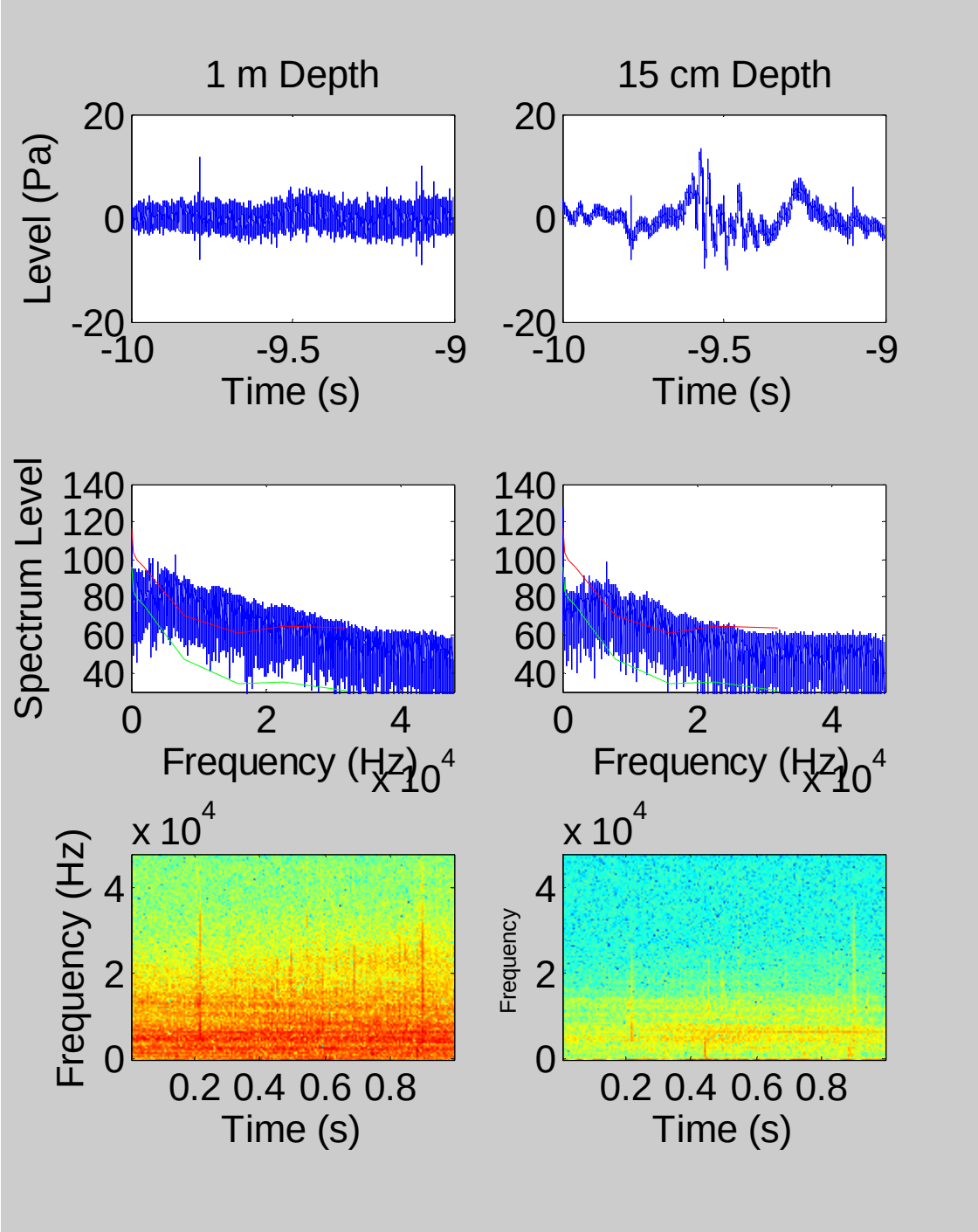

Figure 8. Approach at 35.2 mph. Top row: Time domain signal 10 seconds prior to boat passing. Middle row: Spectrum level power spectra (dB re 1uPa^2/Hz). Note frequency axis is in Hz x10^4. Red line shows audiogram of Buffett. Green line shows audiogram lowered as a function of the frequency-specific critical ratio. Bottom row: Spectrogram of plots from top row.

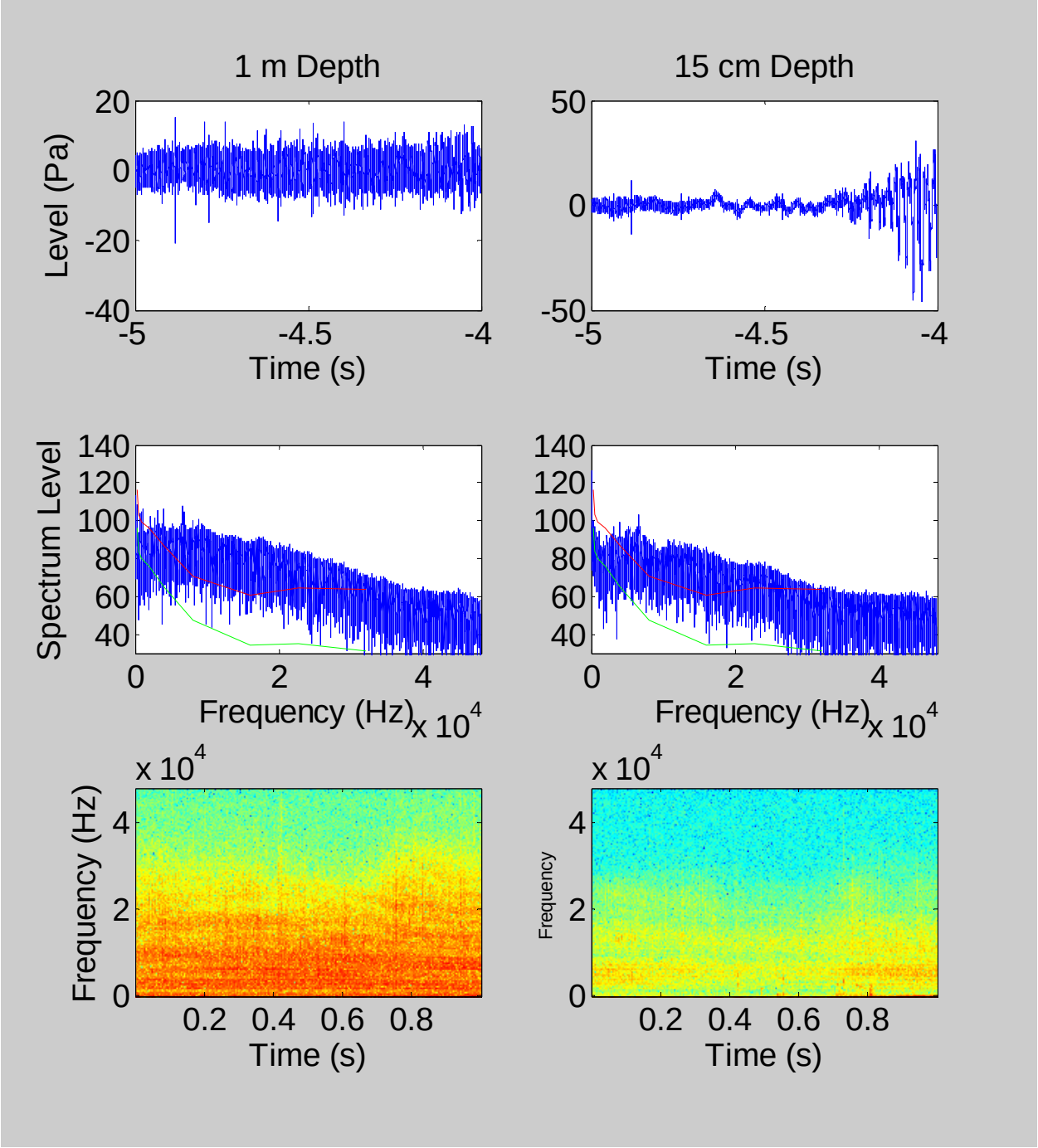

Figure 9. Approach at 35.2 mph. Top row: Time domain signal 5 seconds prior to boat passing. Middle row: Spectrum level power spectra (dB re 1uPa^2/Hz). Note frequency axis is in Hz x10^4. Red line shows audiogram of Buffett. Green line shows audiogram lowered as a function of the frequency-specific critical ratio. Bottom row: Spectrogram of plots from top row.

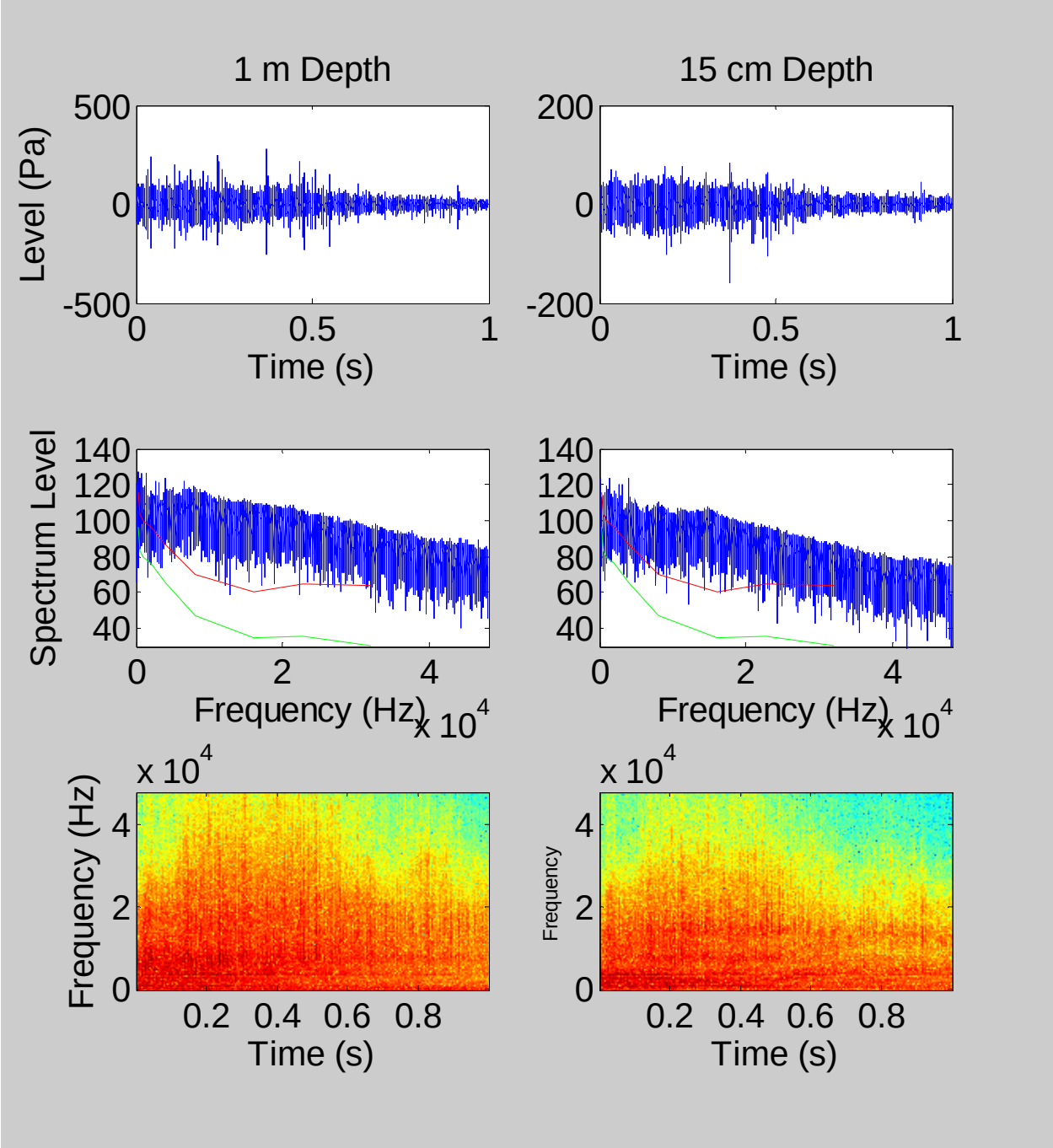

Figure 10. Approach at 35.2 mph. Top row: Time domain signal at time of boat passing. Middle row: Spectrum level power spectra (dB re 1uPa^2/Hz). Note frequency axis is in Hz x10^4. Red line shows audiogram of Buffett. Green line shows audiogram lowered as a function of the frequency-specific critical ratio. Bottom row: Spectrogram of plots from top row.

Nai'a - 225 HP Yamaha 4-stroke
17.8 mph

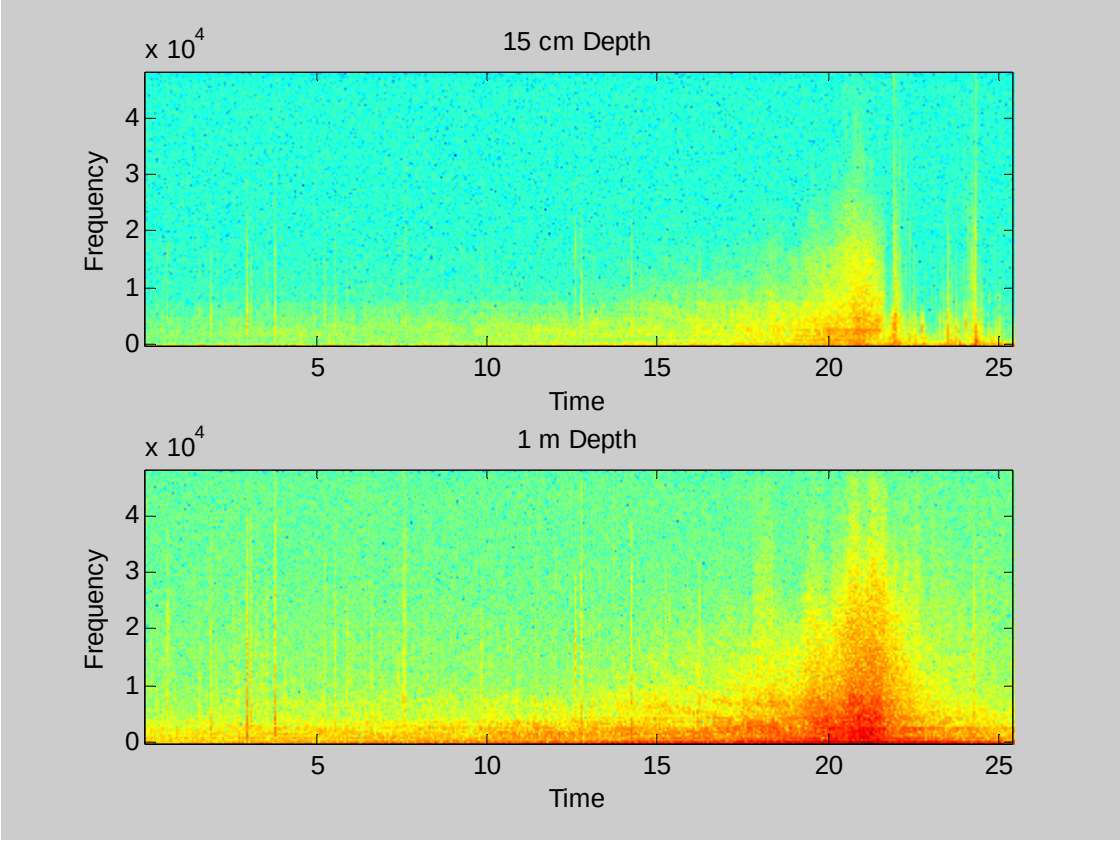

Figure 11. Spectrogram of approach sequence with vessel traveling 17.8 mph. Top plot is with hydrophone at 15 cm depth. Bottom plot is from a hydrophone at 1 m depth.

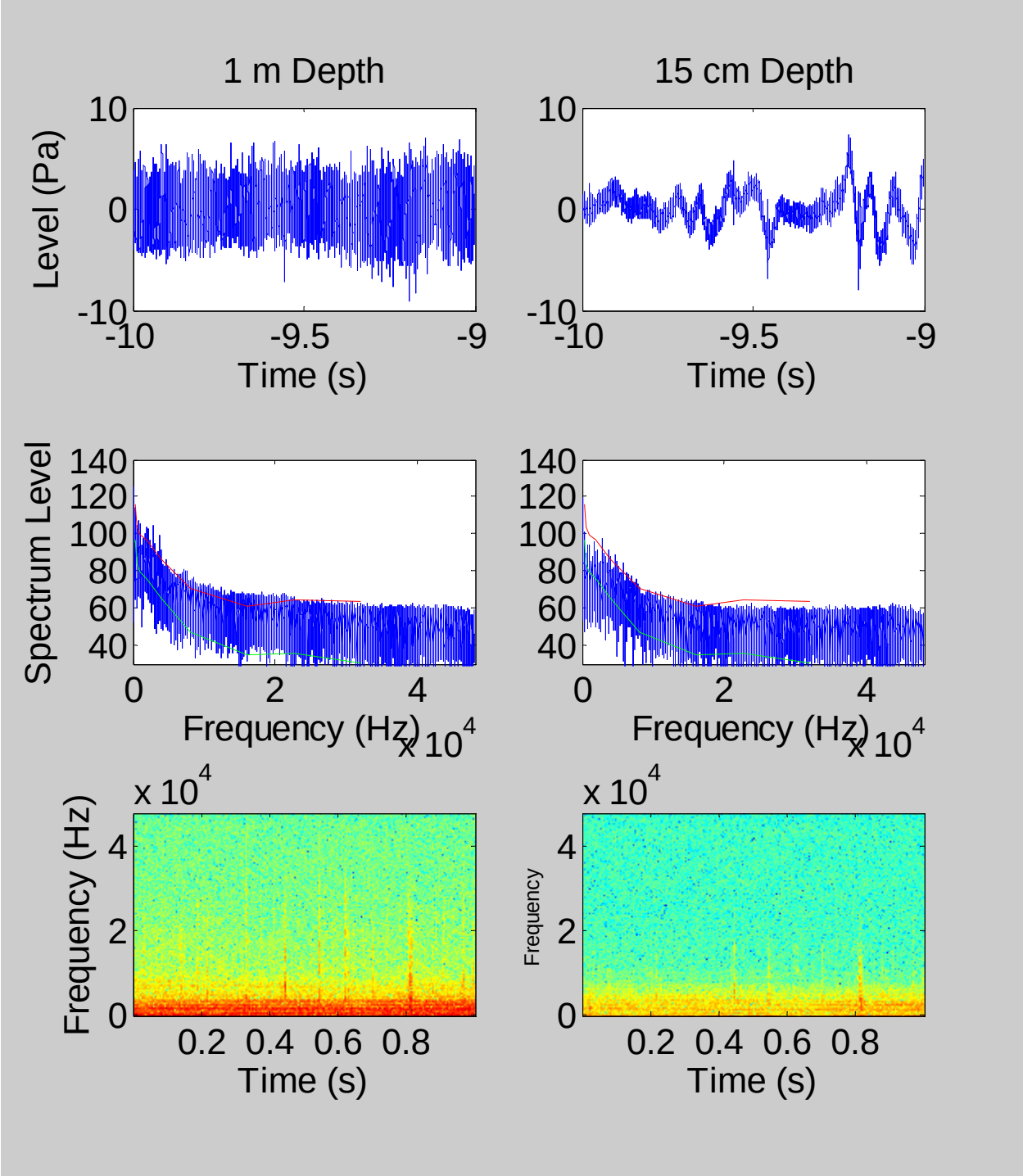

Figure 12. Approach at 17.8 mph. Top row: Time domain signal 10 seconds prior to boat passing. Middle row: Spectrum level power spectra (dB re 1uPa^2/Hz). Note frequency axis is in Hz x10^4. Red line shows audiogram of Buffett. Green line shows audiogram lowered as a function of the frequency-specific critical ratio. Bottom row: Spectrogram of plots from top row.

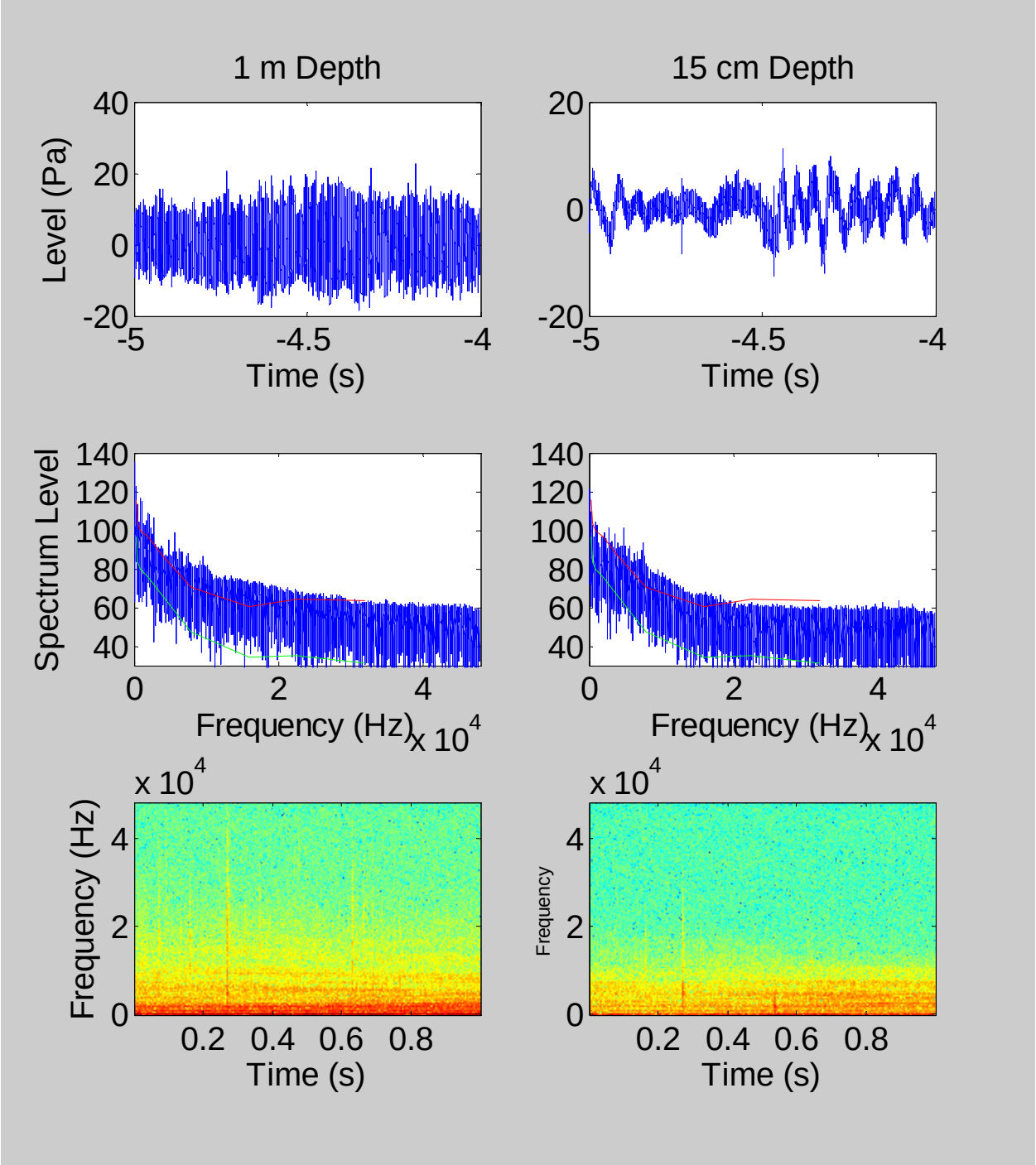

Figure 13. Approach at 17.8 mph. Top row: Time domain signal 5 seconds prior to boat passing. Middle row: Spectrum level power spectra (dB re 1uPa^2/Hz). Note frequency axis is in Hz x10^4. Red line shows audiogram of Buffett. Green line shows audiogram lowered as a function of the frequency-specific critical ratio. Bottom row: Spectrogram of plots from top row.

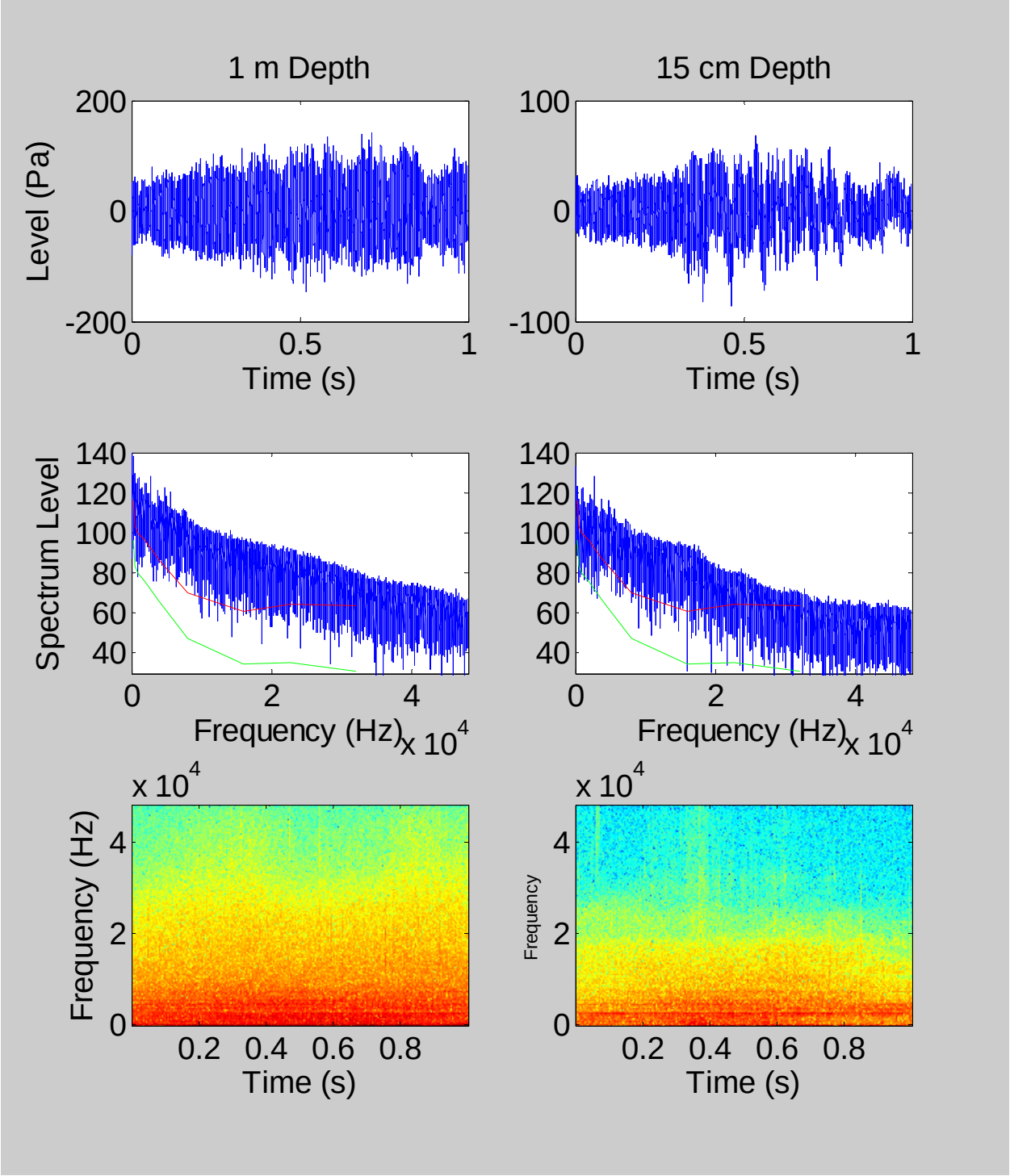

Figure 14. Approach at 17.8mph. Top row: Time domain signal at time of boat passing. Middle row: Spectrum level power spectra (dB re 1uPa^2/Hz). Note frequency axis is in Hz x10^4. Red line shows audiogram of Buffett. Green line shows audiogram lowered as a function of the frequency-specific critical ratio. Bottom row: Spectrogram of plots from top row.

Nai'a - 225 HP Yamaha 4-stroke
7.0 mph (Slow)

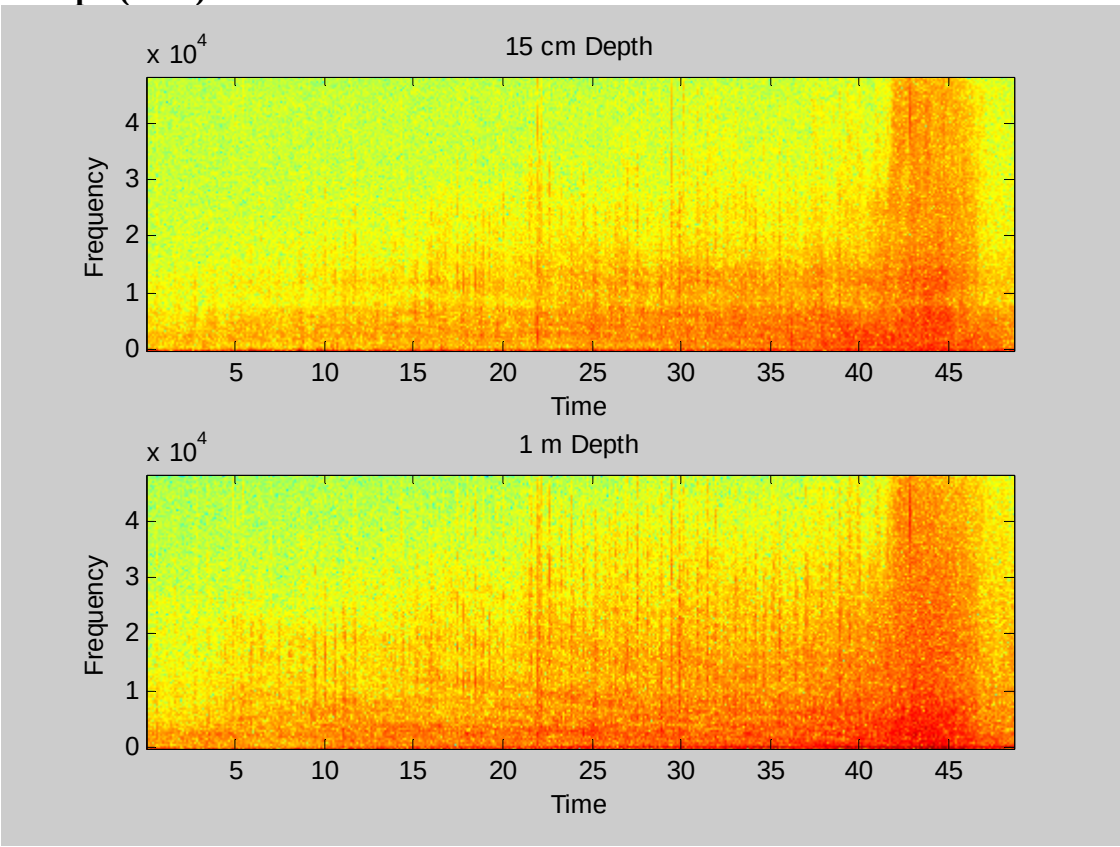

Figure 15. Spectrogram of approach sequence with vessel traveling 7.0 mph. Top plot is with hydrophone at 15 cm depth. Bottom plot is from a hydrophone at 1 m depth.

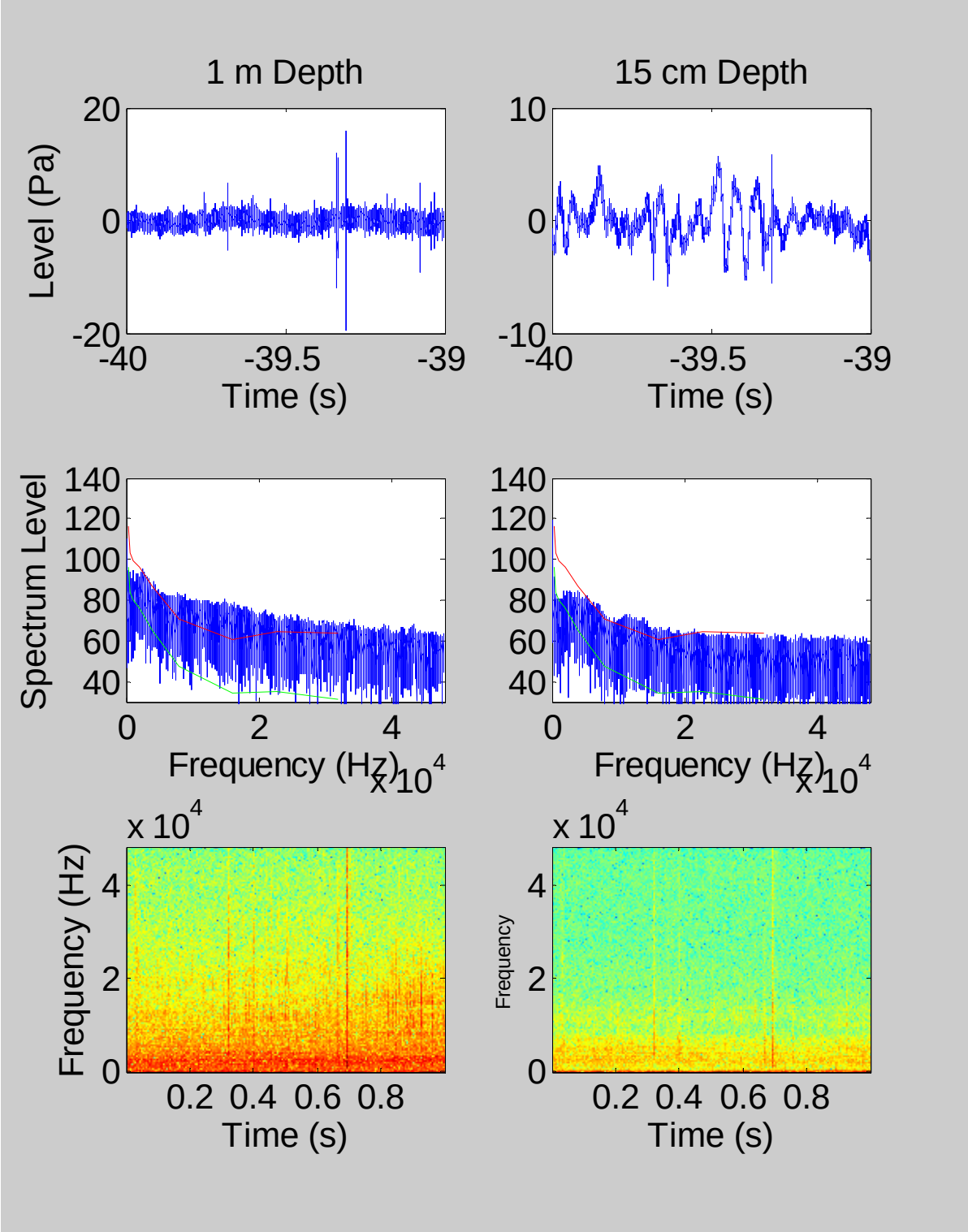

Figure 16. Approach at 7.0 mph. Top row: Time domain signal 40 seconds prior to boat passing. Middle row: Spectrum level power spectra (dB re 1uPa^2/Hz). Note frequency axis is in Hz x10^4. Red line shows audiogram of Buffett. Green line shows audiogram lowered as a function of the frequency-specific critical ratio. Bottom row: Spectrogram of plots from top row.

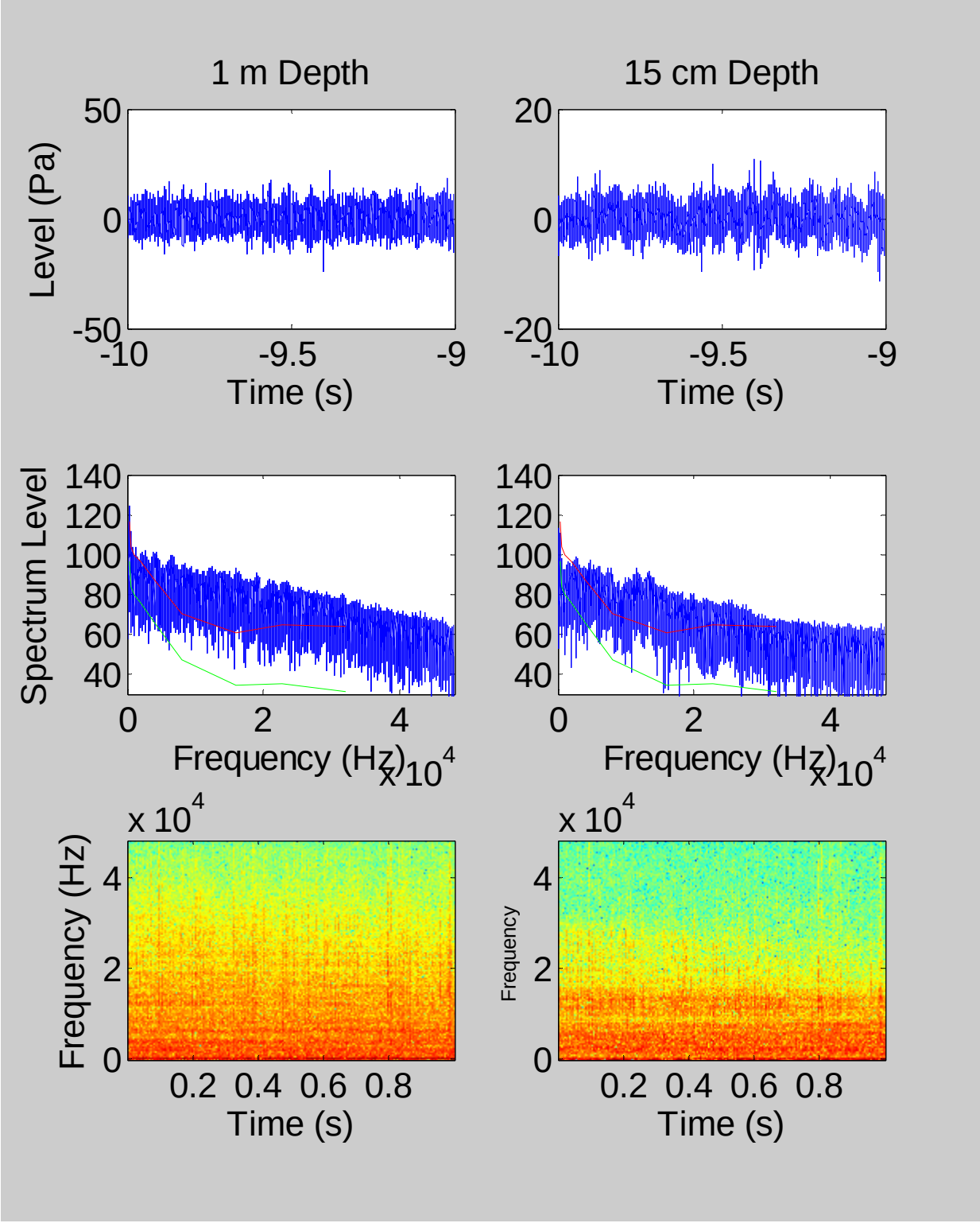

Figure 17. Approach at 7.0 mph. Top row: Time domain signal 10 seconds prior to boat passing. Middle row: Spectrum level power spectra (dB re 1uPa^2/Hz). Note frequency axis is in Hz x10^4. Red line shows audiogram of Buffett. Green line shows audiogram lowered as a function of the frequency-specific critical ratio. Bottom row: Spectrogram of plots from top row.

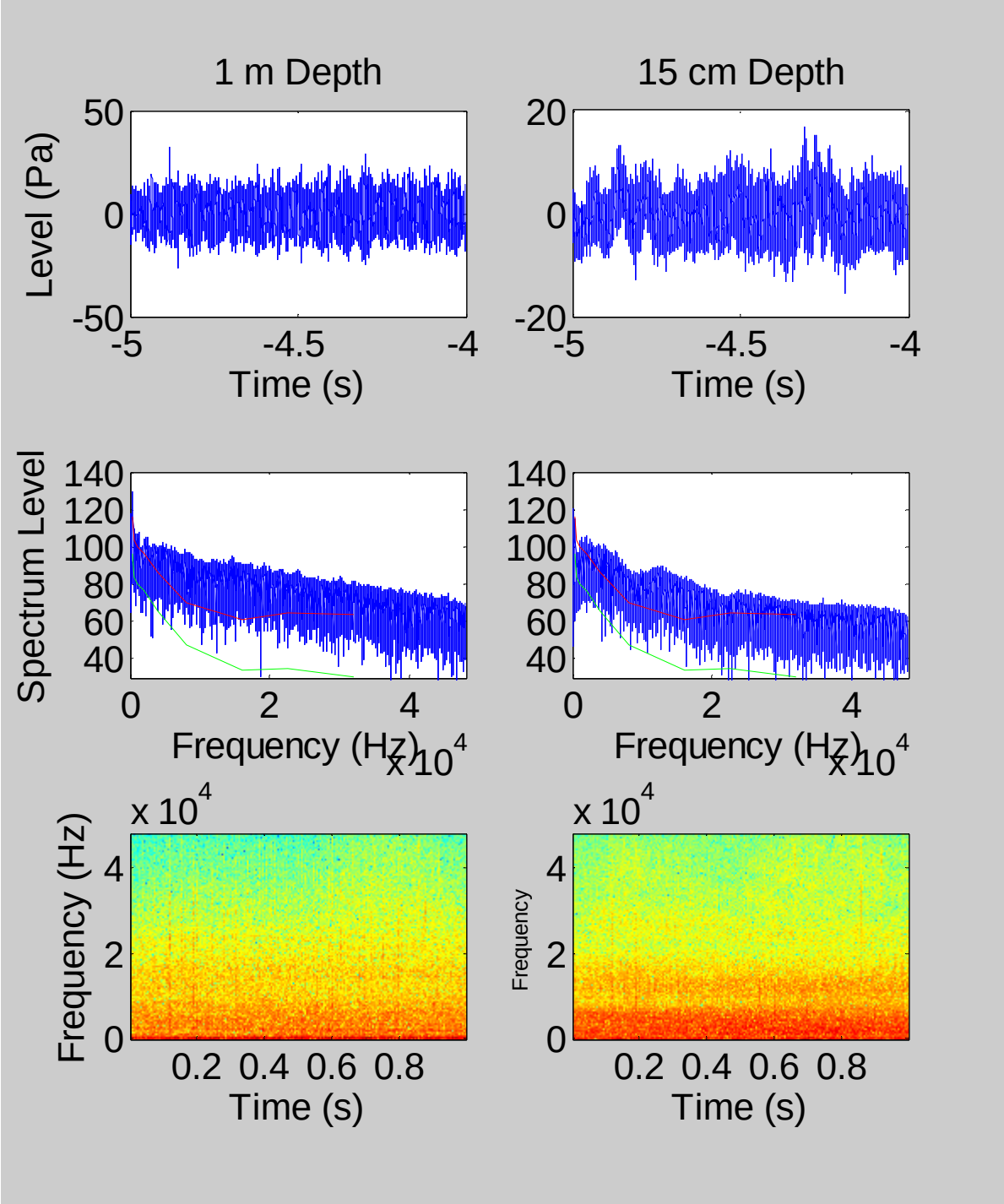

Figure 18. Approach at 7.0 mph. Top row: Time domain signal 5 seconds prior to boat passing. Middle row: Spectrum level power spectra (dB re 1uPa^2/Hz). Note frequency axis is in Hz x10^4. Red line shows audiogram of Buffett. Green line shows audiogram lowered as a function of the frequency-specific critical ratio. Bottom row: Spectrogram of plots from top row.

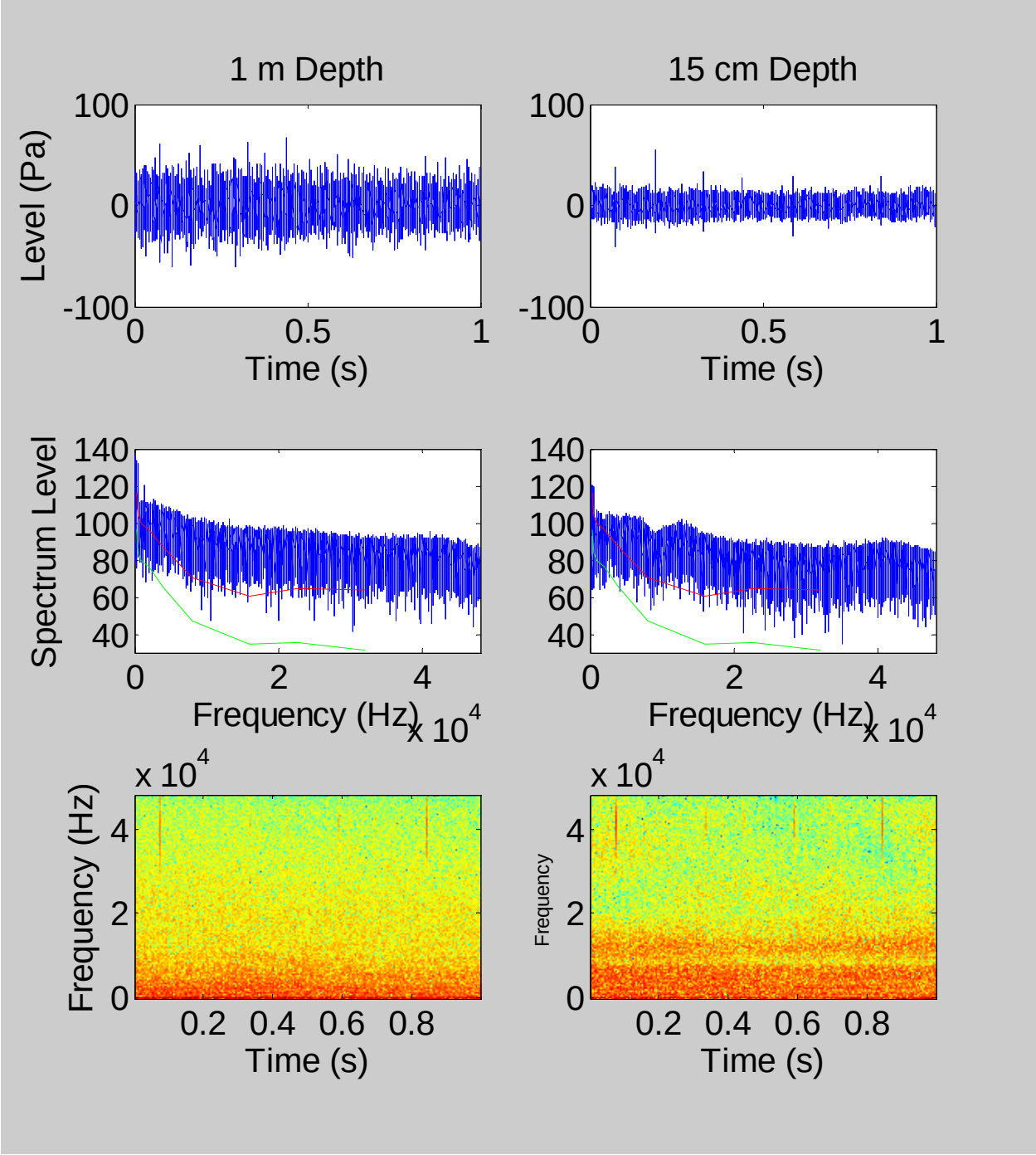

Figure 19. Approach at 7.0 mph. Top row: Time domain signal at time of boat passing. Middle row: Spectrum level power spectra (dB re 1uPa^2/Hz). Note frequency axis is in Hz x10^4. Red line shows audiogram of Buffett. Green line shows audiogram lowered as a function of the frequency-specific critical ratio. Bottom row: Spectrogram of plots from top row.

Nai'a - 225 HP Yamaha 4-stroke
3.2 mph (Idle)

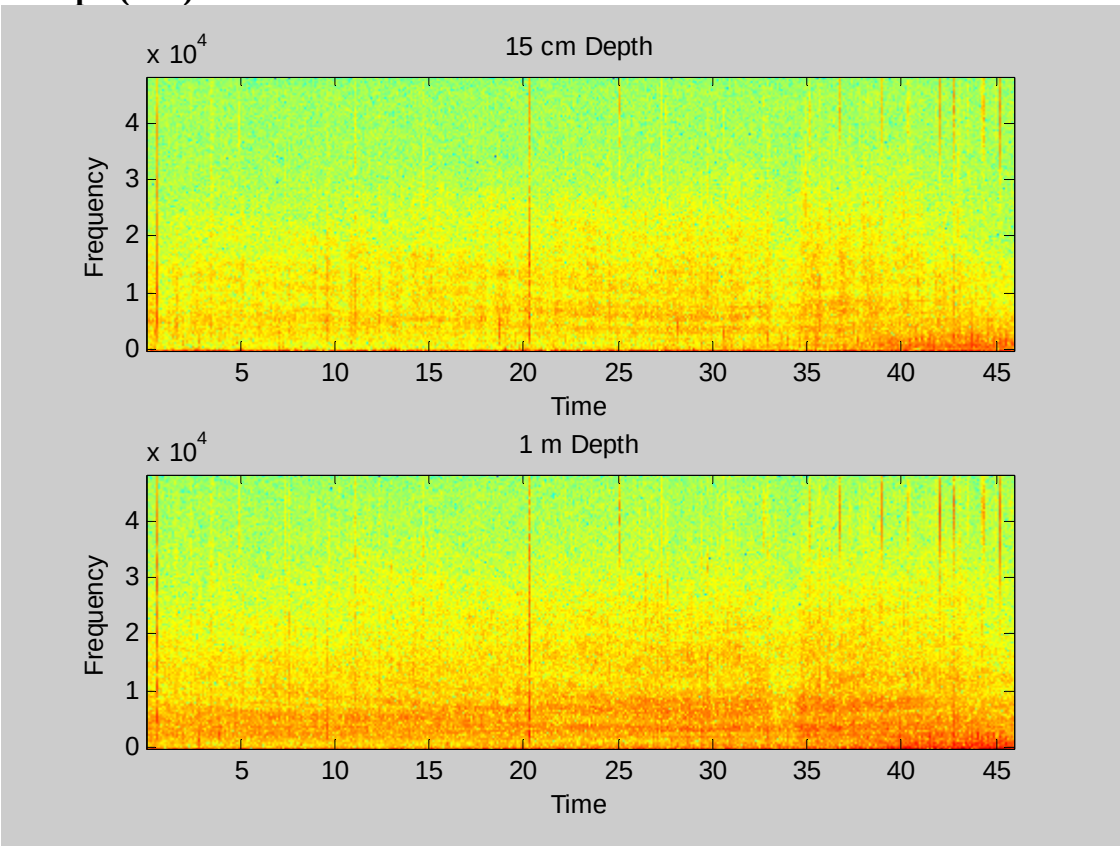

Figure 20. Spectrogram of approach sequence with vessel traveling 3.2 mph. Top plot is with hydrophone at 15 cm depth. Bottom plot is from a hydrophone at 1 m depth.

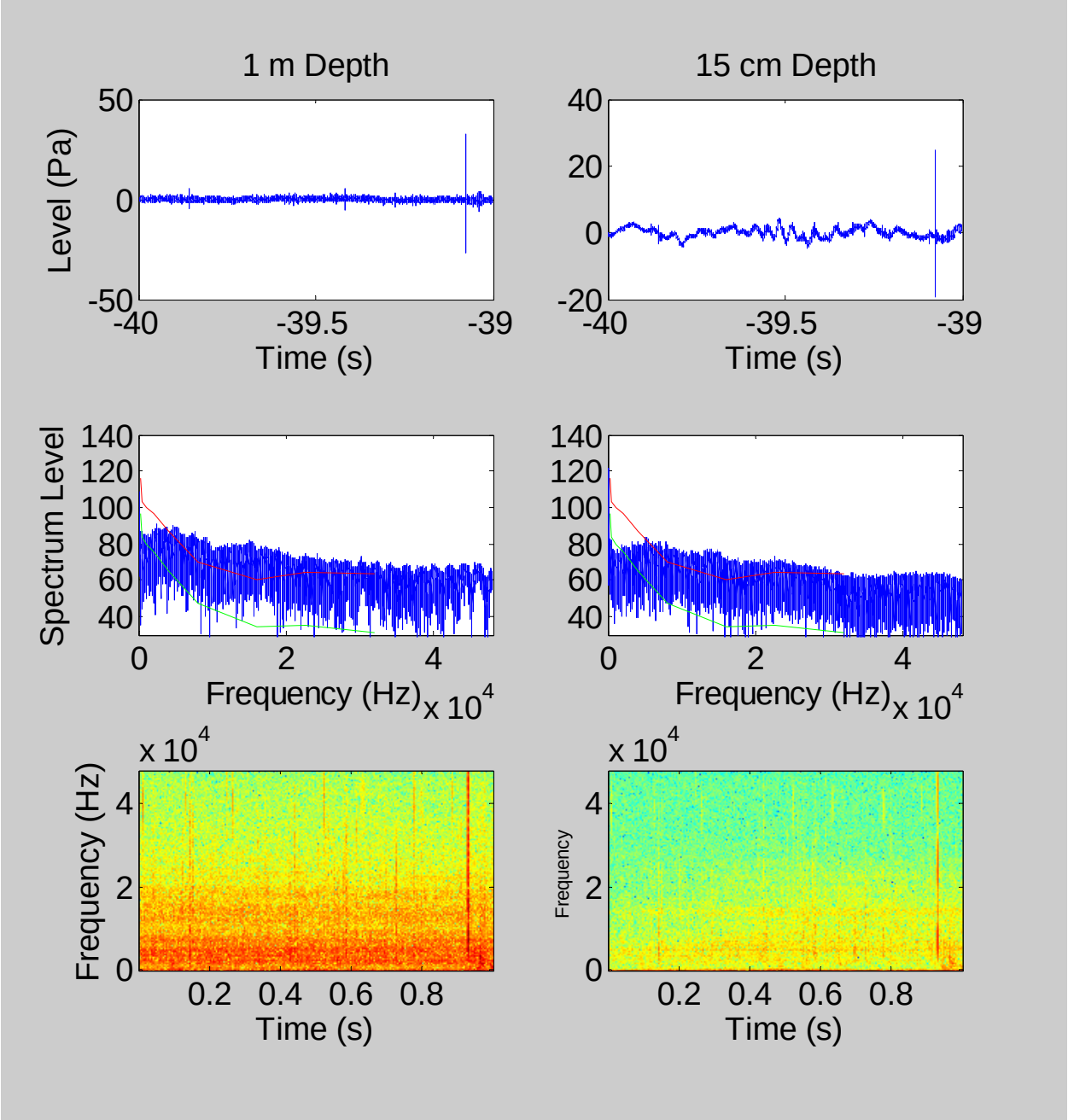

Figure 21. Approach at 3.2 mph. Top row: Time domain signal 40 seconds prior to boat passing. Middle row: Spectrum level power spectra (dB re 1uPa^2/Hz). Note frequency axis is in Hz x10^4. Red line shows audiogram of Buffett. Green line shows audiogram lowered as a function of the frequency-specific critical ratio. Bottom row: Spectrogram of plots from top row.

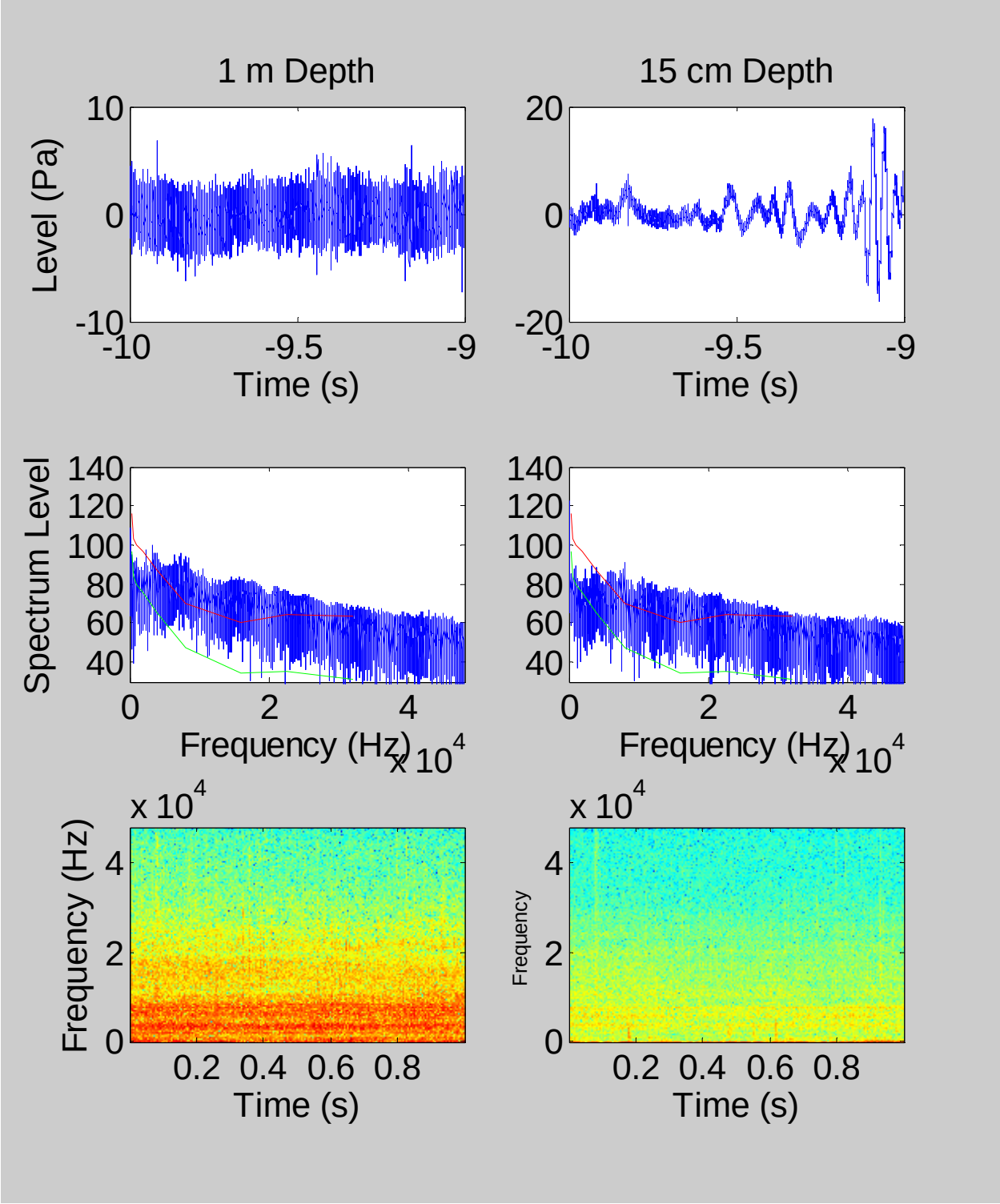

Figure 22. Approach at 3.2 mph. Top row: Time domain signal 10 seconds prior to boat passing. Middle row: Spectrum level power spectra (dB re 1uPa^2/Hz). Note frequency axis is in Hz x10^4. Red line shows audiogram of Buffett. Green line shows audiogram lowered as a function of the frequency-specific critical ratio. Bottom row: Spectrogram of plots from top row.

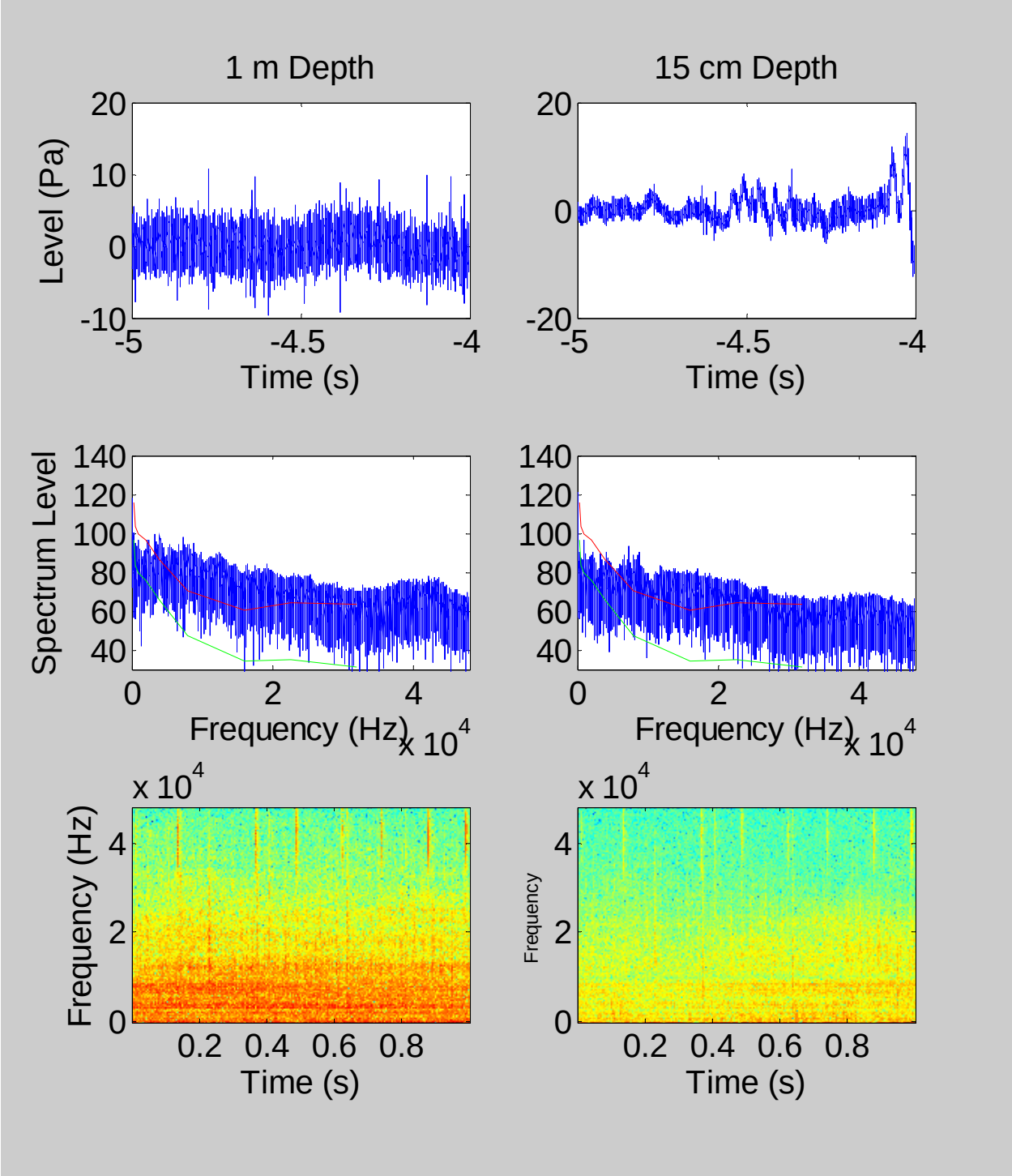

Figure 23. Approach at 3.2 mph. Top row: Time domain signal 5 seconds prior to boat passing. Middle row: Spectrum level power spectra (dB re 1uPa^2/Hz). Note frequency axis is in Hz x10^4. Red line shows audiogram of Buffett. Green line shows audiogram lowered as a function of the frequency-specific critical ratio. Bottom row: Spectrogram of plots from top row.

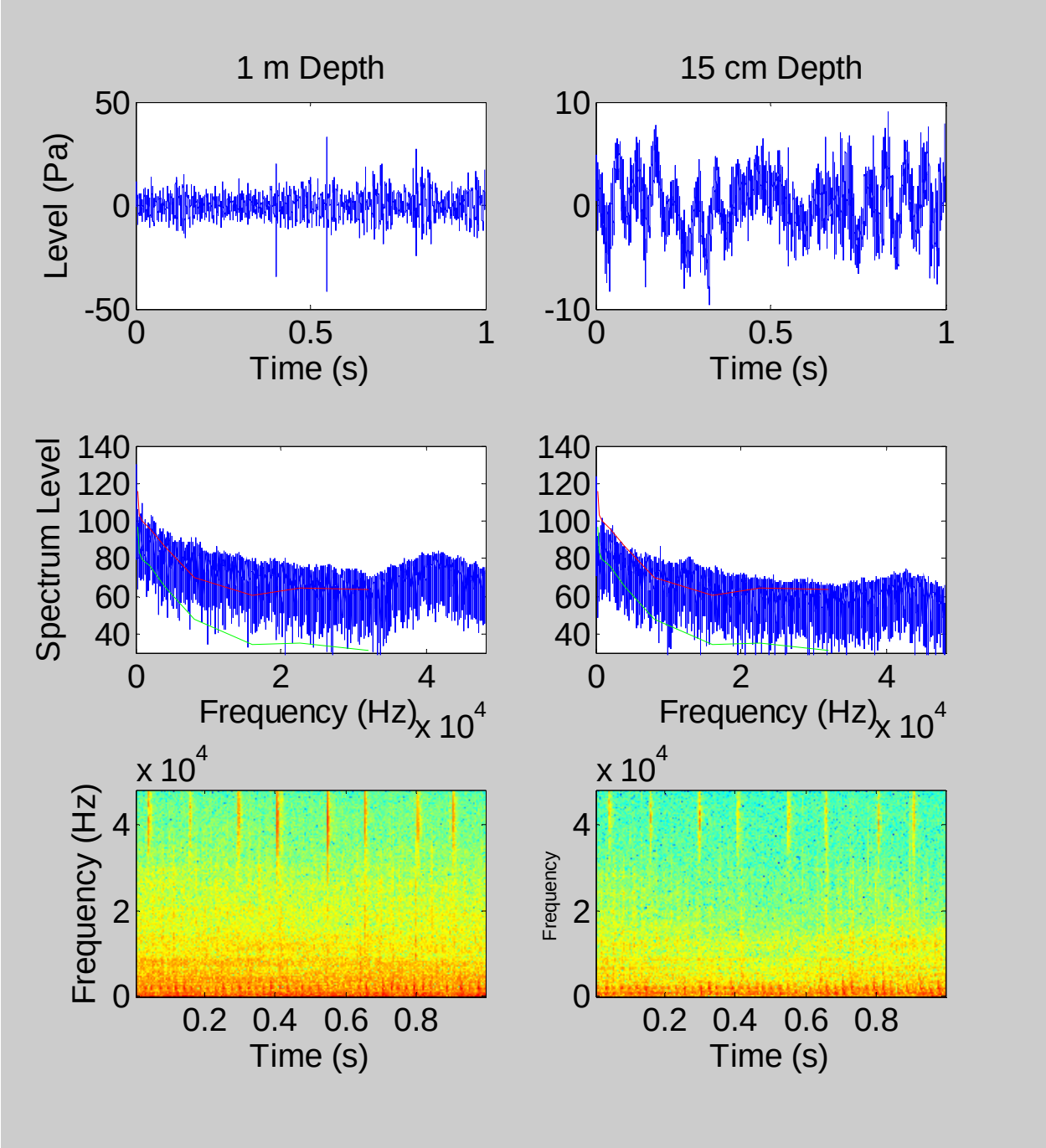

Figure 24. Approach at 3.2 mph. Top row: Time domain signal at time of boat passing. Middle row: Spectrum level power spectra (dB re 1uPa^2/Hz). Note frequency axis is in Hz x10^4. Red line shows audiogram of Buffett. Green line shows audiogram lowered as a function of the frequency-specific critical ratio. Bottom row: Spectrogram of plots from top row.

Fregatta - 150 HP Yamaha 4-stroke
34 miles per hour

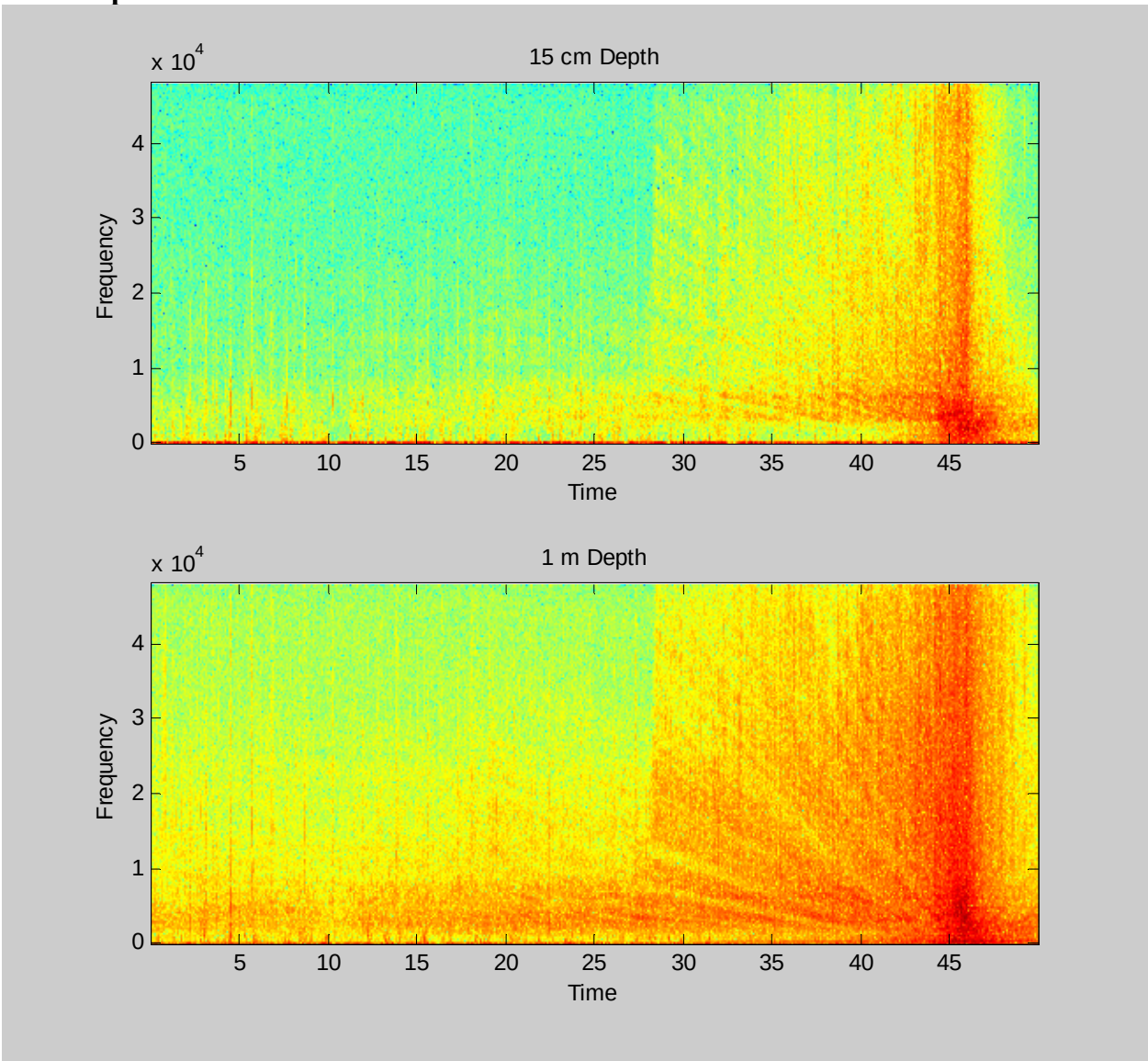

Figure 25. Spectrogram of approach sequence with vessel traveling 34 mph. Top plot is with hydrophone at 15 cm depth. Bottom plot is from a hydrophone at 1 m depth. Note that boat did not reach speed until time of 28 seconds in this plot.

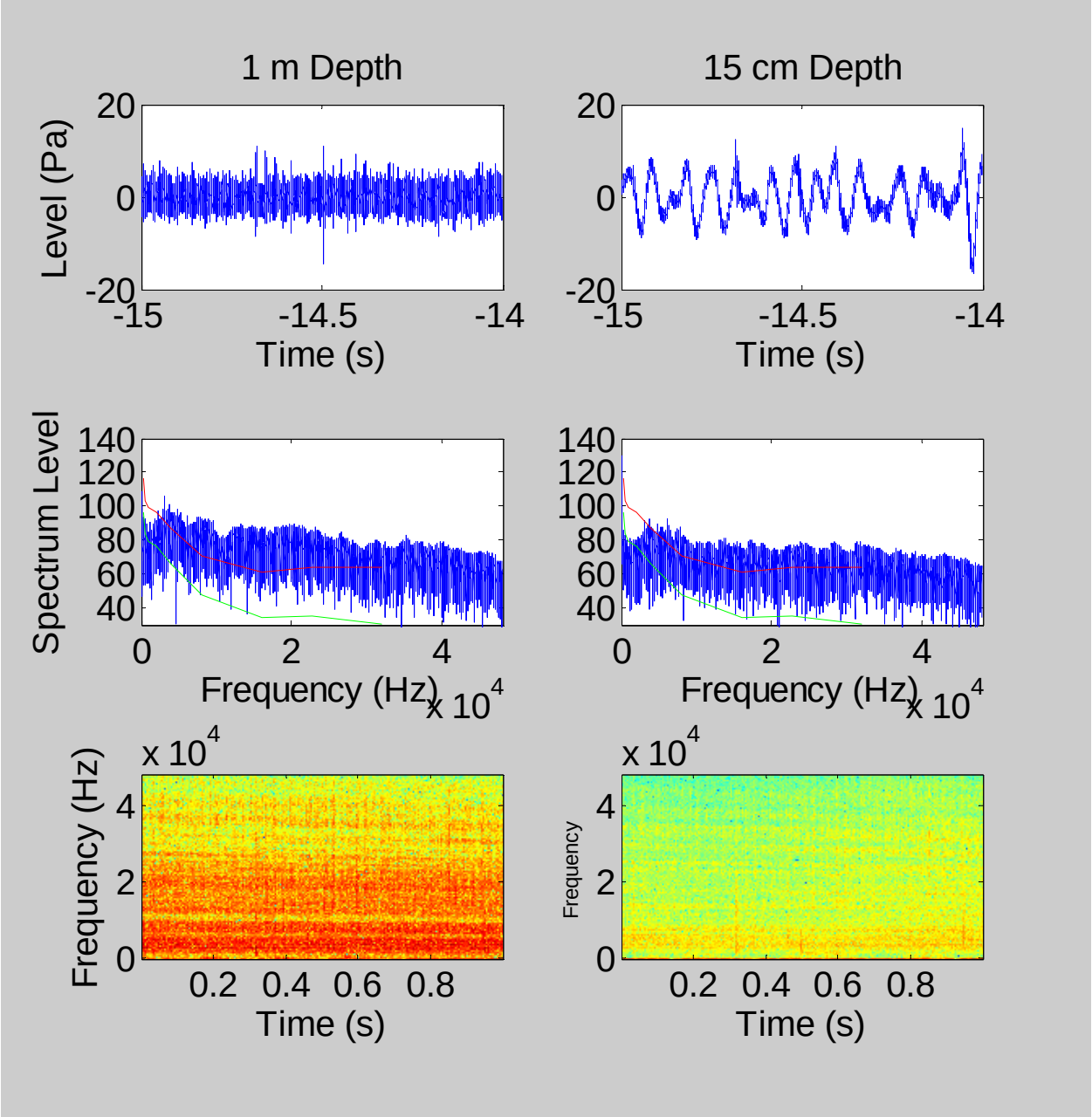

Figure 26. Approach at 34 mph. Top row: Time domain signal 15 seconds prior to boat passing. Middle row: Spectrum level power spectra (dB re 1uPa^2/Hz). Note frequency axis is in Hz x10^4. Red line shows audiogram of Buffett. Green line shows audiogram lowered as a function of the frequency-specific critical ratio. Bottom row: Spectrogram of plots from top row.

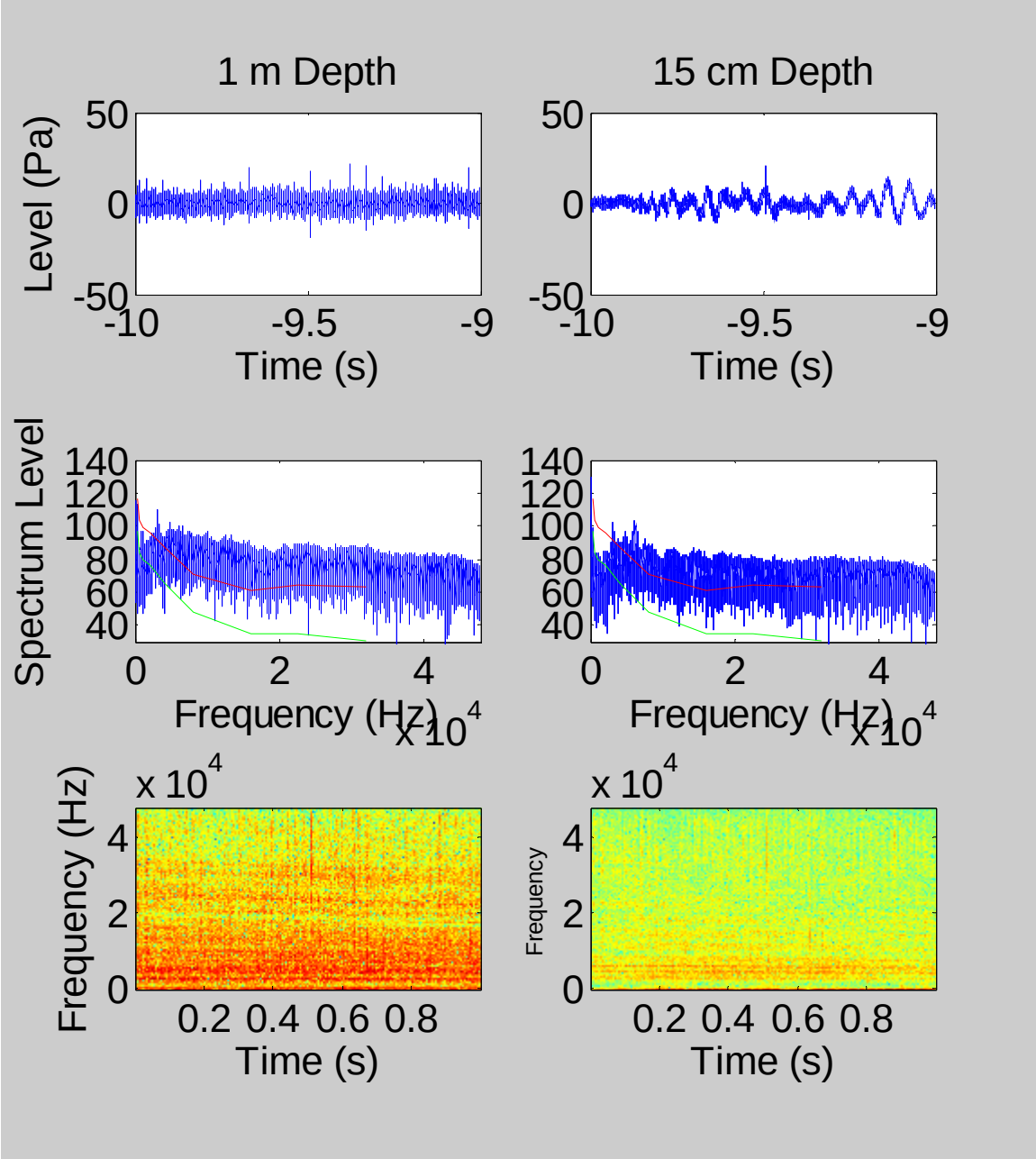

Figure 27. Approach at 34 mph. Top row: Time domain signal 10 seconds prior to boat passing. Middle row: Spectrum level power spectra (dB re 1uPa^2/Hz). Note frequency axis is in Hz x10^4. Red line shows audiogram of Buffett. Green line shows audiogram lowered as a function of the frequency-specific critical ratio. Bottom row: Spectrogram of plots from top row.

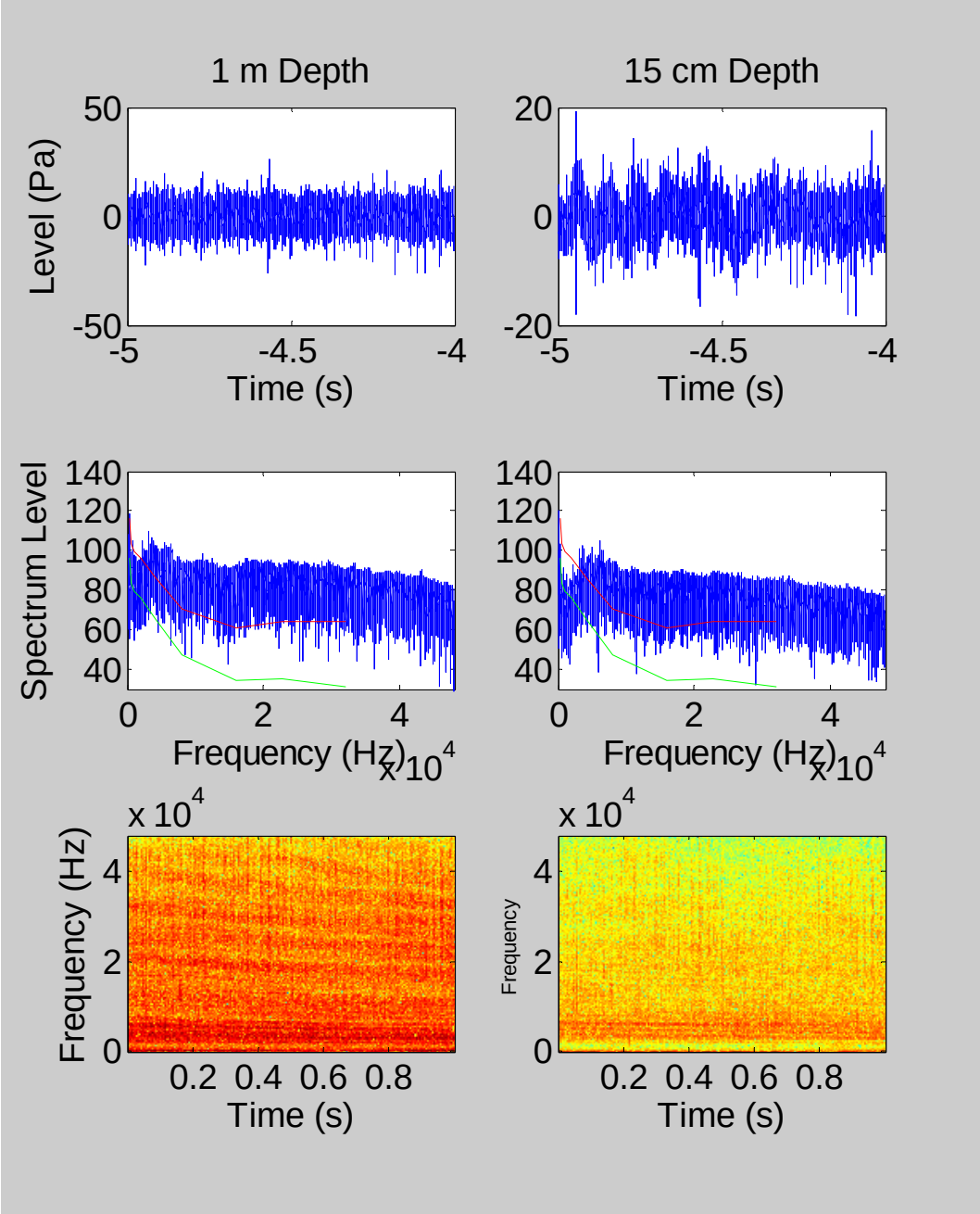

Figure 28. Approach at 34 mph. Top row: Time domain signal 5 seconds prior to boat passing. Middle row: Spectrum level power spectra (dB re 1uPa^2/Hz). Note frequency axis is in Hz x10^4. Red line shows audiogram of Buffett. Green line shows audiogram lowered as a function of the frequency-specific critical ratio. Bottom row: Spectrogram of plots from top row.

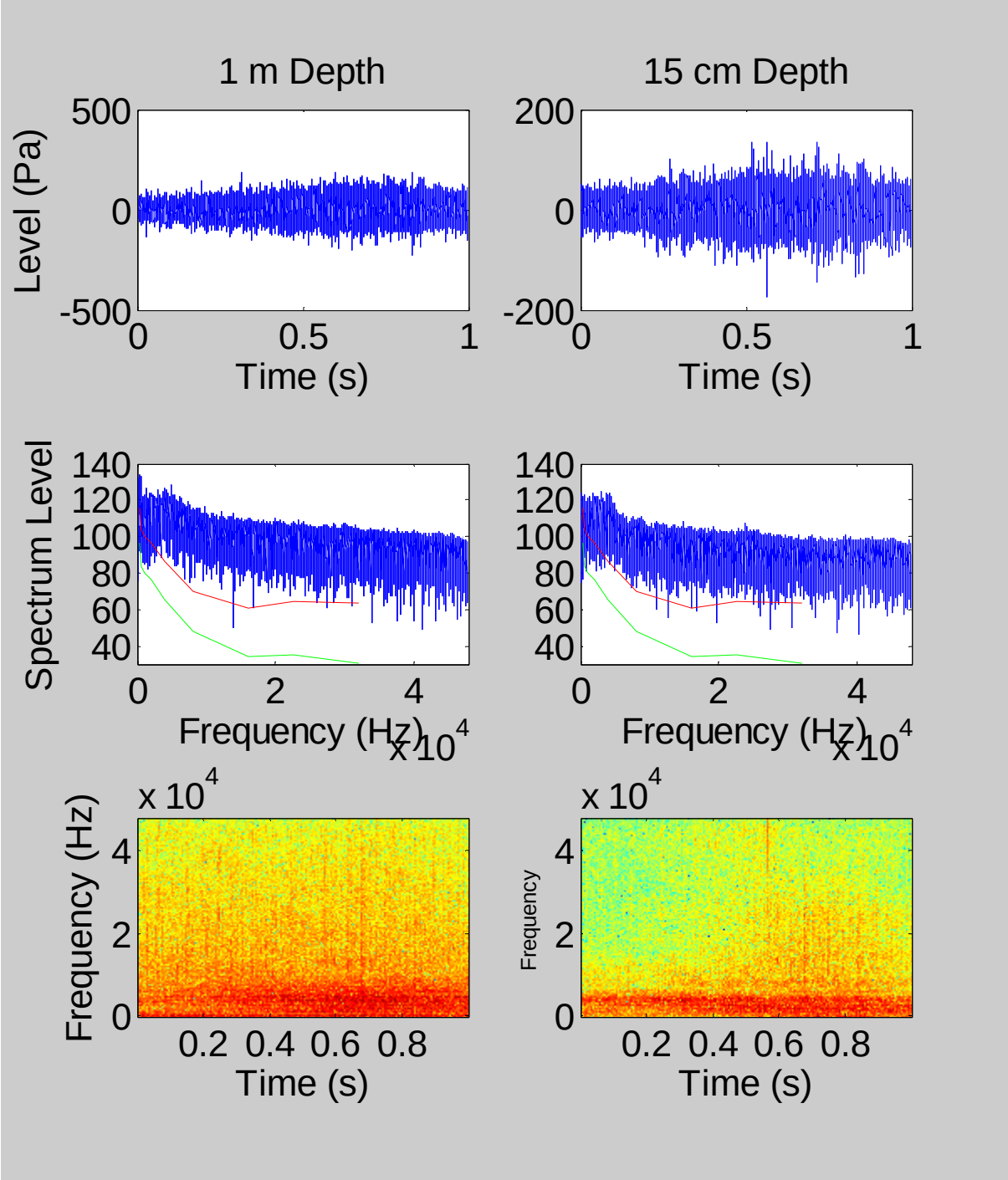

Figure 29. Approach at 34 mph. Top row: Time domain signal at time of boat passing. Middle row: Spectrum level power spectra (dB re 1uPa^2/Hz). Note frequency axis is in Hz x10^4. Red line shows audiogram of Buffett. Green line shows audiogram lowered as a function of the frequency-specific critical ratio. Bottom row: Spectrogram of plots from top row.

17 mph

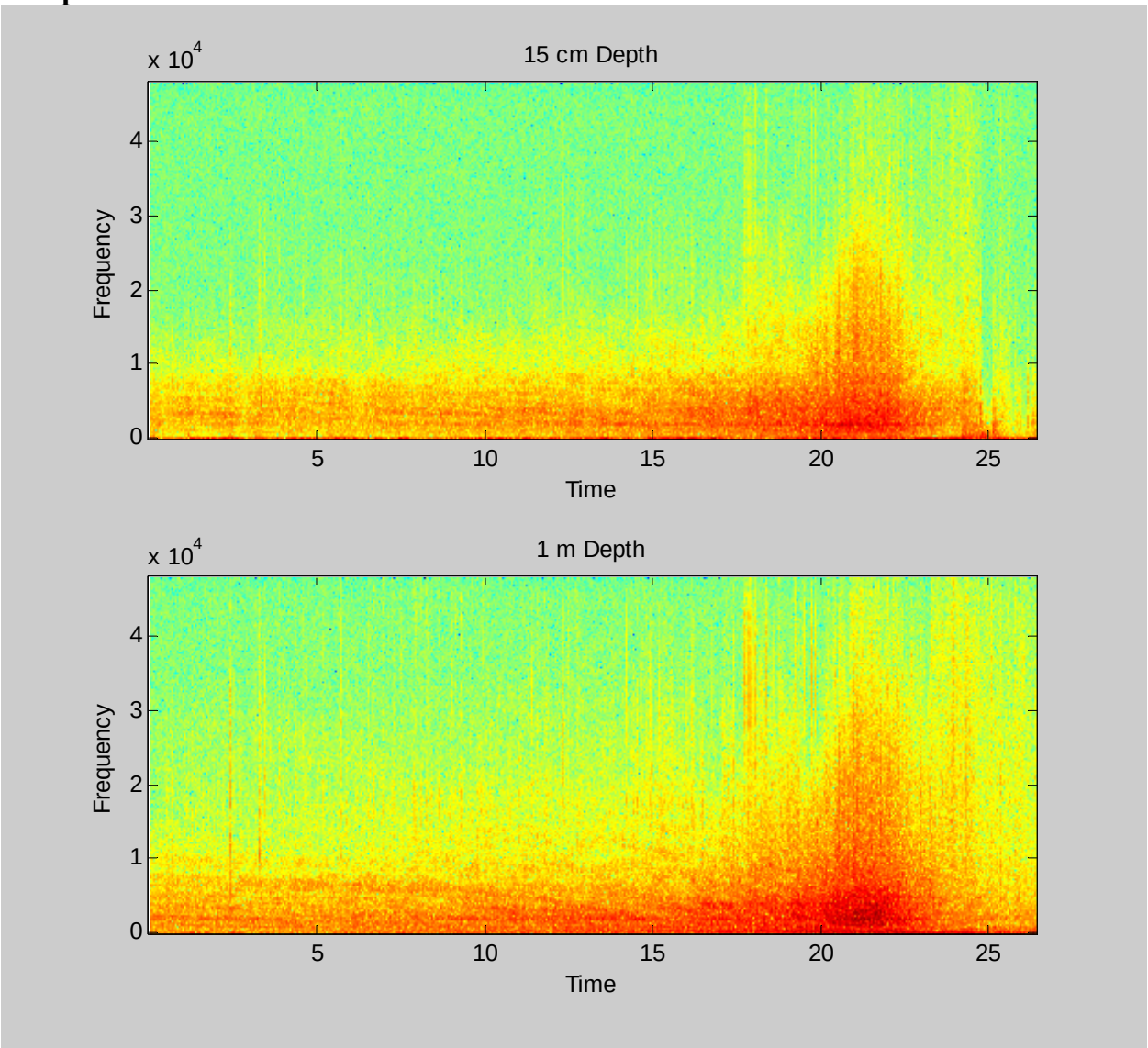

Figure 30. Spectrogram of approach sequence with vessel traveling 17 mph. Top plot is with hydrophone at 15 cm depth. Bottom plot is from a hydrophone at 1 m depth.

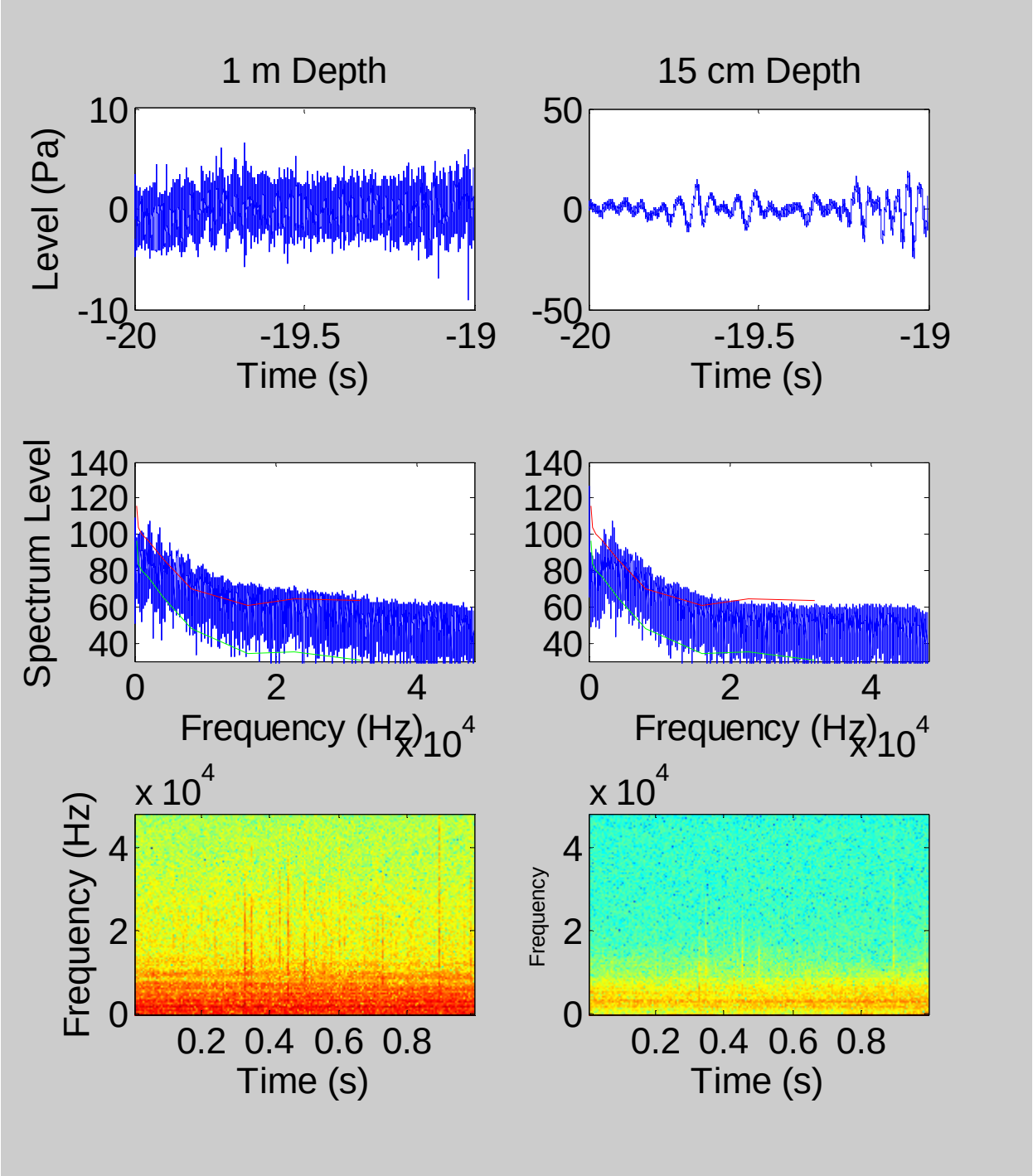

Figure 31. Approach at 17 mph. Top row: Time domain signal 20 seconds prior to boat passing. Middle row: Spectrum level power spectra (dB re 1uPa^2/Hz). Note frequency axis is in Hz x10^4. Red line shows audiogram of Buffett. Green line shows audiogram lowered as a function of the frequency-specific critical ratio. Bottom row: Spectrogram of plots from top row.

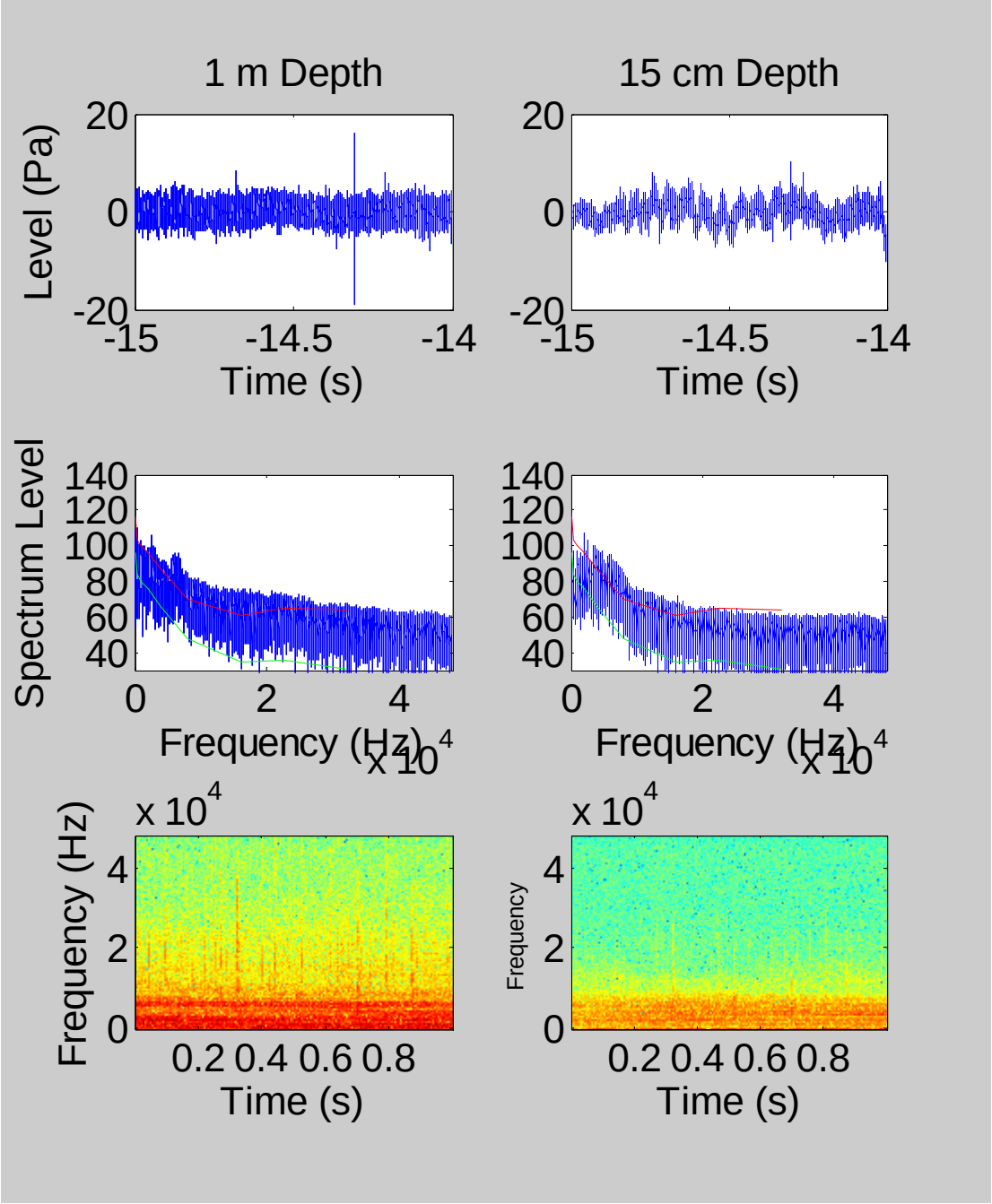

Figure 32. Approach at 17 mph. Top row: Time domain signal 15 seconds prior to boat passing. Middle row: Spectrum level power spectra (dB re 1uPa^2/Hz). Note frequency axis is in Hz x10^4. Red line shows audiogram of Buffett. Green line shows audiogram lowered as a function of the frequency-specific critical ratio. Bottom row: Spectrogram of plots from top row.

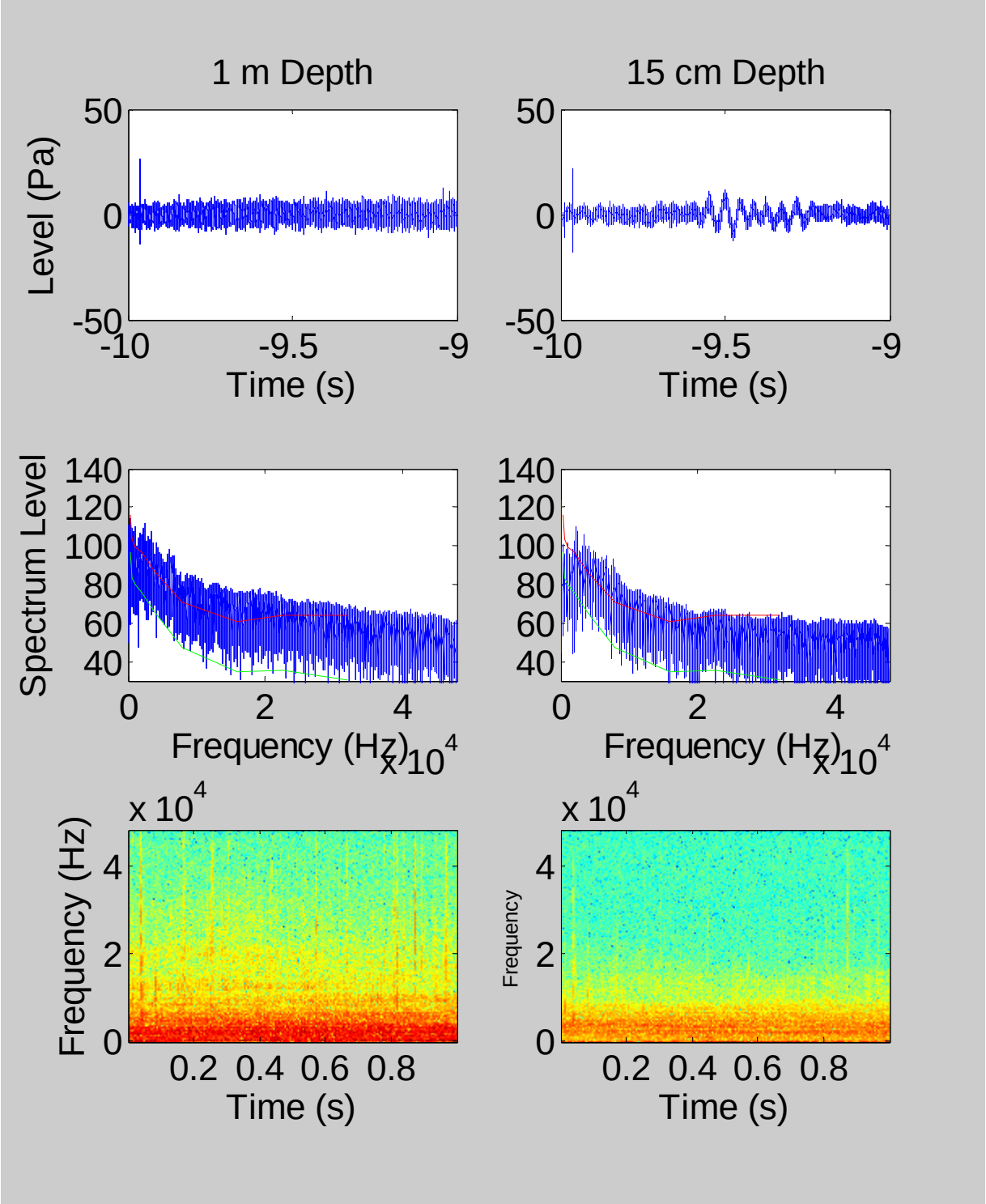

Figure 33. Approach at 17 mph. Top row: Time domain signal 10 seconds prior to boat passing. Middle row: Spectrum level power spectra (dB re 1uPa^2/Hz). Note frequency axis is in Hz x10^4. Red line shows audiogram of Buffett. Green line shows audiogram lowered as a function of the frequency-specific critical ratio. Bottom row: Spectrogram of plots from top row.

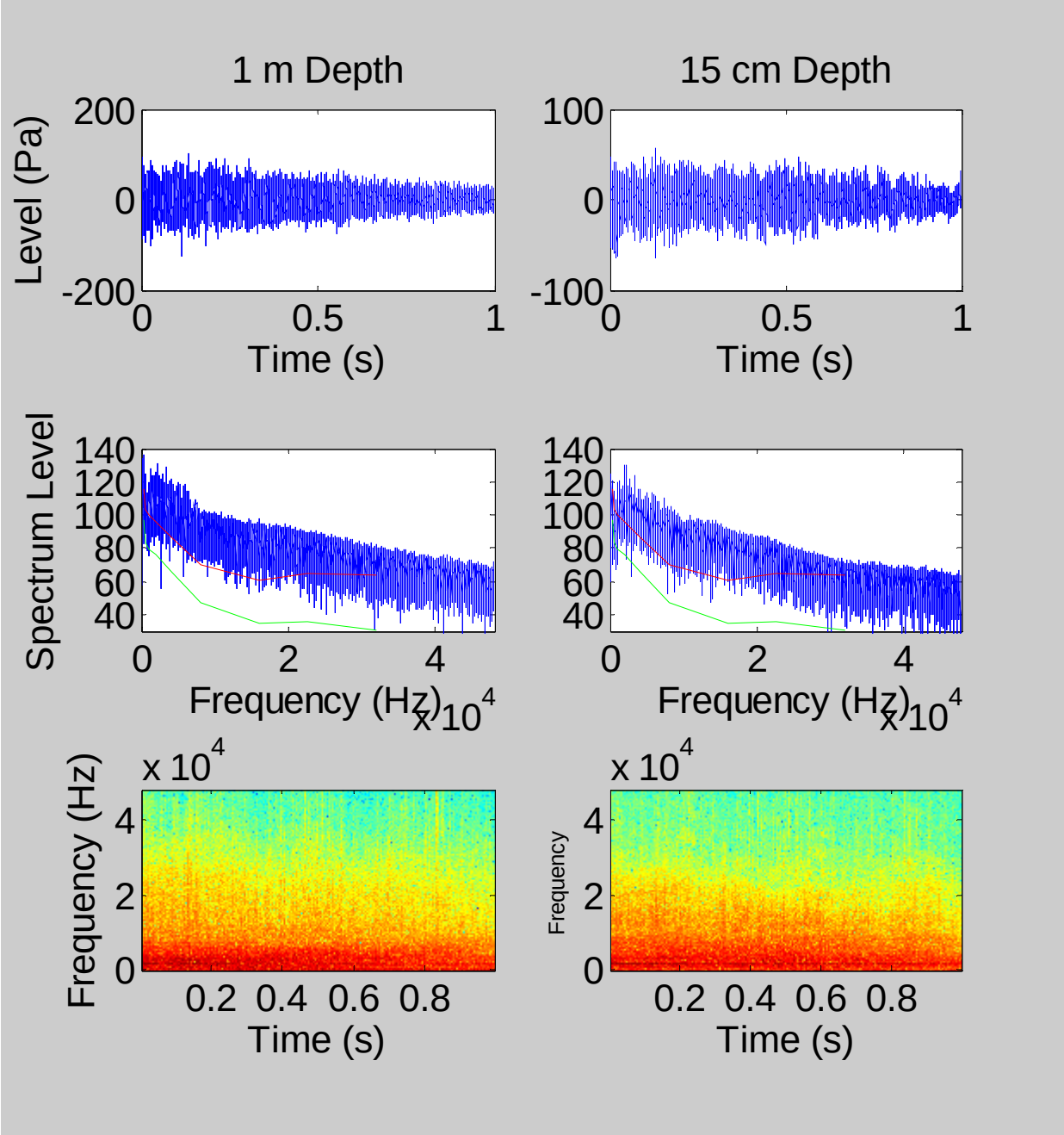

Figure 34. Approach at 17 mph. Top row: Time domain signal at time of boat passing. Middle row: Spectrum level power spectra (dB re 1uPa^2/Hz). Note frequency axis is in Hz x10^4. Red line shows audiogram of Buffett. Green line shows audiogram lowered as a function of the frequency-specific critical ratio. Bottom row: Spectrogram of plots from top row.

4 mph (Idle)

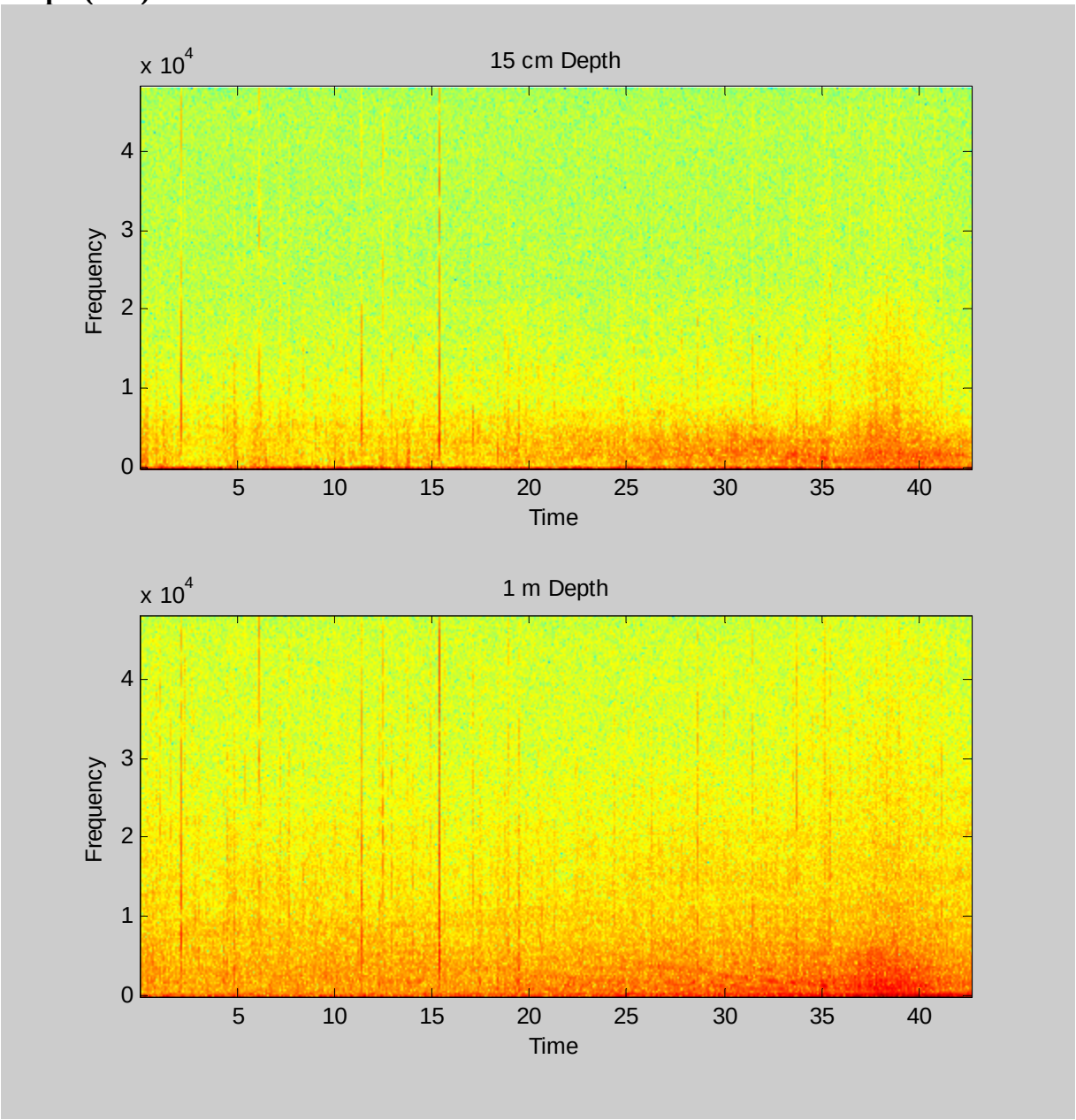

Figure 35. Spectrogram of approach sequence with vessel traveling 4 mph. Top plot is with hydrophone at 15 cm depth. Bottom plot is from a hydrophone at 1 m depth.

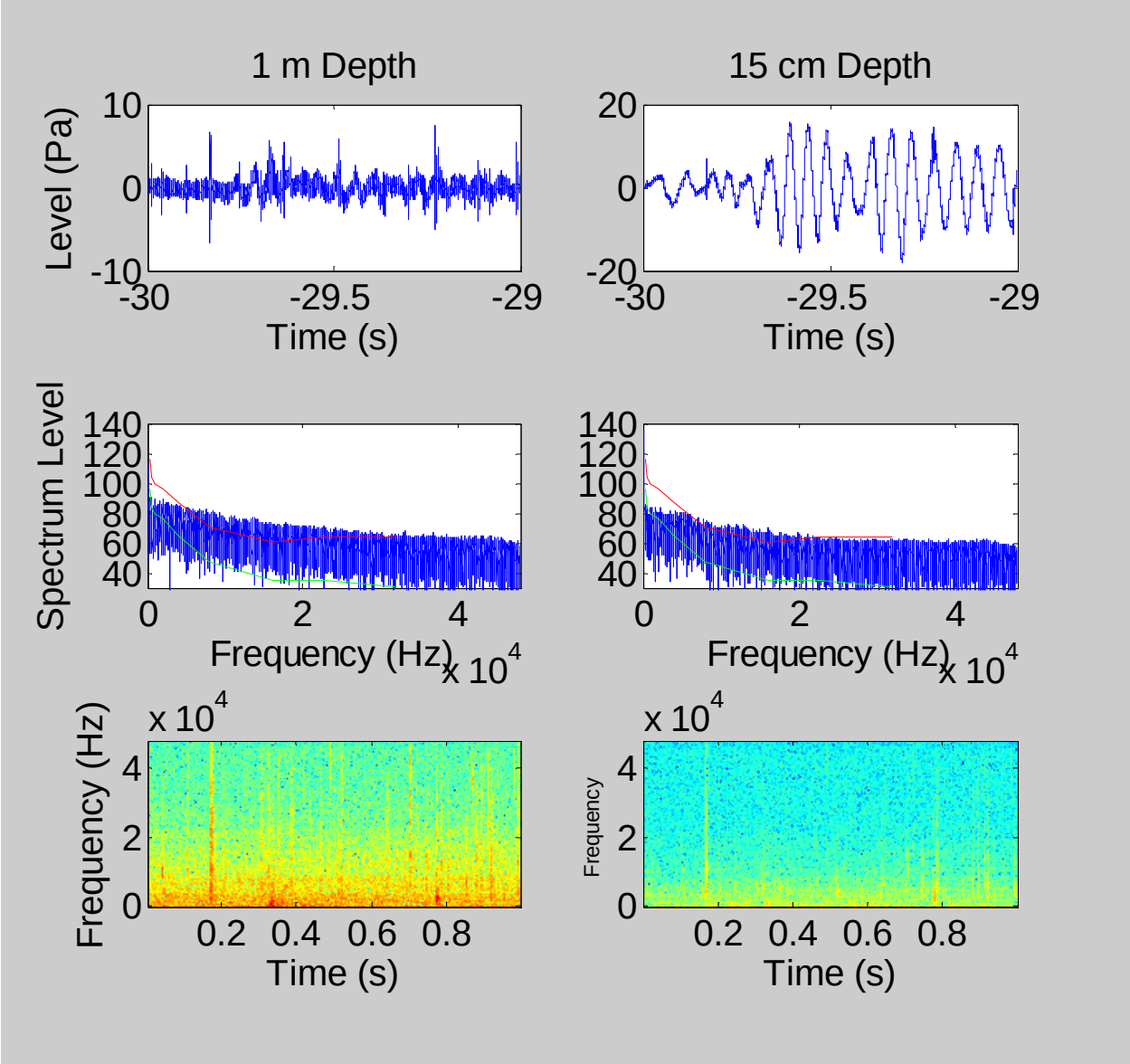

Figure 36. Approach at 4 mph. Top row: Time domain signal 30 seconds prior to boat passing. Middle row: Spectrum level power spectra (dB re 1uPa^2/Hz). Note frequency axis is in Hz x10^4. Red line shows audiogram of Buffett. Green line shows audiogram lowered as a function of the frequency-specific critical ratio. Bottom row: Spectrogram of plots from top row.

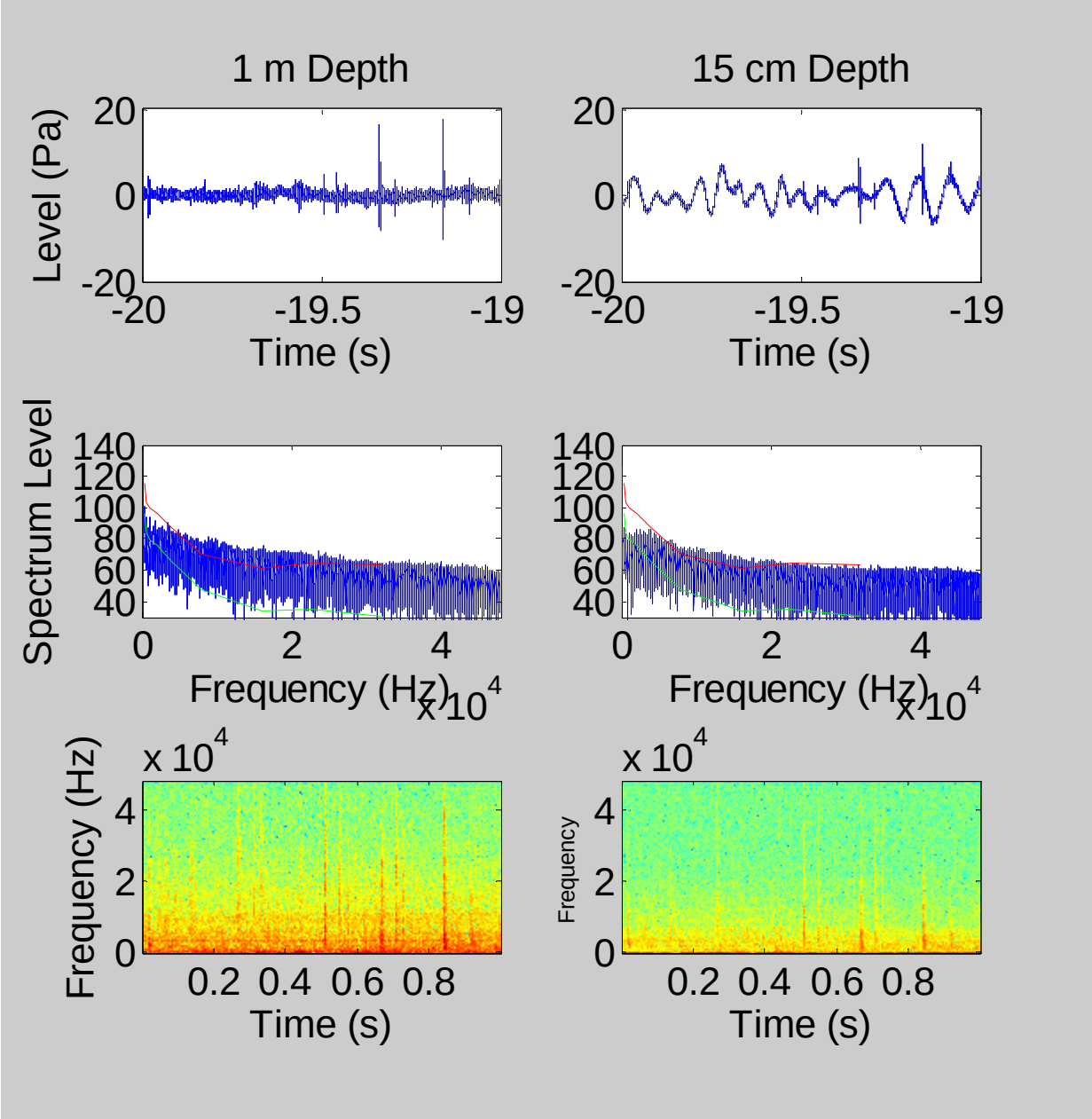

Figure 37. Approach at 4 mph. Top row: Time domain signal 20 seconds prior to boat passing. Middle row: Spectrum level power spectra (dB re 1uPa^2/Hz). Note frequency axis is in Hz x10^4. Red line shows audiogram of Buffett. Green line shows audiogram lowered as a function of the frequency-specific critical ratio. Bottom row: Spectrogram of plots from top row.

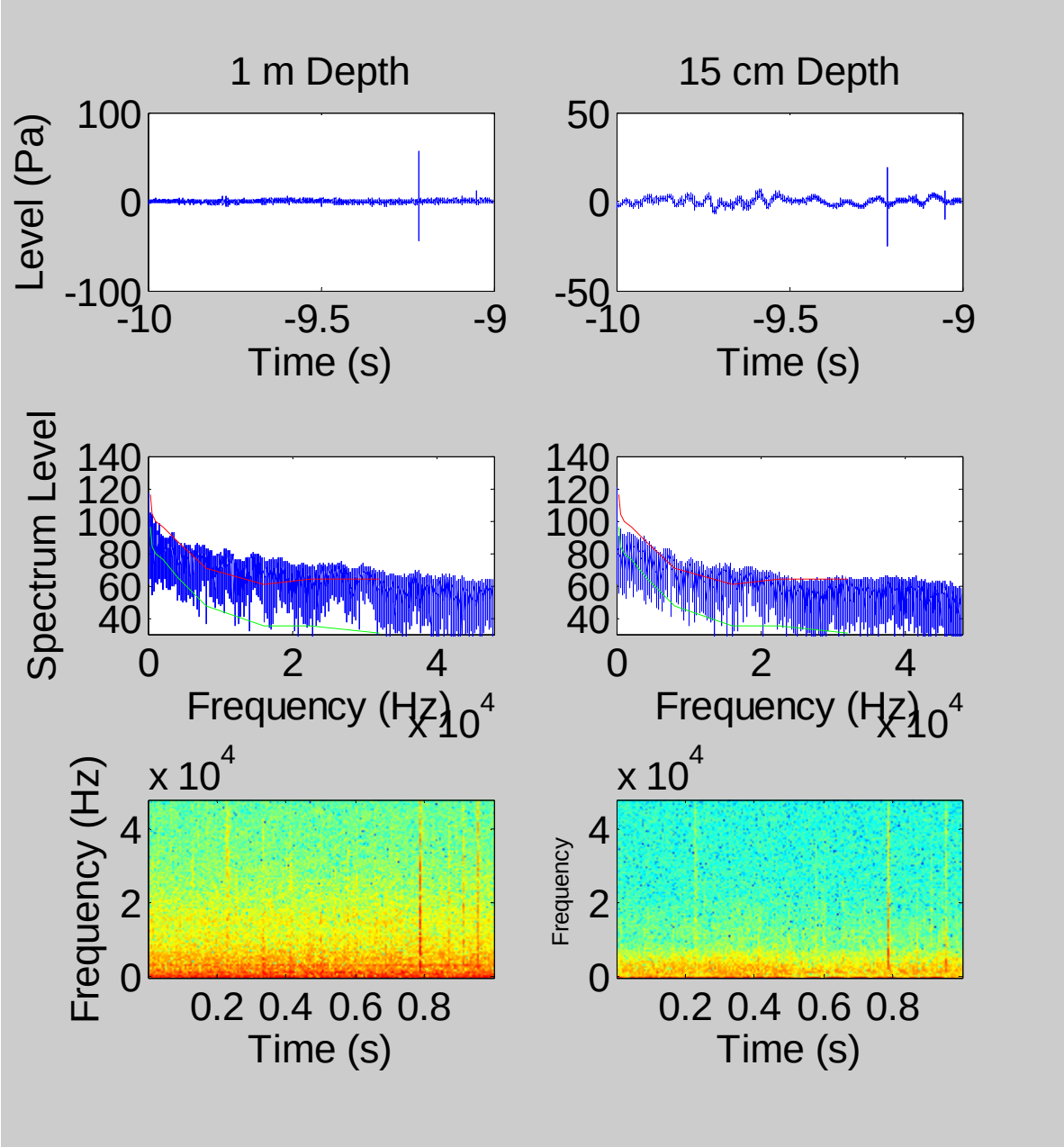

Figure 38. Approach at 4 mph. Top row: Time domain signal 10 seconds prior to boat passing. Middle row: Spectrum level power spectra (dB re 1uPa^2/Hz). Note frequency axis is in Hz x10^4. Red line shows audiogram of Buffett. Green line shows audiogram lowered as a function of the frequency-specific critical ratio. Bottom row: Spectrogram of plots from top row.

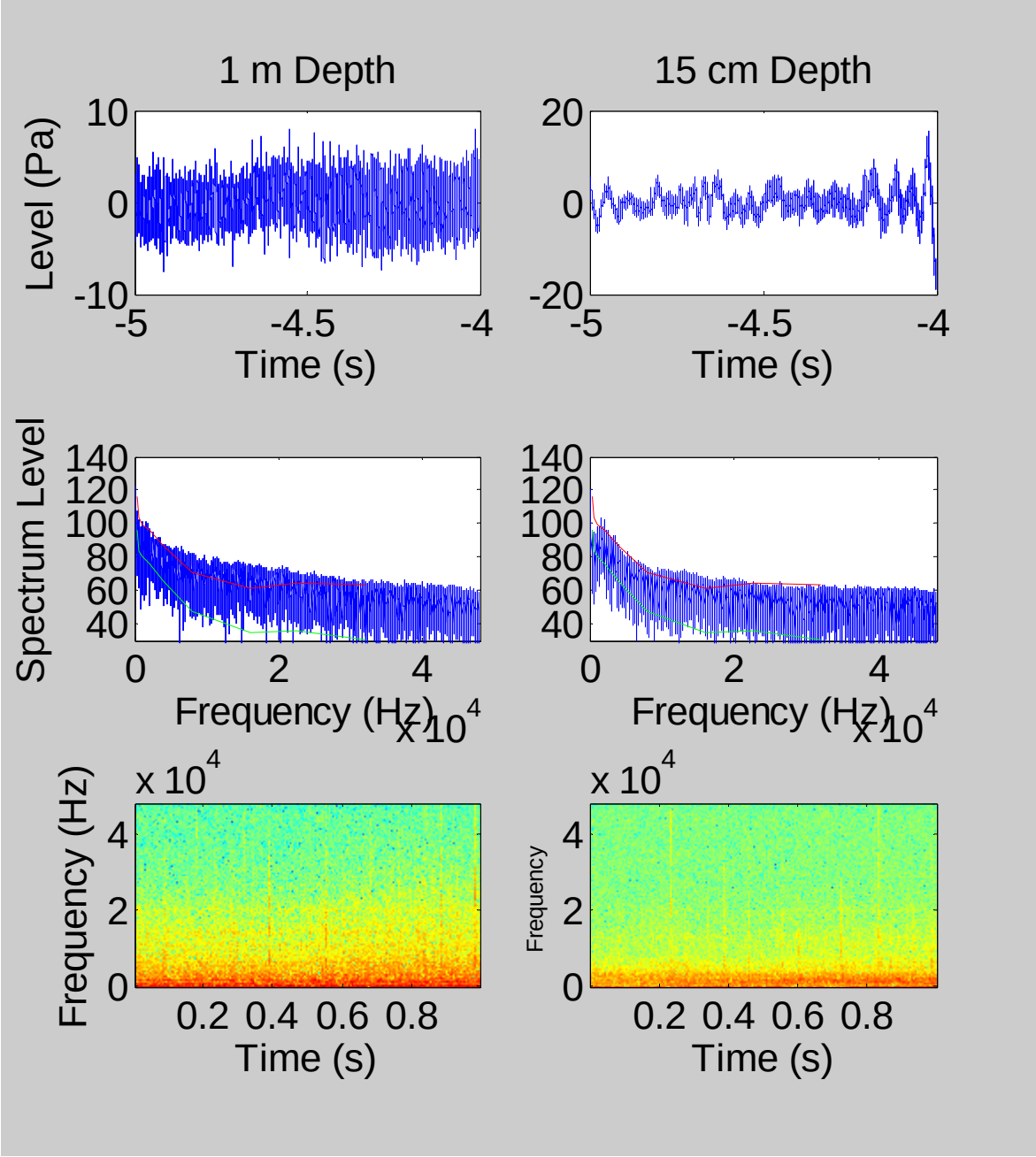

Figure 39. Approach at 4 mph. Top row: Time domain signal 5 seconds prior to boat passing. Middle row: Spectrum level power spectra (dB re 1uPa^2/Hz). Note frequency axis is in Hz x10^4. Red line shows audiogram of Buffett. Green line shows audiogram lowered as a function of the frequency-specific critical ratio. Bottom row: Spectrogram of plots from top row.

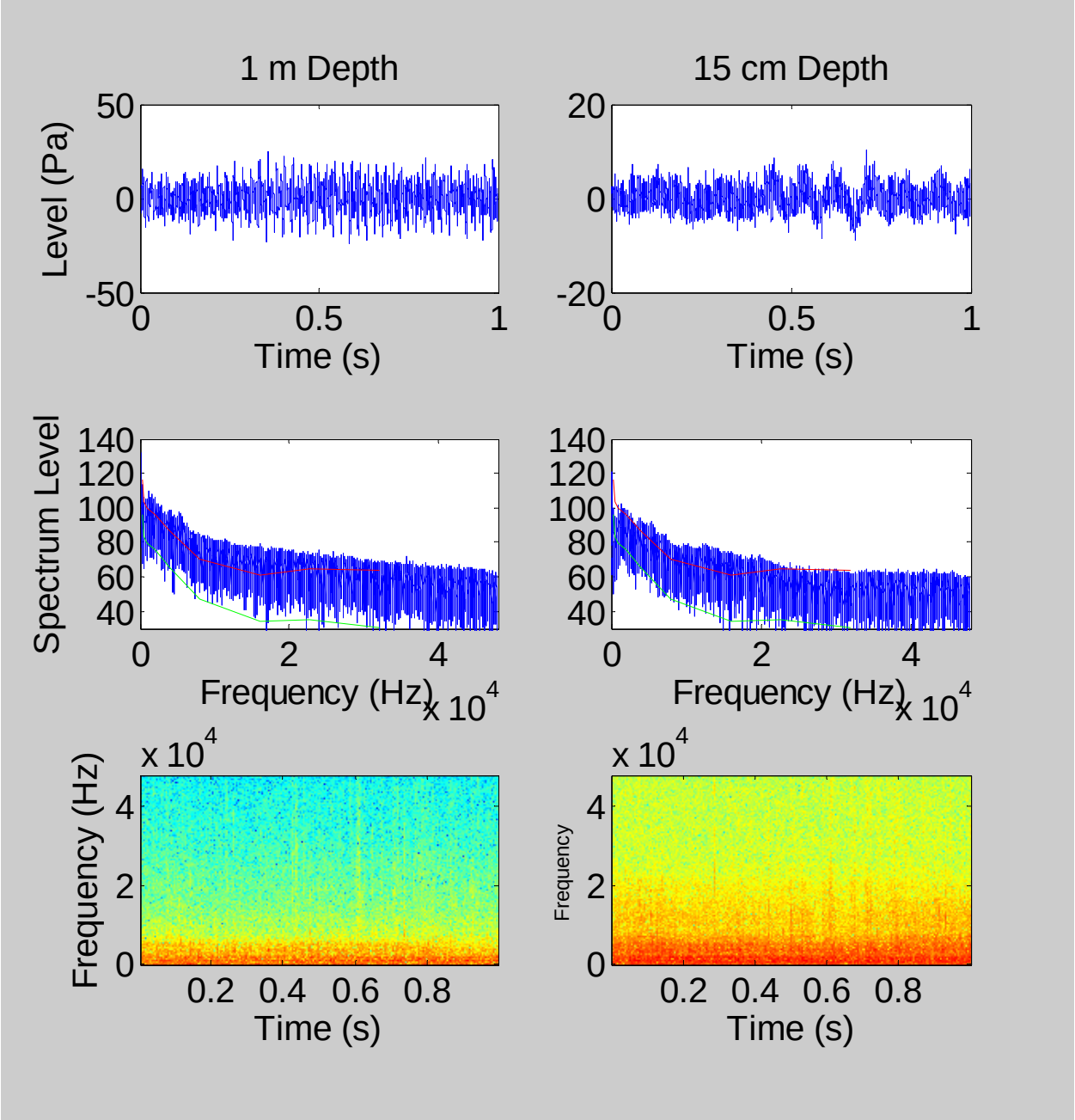

Figure 40. Approach at 4 mph. Top row: Time domain signal at time of boat passing. Middle row: Spectrum level power spectra (dB re 1uPa^2/Hz). Note frequency axis is in Hz x10^4. Red line shows audiogram of Buffett. Green line shows audiogram lowered as a function of the frequency-specific critical ratio. Bottom row: Spectrogram of plots from top row.

Mini Mako - 115 HP Yamaha 4-stroke
34.5 mph

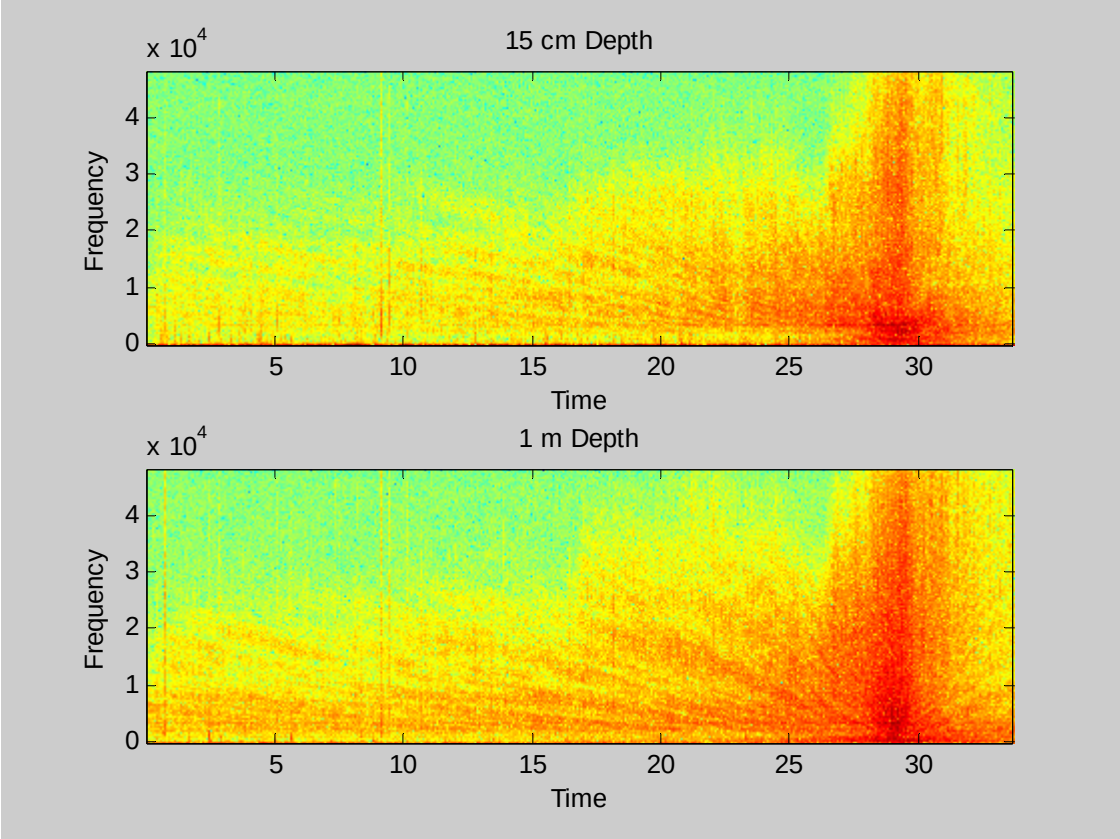

Figure 41. Spectrogram of approach sequence with vessel traveling 34.5 mph. Top plot is with hydrophone at 15 cm depth. Bottom plot is from a hydrophone at 1 m depth.

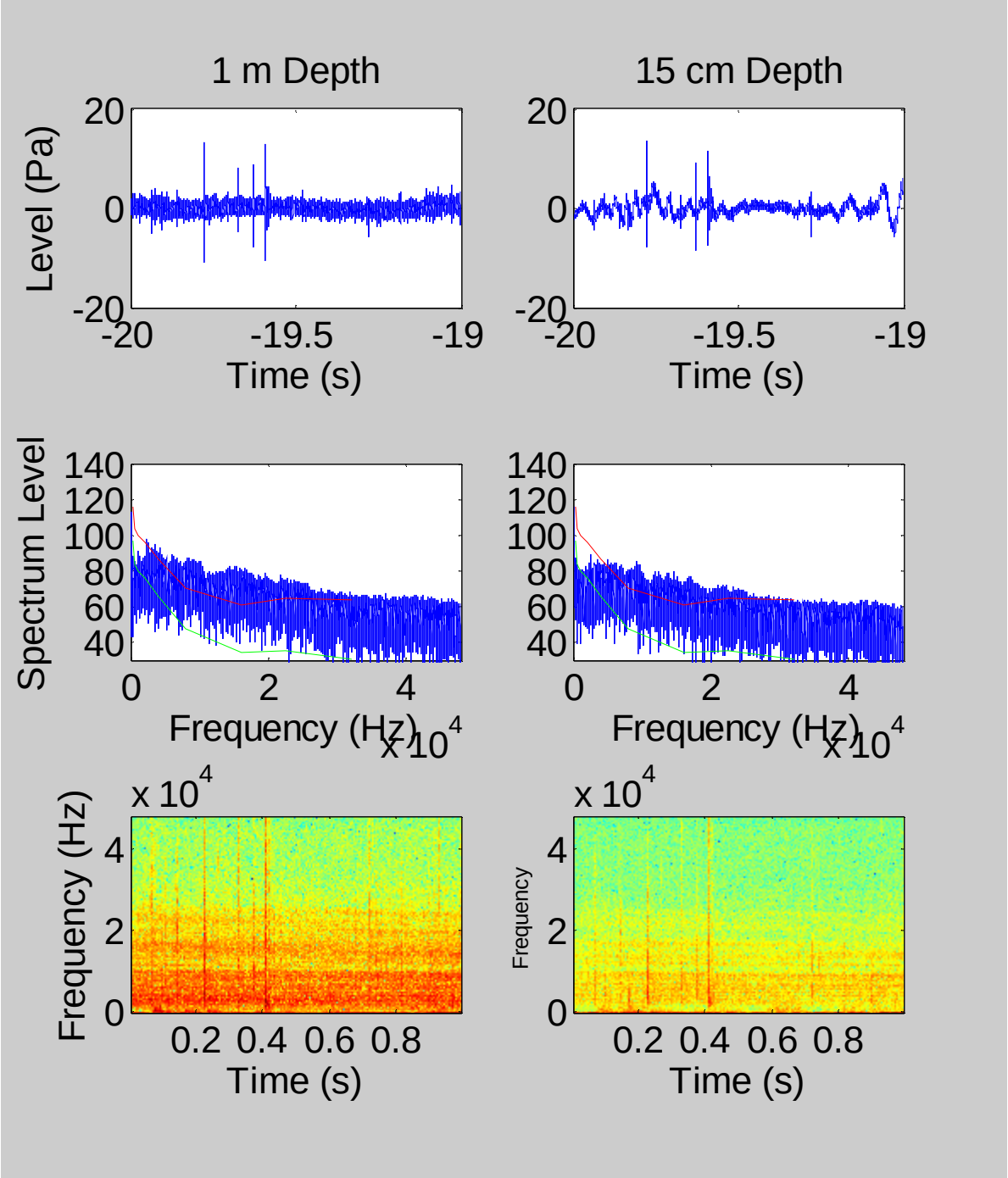

Figure 42. Approach at 34.5 mph. Top row: Time domain signal 20 seconds prior to boat passing. Middle row: Spectrum level power spectra (dB re 1uPa^2/Hz). Note frequency axis is in Hz x10^4. Red line shows audiogram of Buffett. Green line shows audiogram lowered as a function of the frequency-specific critical ratio. Bottom row: Spectrogram of plots from top row.

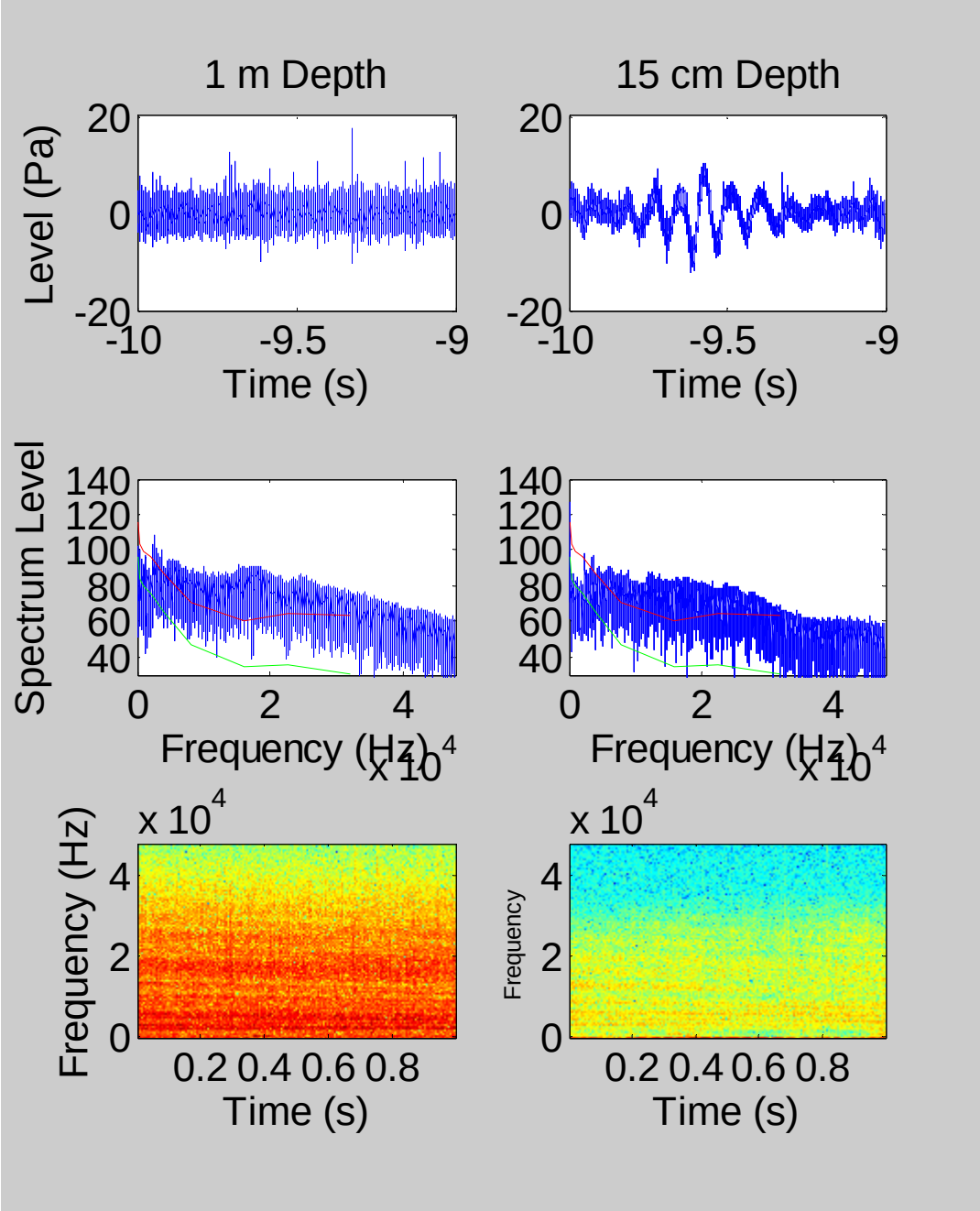

Figure 43. Approach at 34.5 mph. Top row: Time domain signal 10 seconds prior to boat passing. Middle row: Spectrum level power spectra (dB re 1uPa^2/Hz). Note frequency axis is in Hz x10^4. Red line shows audiogram of Buffett. Green line shows audiogram lowered as a function of the frequency-specific critical ratio. Bottom row: Spectrogram of plots from top row.

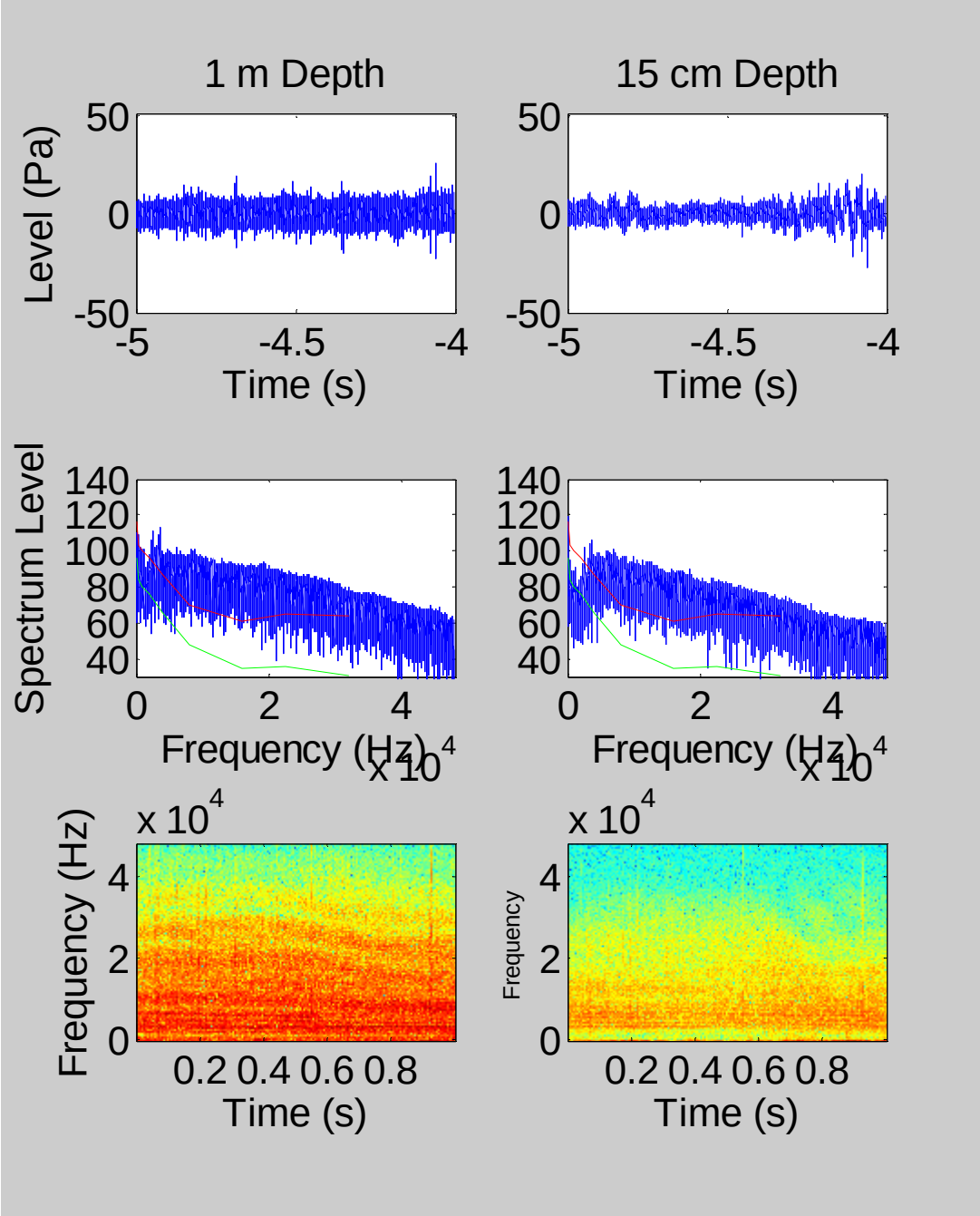

Figure 44. Approach at 34.5 mph. Top row: Time domain signal 5 seconds prior to boat passing. Middle row: Spectrum level power spectra (dB re 1uPa^2/Hz). Note frequency axis is in Hz x10^4. Red line shows audiogram of Buffett. Green line shows audiogram lowered as a function of the frequency-specific critical ratio. Bottom row: Spectrogram of plots from top row.

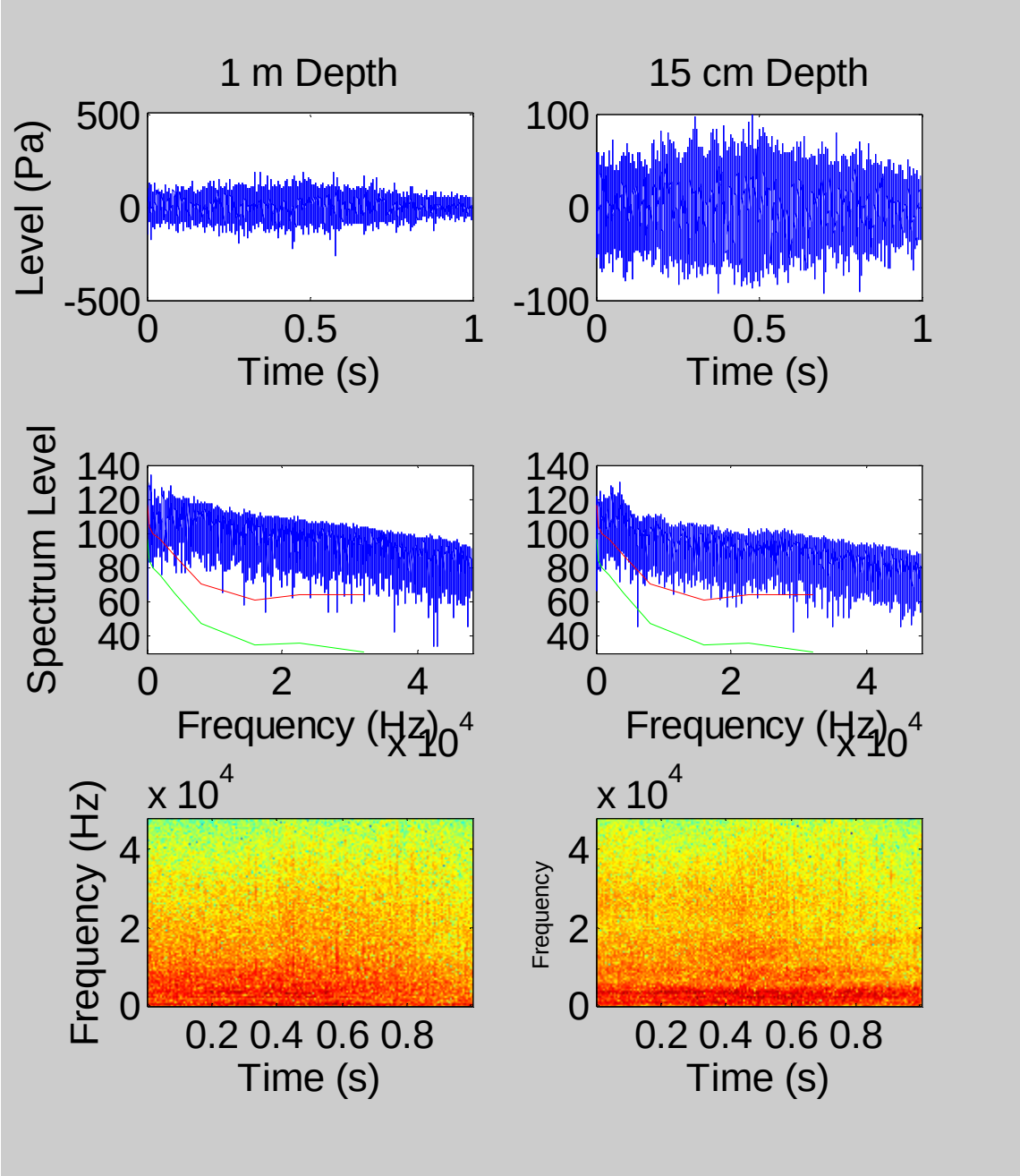

Figure 45. Approach at 34.5 mph. Top row: Time domain signal at time of boat passing. Middle row: Spectrum level power spectra (dB re 1uPa^2/Hz). Note frequency axis is in Hz x10^4. Red line shows audiogram of Buffett. Green line shows audiogram lowered as a function of the frequency-specific critical ratio. Bottom row: Spectrogram of plots from top row.

10.7 mph

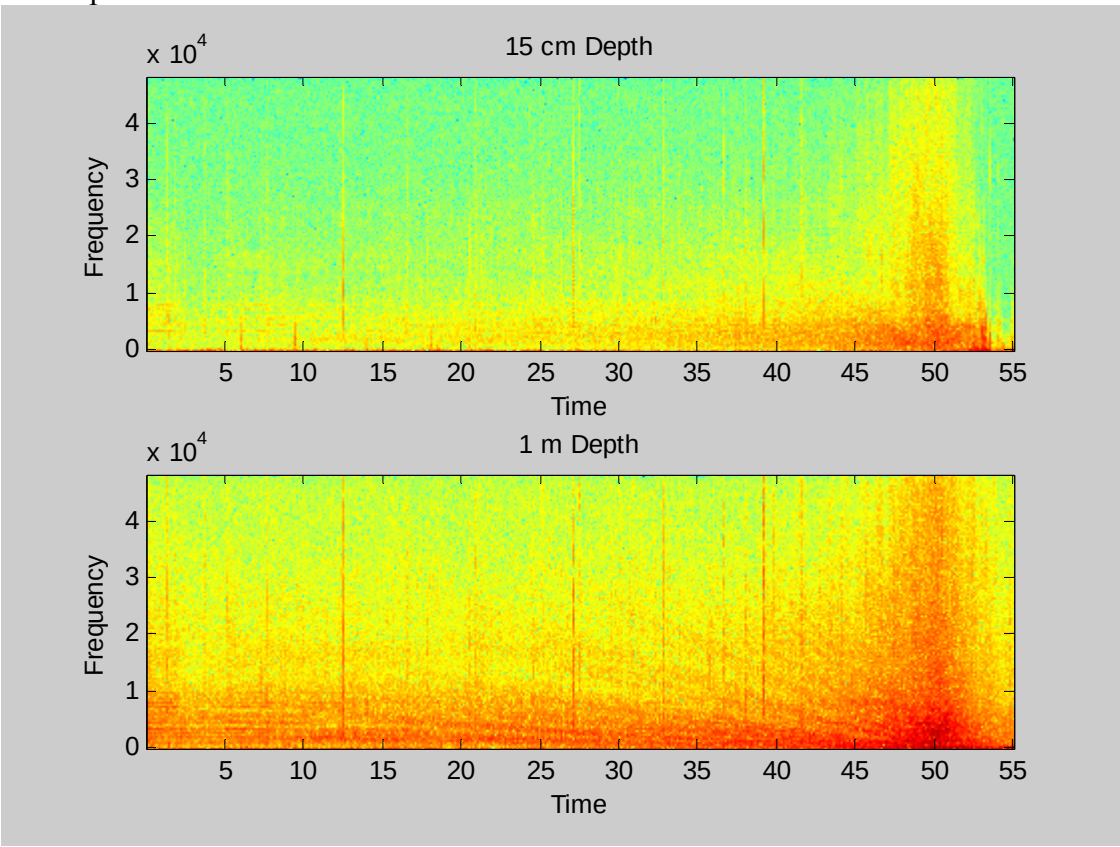

Figure 46. Spectrogram of approach sequence with vessel traveling 10.7 mph. Top plot is with hydrophone at 15 cm depth. Bottom plot is from a hydrophone at 1 m depth.

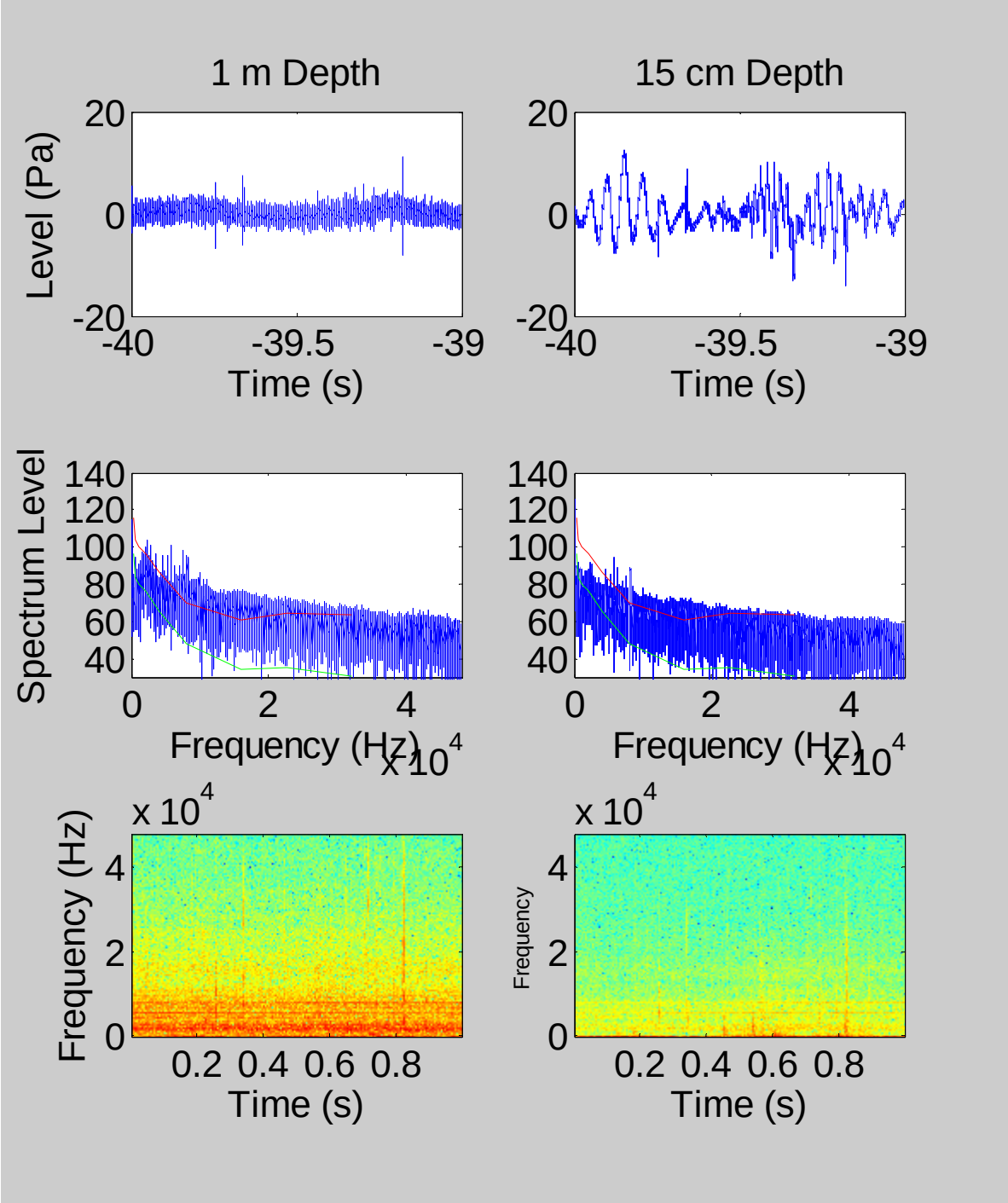

Figure 47. Approach at 10.7 mph. Top row: Time domain signal 40 seconds prior to boat passing. Middle row: Spectrum level power spectra (dB re 1uPa^2/Hz). Note frequency axis is in Hz x10^4. Red line shows audiogram of Buffett. Green line shows audiogram lowered as a function of the frequency-specific critical ratio. Bottom row: Spectrogram of plots from top row.

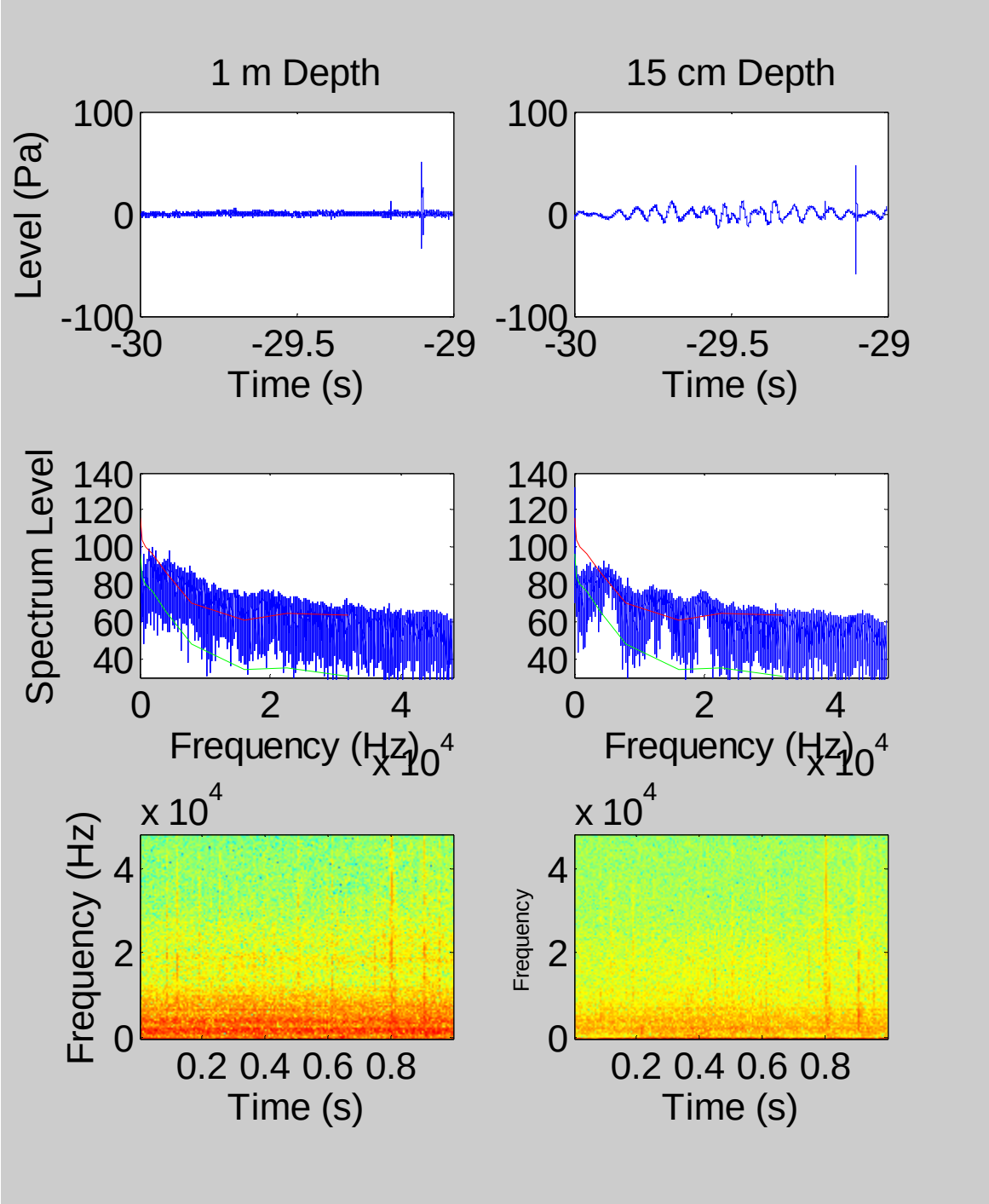

Figure 48. Approach at 10.7 mph. Top row: Time domain signal 30 seconds prior to boat passing. Middle row: Spectrum level power spectra (dB re 1uPa^2/Hz). Note frequency axis is in Hz x10^4. Red line shows audiogram of Buffett. Green line shows audiogram lowered as a function of the frequency-specific critical ratio. Bottom row: Spectrogram of plots from top row.

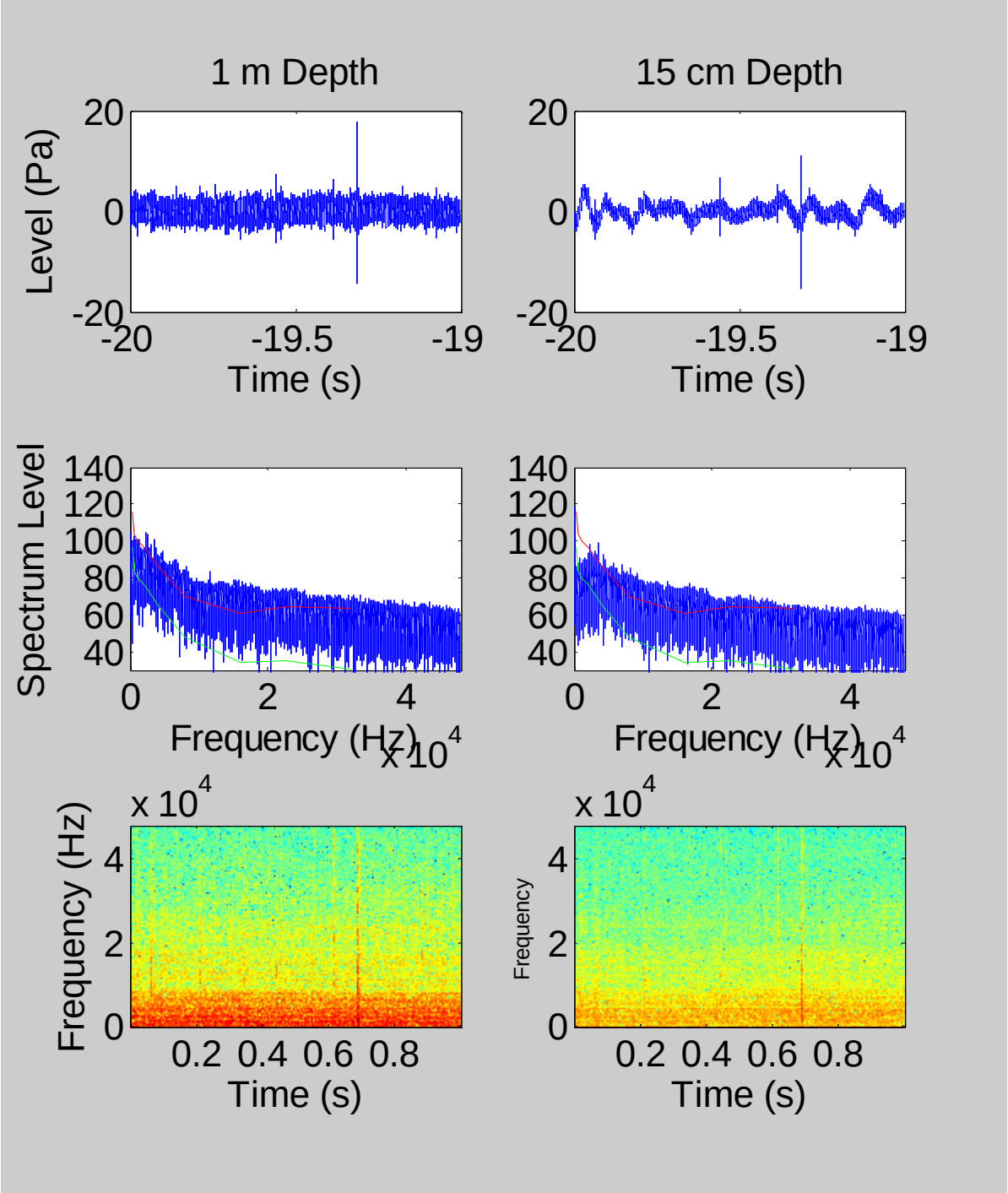

Figure 49. Approach at 10.7 mph. Top row: Time domain signal 20 seconds prior to boat passing. Middle row: Spectrum level power spectra (dB re 1uPa^2/Hz). Note frequency axis is in Hz x10^4. Red line shows audiogram of Buffett. Green line shows audiogram lowered as a function of the frequency-specific critical ratio. Bottom row: Spectrogram of plots from top row.

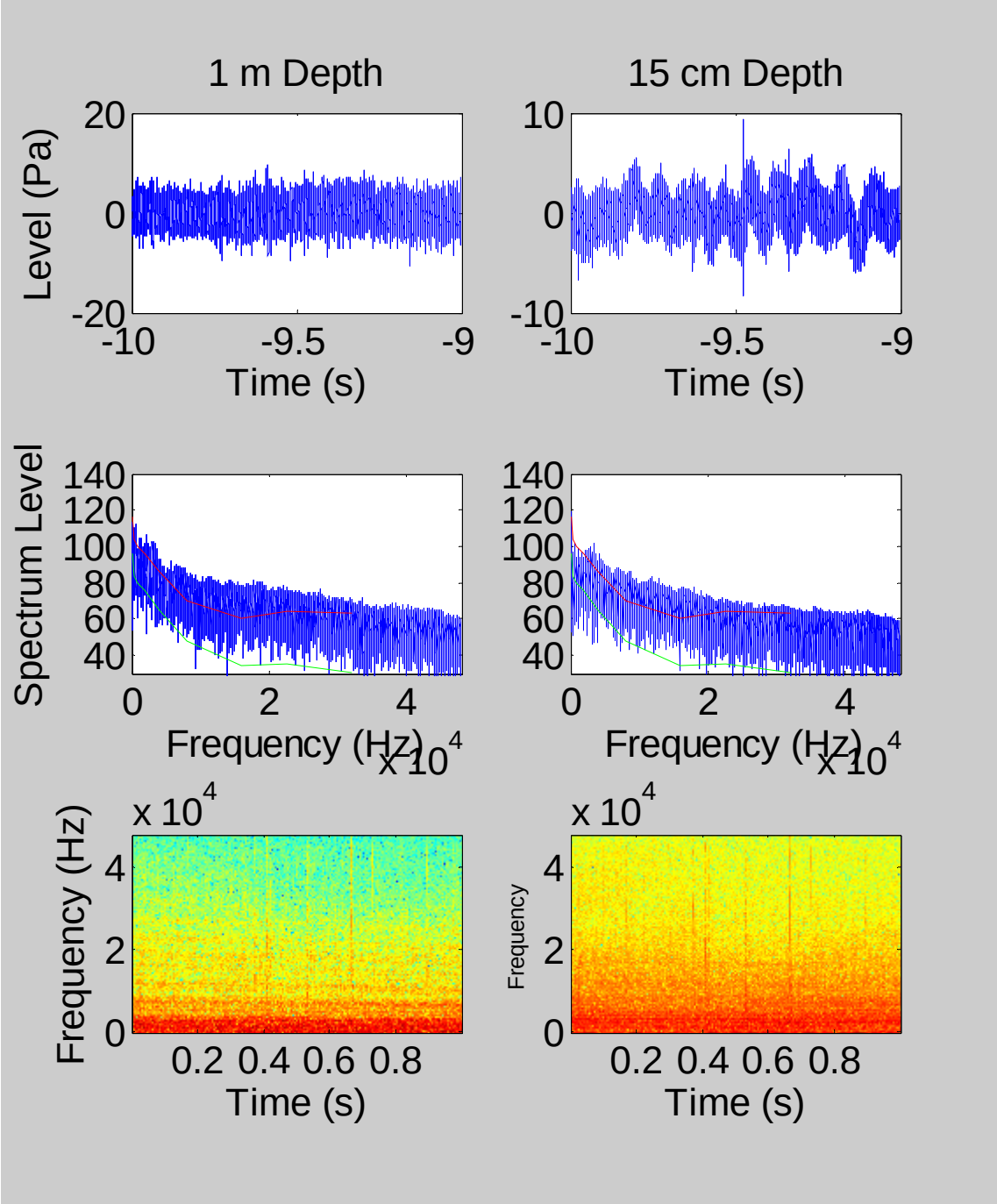

Figure 50. Approach at 10.7 mph. Top row: Time domain signal 10 seconds prior to boat passing. Middle row: Spectrum level power spectra (dB re 1uPa^2/Hz). Note frequency axis is in Hz x10^4. Red line shows audiogram of Buffett. Green line shows audiogram lowered as a function of the frequency-specific critical ratio. Bottom row: Spectrogram of plots from top row.

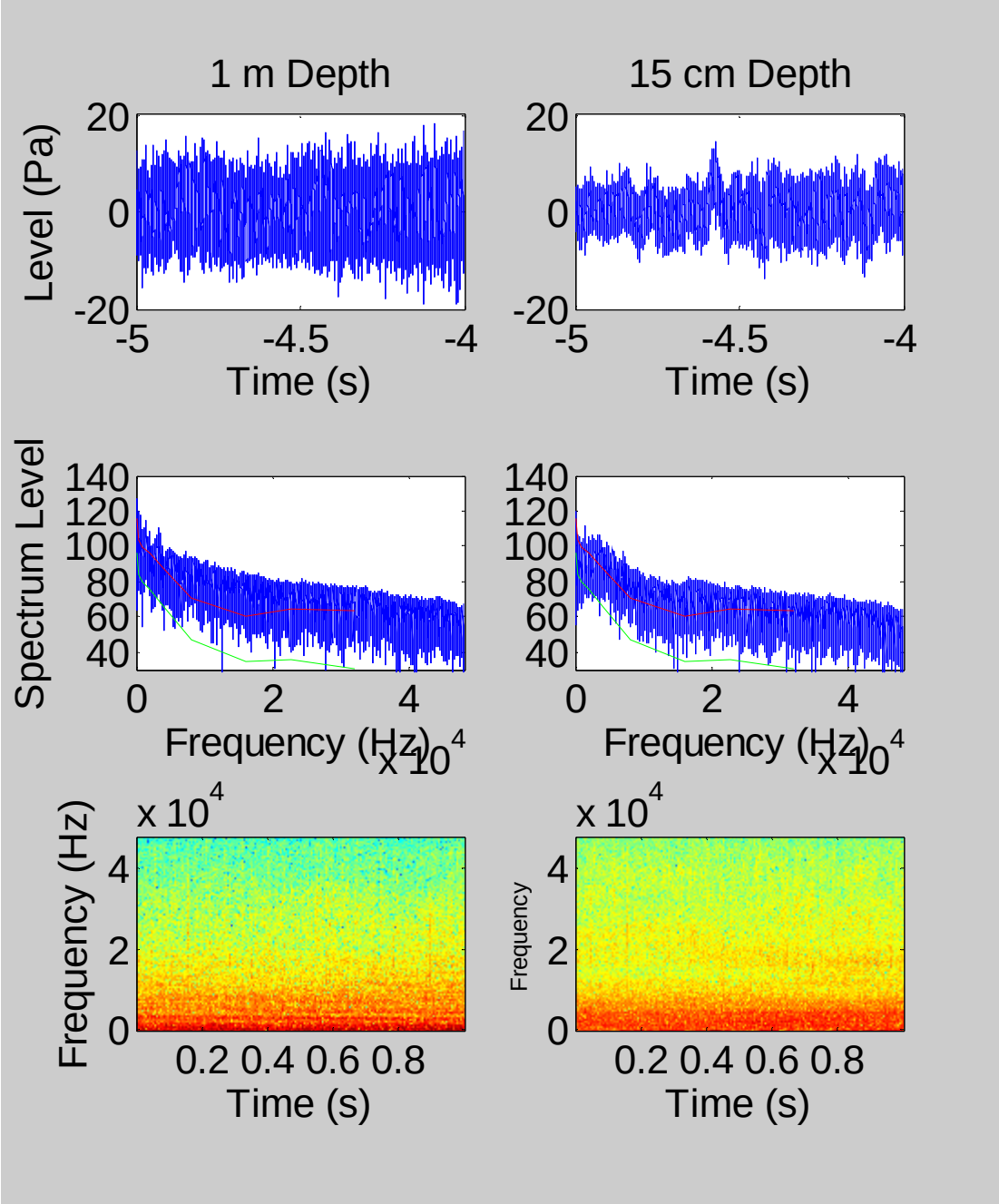

Figure 51. Approach at 10.7 mph. Top row: Time domain signal 5 seconds prior to boat passing. Middle row: Spectrum level power spectra (dB re 1uPa^2/Hz). Note frequency axis is in Hz x10^4. Red line shows audiogram of Buffett. Green line shows audiogram lowered as a function of the frequency-specific critical ratio. Bottom row: Spectrogram of plots from top row.

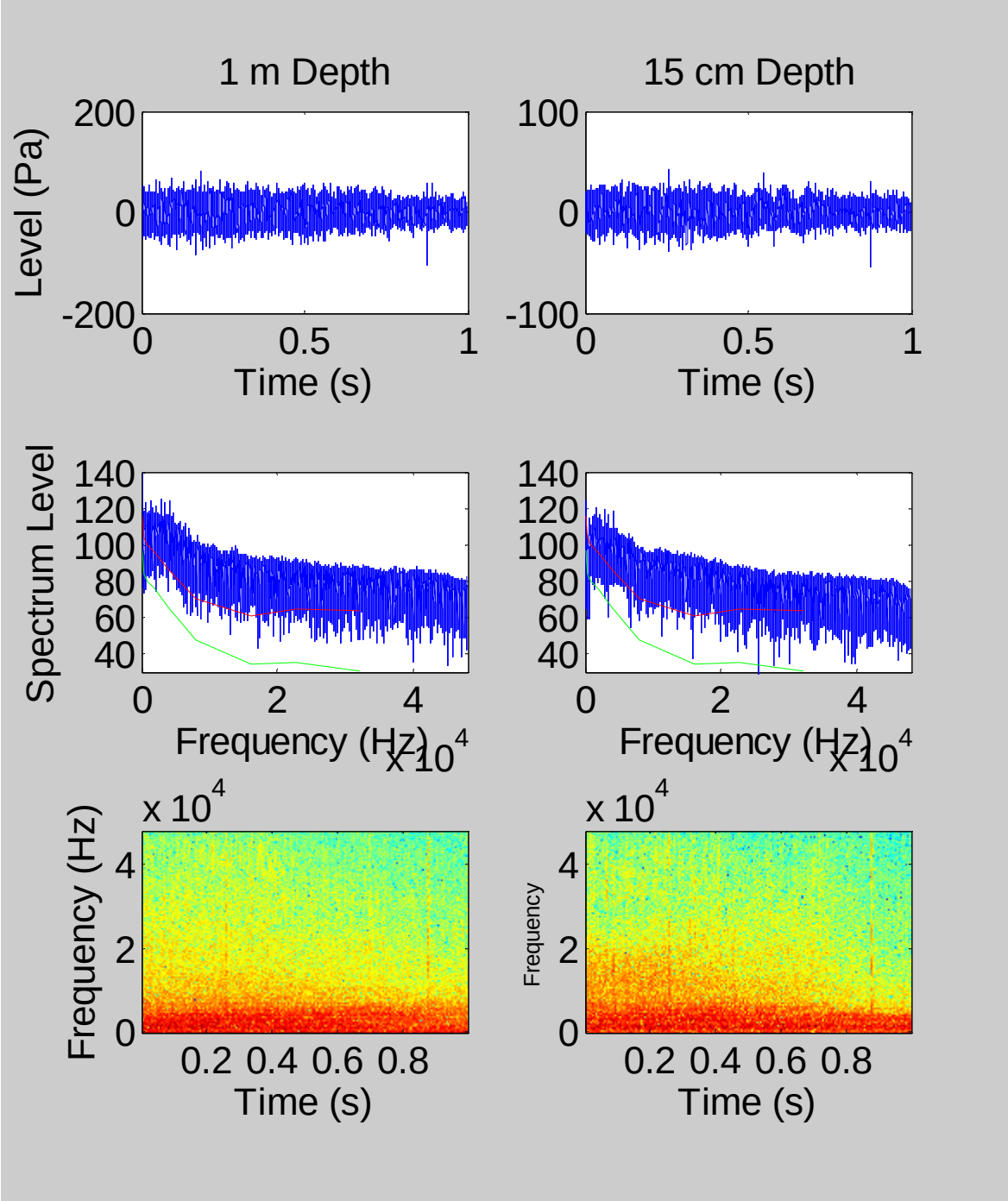

Figure 52. Approach at 10.7 mph. Top row: Time domain signal at time of boat passing. Middle row: Spectrum level power spectra (dB re 1uPa^2/Hz). Note frequency axis is in Hz x10^4. Red line shows audiogram of Buffett. Green line shows audiogram lowered as a function of the frequency-specific critical ratio. Bottom row: Spectrogram of plots from top row.

3.2 mph (Idle)

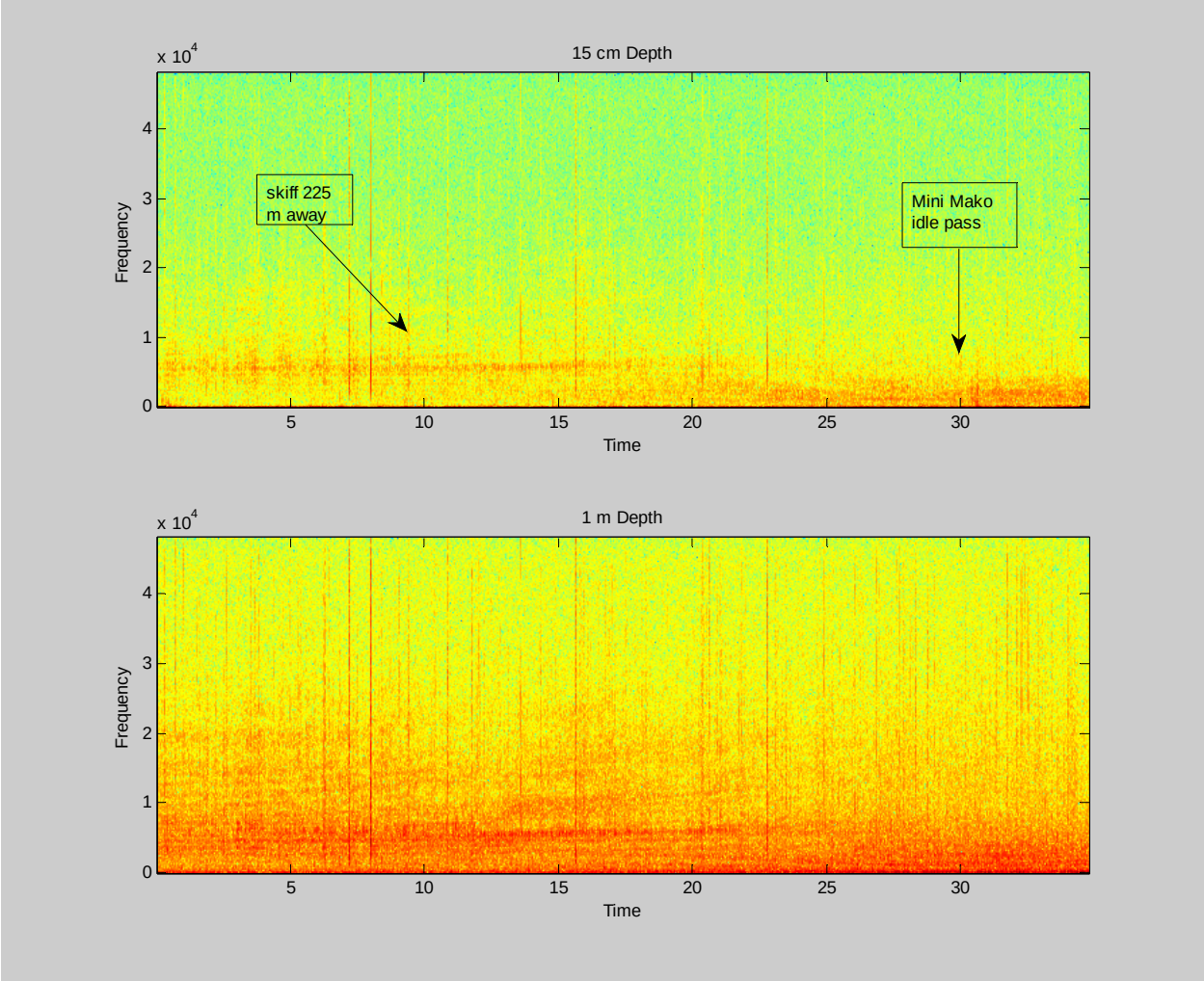

Figure 53. Spectrogram of approach sequence with vessel traveling 3.2 mph. Note that a skiff passed 225 m away (measured with laser range finders) prior to the pass of the idling boat. This is evident from 0-25 seconds in the spectrogram. Top plot is with hydrophone at 15 cm depth. Bottom plot is from a hydrophone at 1 m depth.

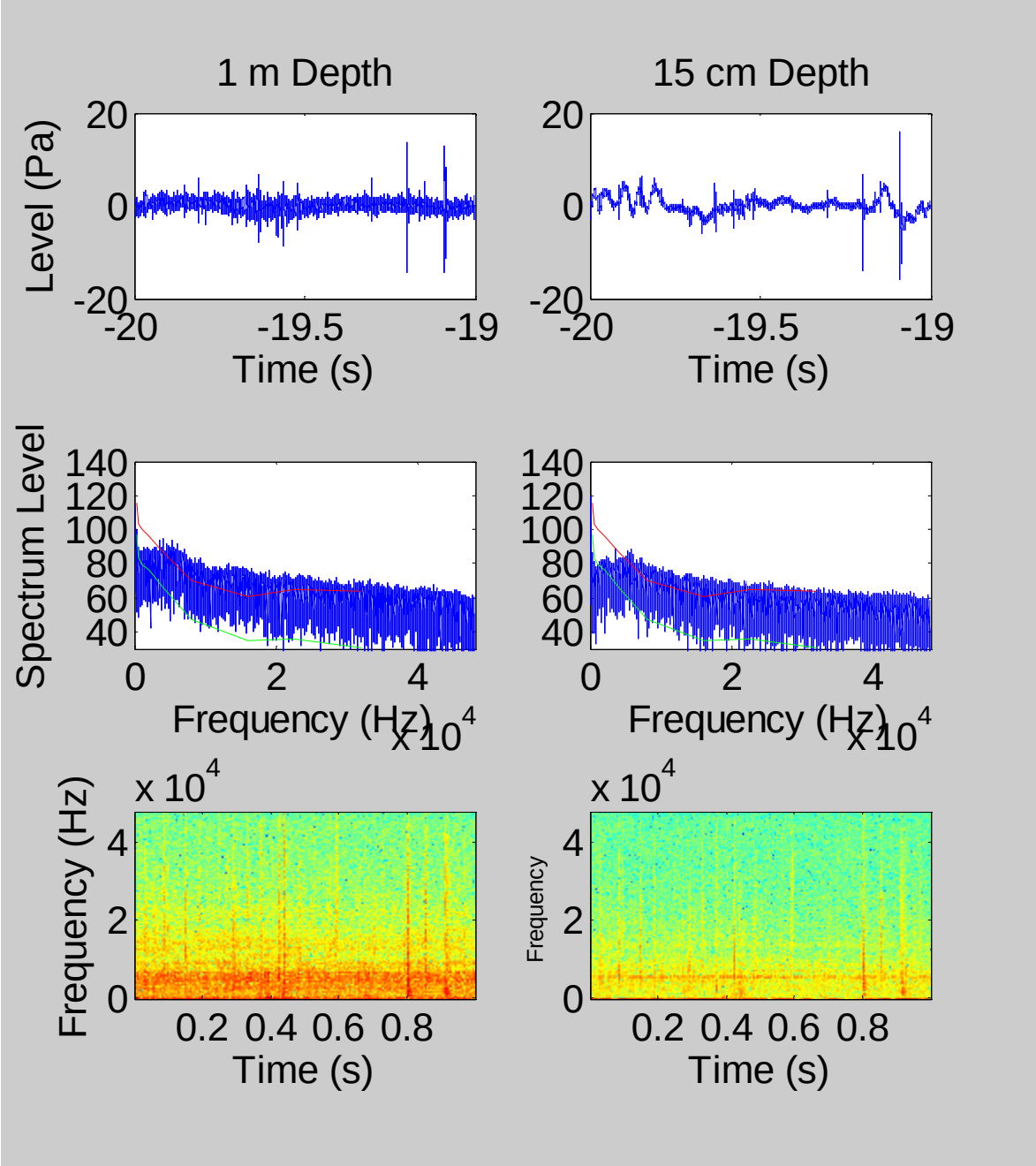

Figure 54. Approach at 3.2 mph. Top row: Time domain signal 20 seconds prior to boat passing. Middle row: Spectrum level power spectra (dB re 1uPa^2/Hz). Note frequency axis is in Hz x10^4. Red line shows audiogram of Buffett. Green line shows audiogram lowered as a function of the frequency-specific critical ratio. Bottom row: Spectrogram of plots from top row.

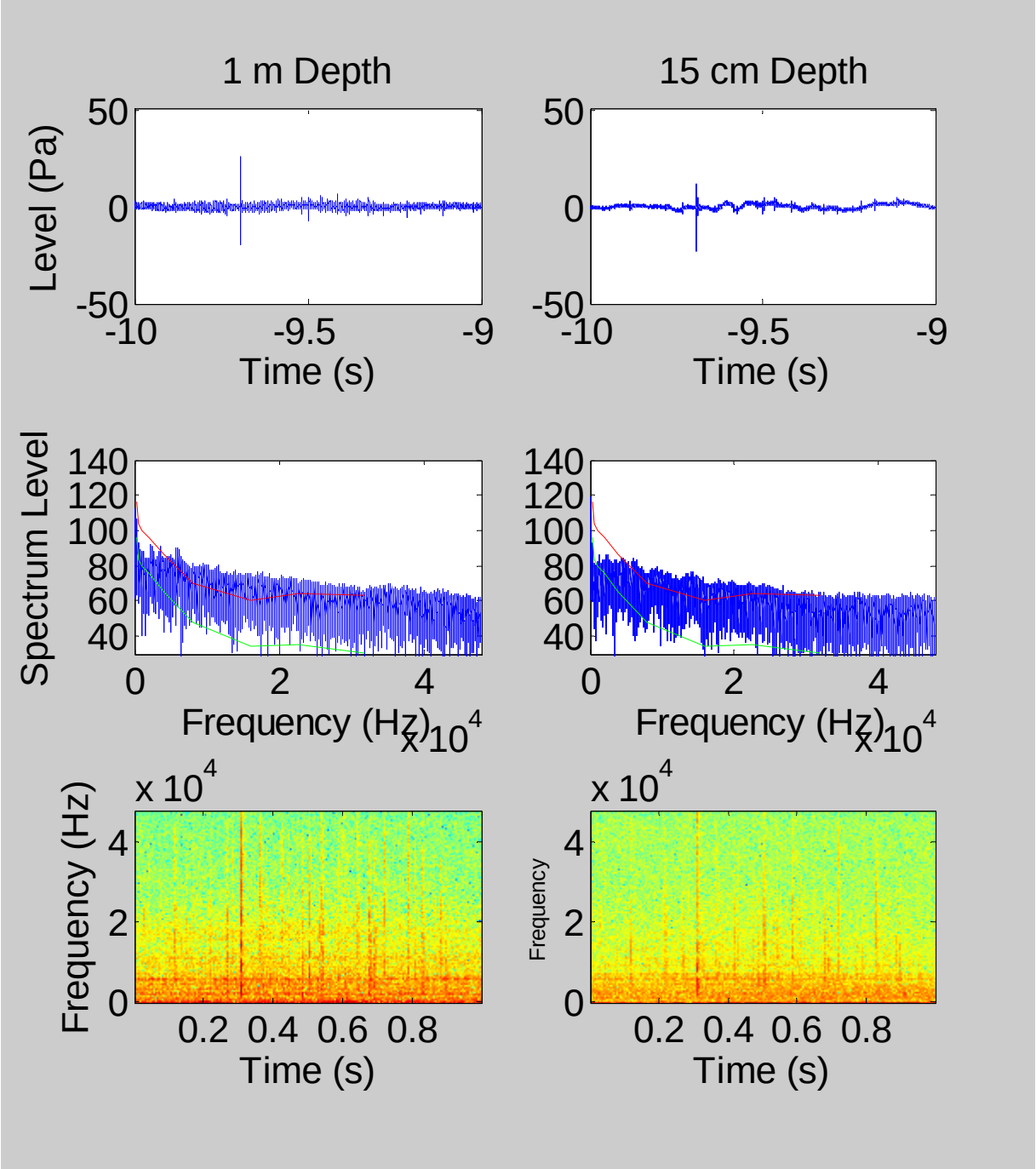

Figure 55. Approach at 3.2 mph. Top row: Time domain signal 10 seconds prior to boat passing. Middle row: Spectrum level power spectra (dB re 1uPa^2/Hz). Note frequency axis is in Hz x10^4. Red line shows audiogram of Buffett. Green line shows audiogram lowered as a function of the frequency-specific critical ratio. Bottom row: Spectrogram of plots from top row.

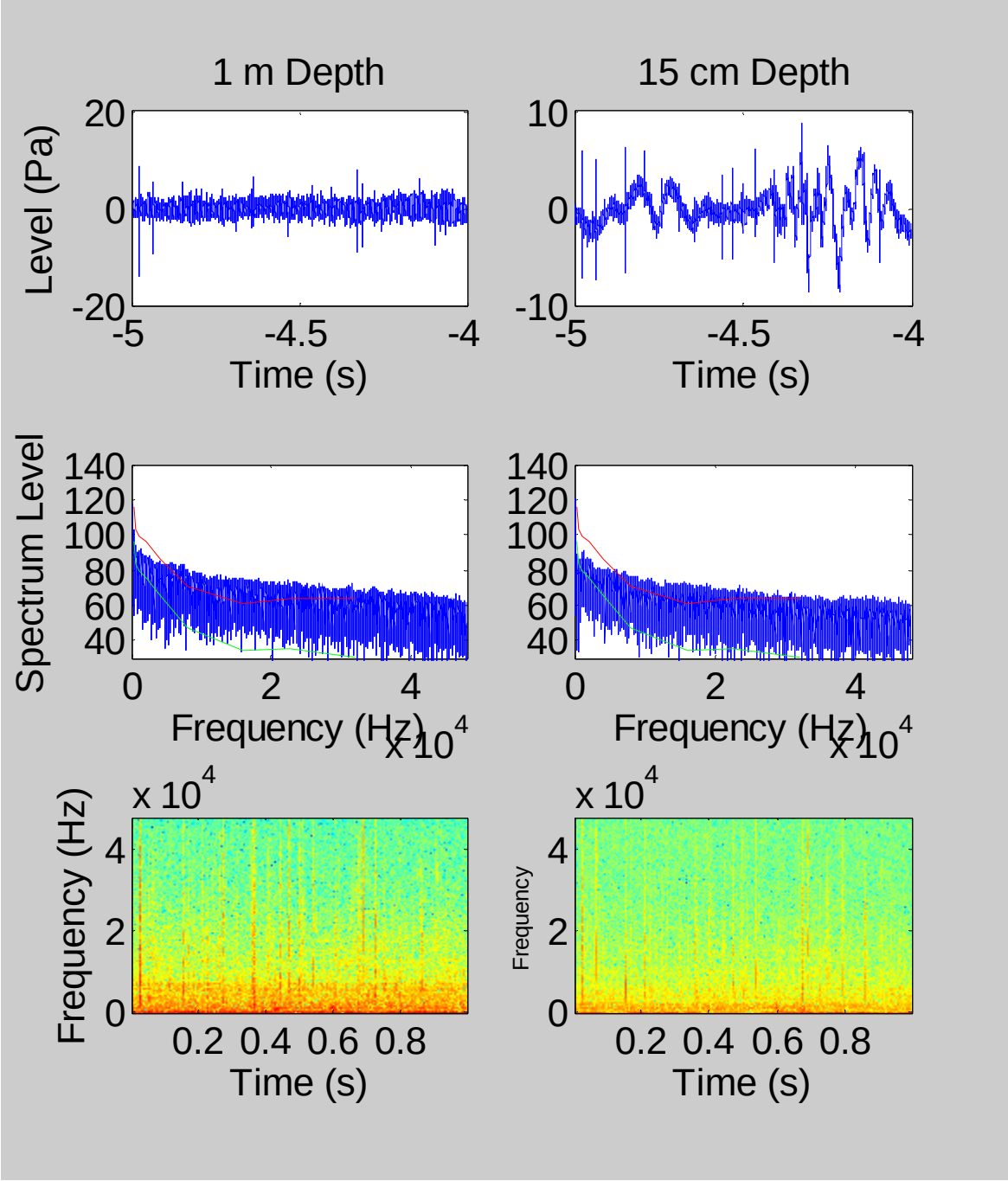

Figure 56. Approach at 3.2 mph. Top row: Time domain signal 5 seconds prior to boat passing. Middle row: Spectrum level power spectra (dB re 1uPa^2/Hz). Note frequency axis is in Hz x10^4. Red line shows audiogram of Buffett. Green line shows audiogram lowered as a function of the frequency-specific critical ratio. Bottom row: Spectrogram of plots from top row.

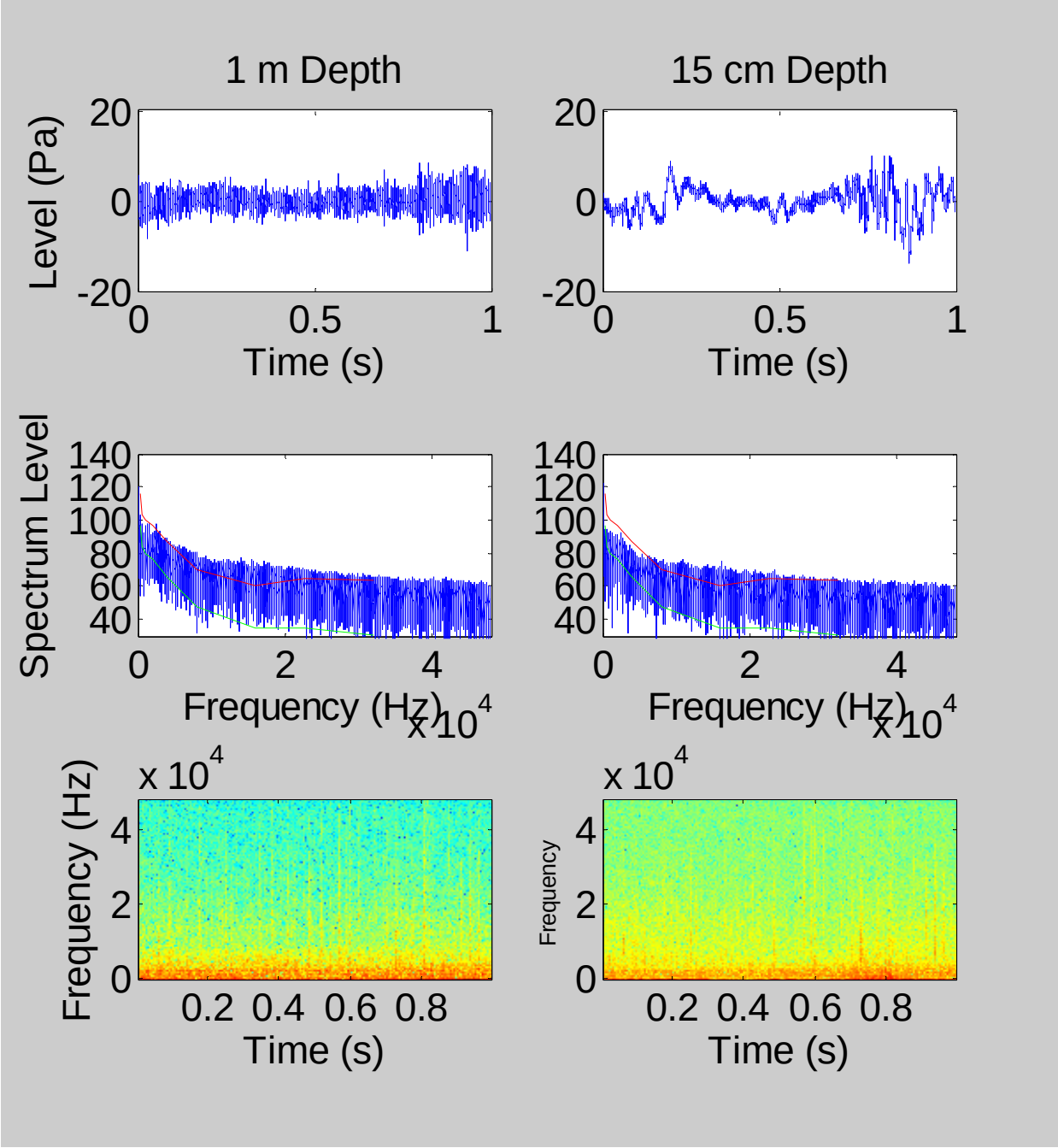

Figure 57. Approach at 3.2 mph. Top row: Time domain signal at time of boat passing. Middle row: Spectrum level power spectra (dB re 1uPa^2/Hz). Note frequency axis is in Hz x10^4. Red line shows audiogram of Buffett. Green line shows audiogram lowered as a function of the frequency-specific critical ratio. Bottom row: Spectrogram of plots from top row.

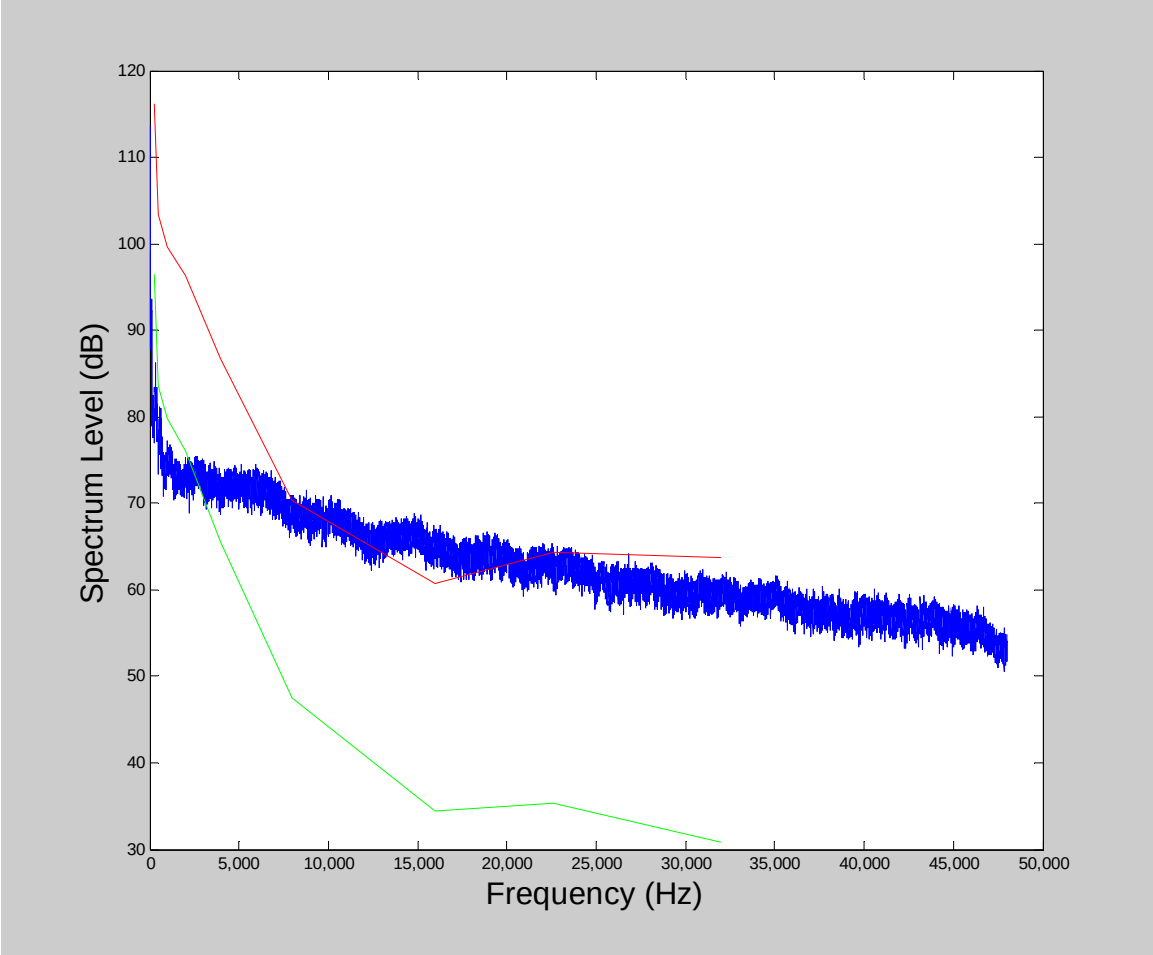

Figure 58. Background noise in Sarasota Bay at the time of the boat noise measurments. The sound level is given as spectrum level (dB re 1uPa^2/Hz). The audiogram of Buffett is overlaid in red, and the audiogram adjusted for the critical ratio is shown in green.

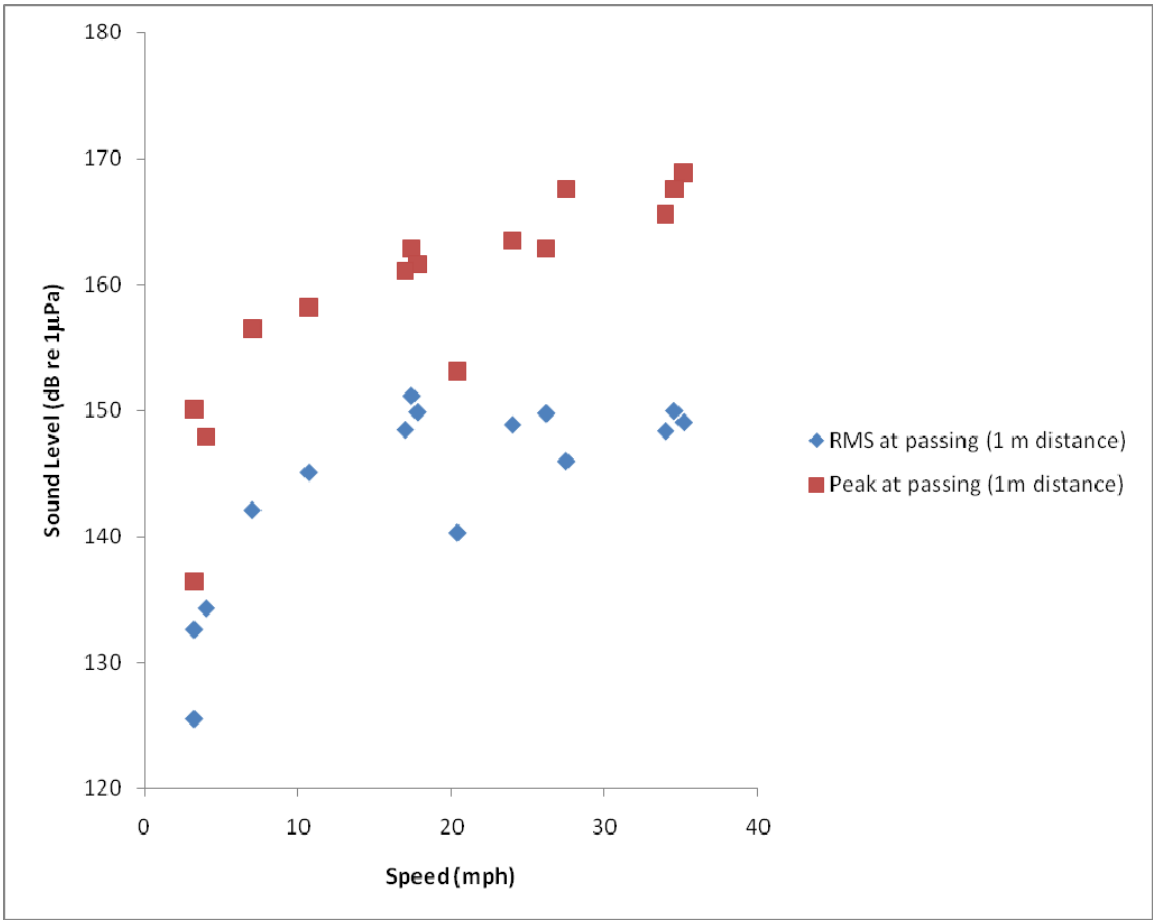

Figure 59. Estimated boat source levels as a function of boat speed. Data are from three different small boats. RMS sound levels are calculated from 1 second of recording when the boat passed approximately 1 m from the hydrophone. All recordings are from 1 m depth. Peak sound levels are measured from the same sound segment.

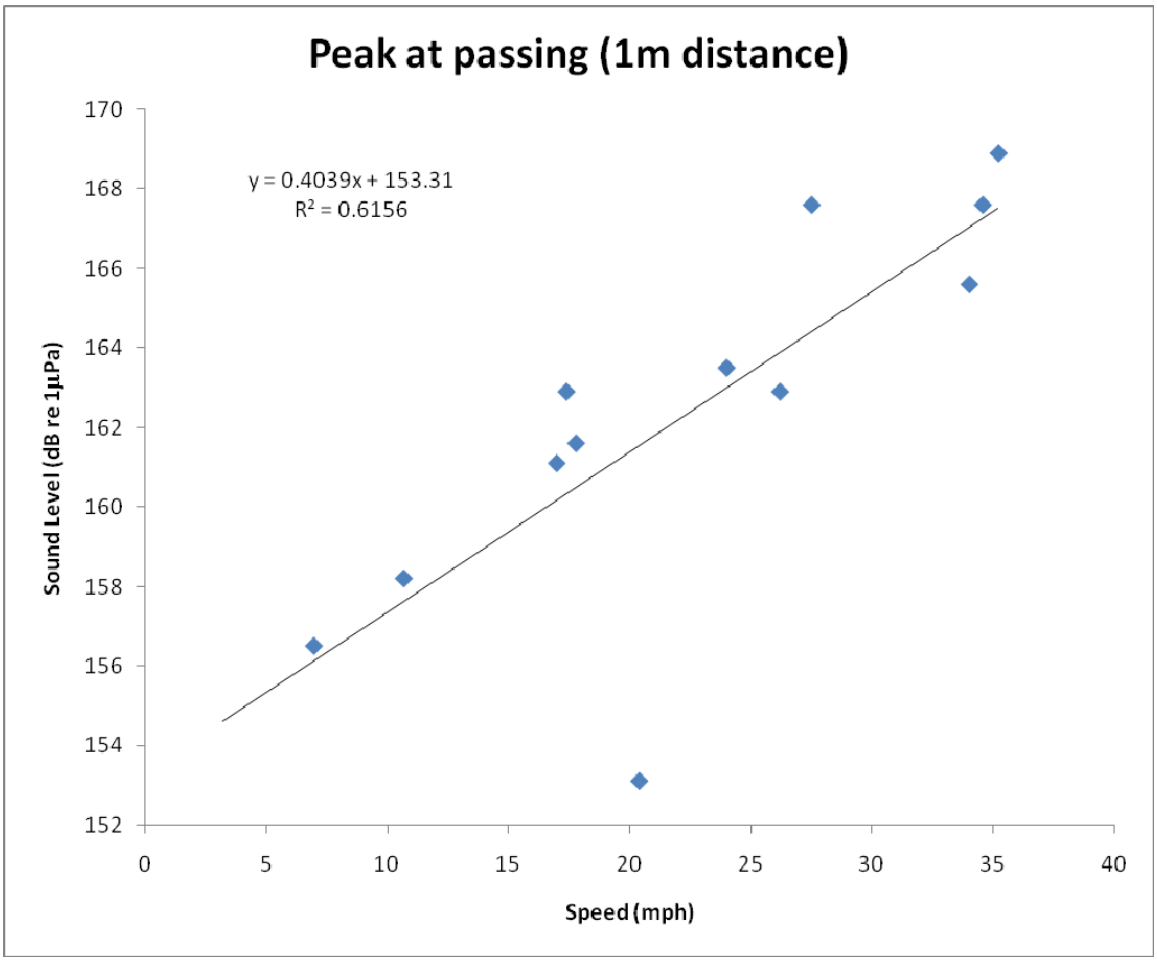

Figure 60. Regression of boat source levels as a function of boat speed. Data from Figure 59, except data from idle speed measurements was excluded from analysis. The slope of 0.4 indicates that the peak sound level will increase 6 dB for every 15 mph increase in speed.

References

Bauer, G.B., Colbert, D.E., Gaspard, J.C. III, Littlefield, B., and Fellner, W. (2003) Underwater visual acuity of Florida manatees. Int. J. Comp. Psychol. 16:130-142.

Bauer, G.B., Gaspard III, J.C., Colbert, D.E., Leach, J.B., and Reep, R. (2005) Tactile Discrimination of Textures by Florida Manatees, *Trichechus manatus latirostris.* The 12th Annual International Conference on Comparative Cognition, Melbourne, FL, March 19 – 22, 2005.

Bullock, T.H., Domning, and Best, R.C. 1980. Evoked brain potentials demonstrate hearing in a manatee (*Trichechus inunguis).* Journal of Mammalogy 61:130-133.

Bullock, T.H., O'Shea, T.J., and McClune, M.C. 1982. Auditory evoked potentials in the West Indian manatee (Sirenia: *Trichechus manatus).* Journal of Comparative Physiology 148:547-554.

Calleson, C.S., and Frohlich, R.K. 2007. Slower boat speeds reduce risks to manatees. Endangered Species Research. 3: 295-304.

Colbert, D. & Bauer, G.B. (1999). Basic husbandry training of two West Indian manatees, *Trichechus manatus latirostris.* Soundings 24: 18-21.

Colbert, D., Fellner, W., Bauer, G.B., Manire,C.A., & Rhinehart, H.L. (2001). Husbandry and research training of two Florida manatees, (*Trichechus manatus latirostris*). Aquatic Mammals 27: 16-23.

Colbert, D.E., Gaspard, J.C., Mann, D., Bauer, G.B., Dziuk, K. Sound localization abilities of two Florida manatees, *Trichechus manatus latirostris.* Presented at the Sirenian International Symposium, Conference on the Biology of Marine Mammals, San Diego, December 2005.

Colbert, D.E., Gaspard, J.C. III, Mann, D.A., Bauer, G.B., & Reep, R. Manatee Sound Localization Performance Abilities and Interaural Level Cue Availability. Presented at 36th Annual Conference of the International Marine Animal Trainer's Association, November 9-14, 2008, Cancun, Mexico.

Coombs, S. (1994) Nearfield detection of dipole sources by the goldfish (*Carassius auratus*) and the mottled sculpin (*Cottus bairdi),* J. Exp. Biol. 190:109-129.

Cornsweet, T.N. (1962) The staircase method in psychophysics. American Journal of Psychology 75:485-491.

Dehnhardt, G., Mauck, B., and Bleckmann, H. (1998) Seal whiskers detect water movements. Nature 394: 235-236.

Gerstein, E.R., L. Gerstein, S.E. Forsythe, and J.E. Blue. 1999. The underwater audiogram of the West Indian manatee (*Trichechus manatus*). Journal of the Acoustical Society of America 105(6):3575-3583.

Green, D.M. and Swets, J.A. (1966) Signal detection theory and psychophysics. Los Altos, CA: Peninsula.

Johnson, C.S. (1968) Masked Tonal Thresholds in the bottle-nosed porpoise. Journal of the Acoustical Society of America 44,965-967.

Kalmijn, A. J. (1988) Hydrodynamics and acoustic field detection. In Sensory Biology of Aquatic Animals, Atema, J., Fay, R. R., Popper, A. N., Tavolga, W. N., (Eds.), Springer-Verlag, New York, pp. 83–130.

Ketten, D.R., D.K. Odell, and D.P. Domning. 1992. Structure, function, and adaptation of the manatee ear. Pp. 77-95. IN: J.A. Thomas, R. A. Kastelein and A. Supin (eds.), Marine Mammal Sensory Systems, Plenum Press, New York.

Klishin, V.O., Diaz, R.P., Popov, V.V., & Supin, A.Y. (1990). Some characteristics of the Brazilian manatee, Trichechus inunguis. Aquatic Mammals, 16, 140 – 144.

Mann, D.A., D. E. Colbert, J. C. Gaspard, B. M. Casper, M. L. H. Cook, R.L. Reep, G. B. Bauer (2005) Auditory Temporal Resolution of the Manatee (*Trichechus manatus latirostris*) Auditory System. J Comp Physiol. A 191:903-908.

Miksis-Olds, JL, Donaghay, PL, Miller, JH, Tyack, PL, Reynolds, JE. (2007). Simulated vessel approaches elicit differential responses from manatees. Marine Mammal Science 23: 629-649.

Miller, G.A. (1947). Sensitivity to changes in the intensity of white noise and its relation to masking and loudness. Journal of the Acoustical Society of America. 19: 609-619.

Mohl, B., W.W.L. Au, J. Pawloski, and P.E. Natchigall. 1999. Dolphin hearing: relative sensitivity as a function of point of application of a contact sound source in the jaw and head region. Journal of the Acoustical Society of America. 105: 3421-3424.

Popov, V.V. and Supin, A.Y. 1990. Electrophysiological studies on hearing in some cetaceans and a manatee. IN: J.A. Thomas, and R. A. Kastelein (eds.), Sensory Abilities of Cetaceans: Laboratory and Field Evidence. Plenum Press, New York.

Reep, R. L., Marshall, C. D., and Stoll, M.L. (2002) Tactile hairs on the postcranial body in Florida manatees: A mammalian lateral line? Brain Behavior and Evolution 59:141-154.

Terhune, J.M. and Ronald, K. (1975). Masked hearing thresholds of ring seals. Journal of the Acoustical Society of America. 58, 515-516.

U.S. Fish and Wildlife Service. 2001. Florida Manatee Recovery Plan (*Trichechus manatus latirostris*), Third Revision. U.S. Fish and Wildlife Service. Atlanta, Georgia. 144pp. + appendices.

Permits

Training and testing was implemented under USFWS Permit: MA837923-7 to Gordon B. Bauer, which expires in 2013. This permit allows sensory processes and cognitive testing including playing sounds, including low frequency sound, to manatees and instrumental conditioning for stimulus discrimination. All research was reviewed and approved by the Mote Marine Laboratory IACUC.